Version 10
June 2001

Fine Guidance Sensor Instrument Handbook for Cycle 11

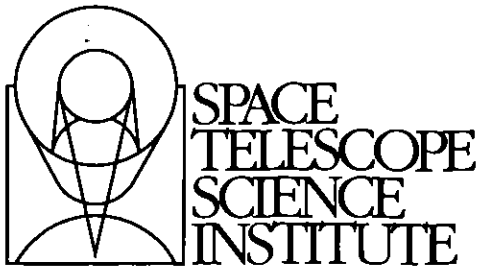

Hubble Division
3700 San Martin Drive
Baltimore, Maryland 21218
help@stsci.edu

Operated by the Association of Universities for Research in Astronomy, Inc., for the National Aeronautics and Space Administration

User Support

For prompt answers to any question, please contact the Science Support Division Help Desk.

- **E-mail:** `help@stsci.edu`
- **Phone:** (410) 338-1082

World Wide Web

Information and other resources are available on the FGS World Wide Web pages:

- **URL:** `http://www.stsci.edu/instruments/fgs/`

FGS Instrument Team

Name	Title	Phone	e-mail
Ed Nelan	Instrument Scientist	(410) 338-4992	nelan@stsci.edu
Diana Jong	Data Analyst	(410) 338-4396	jong@stsci.edu
Russ Makidon	Data Analyst	(410) 338-4946	makidon@stsci.edu

Revision History

Version	Date	Editor
1.0	October 1985	Alain Fresneau
5.0	June 1995	S. T. Holfeltz, E. P. Nelan, L. G. Taff, and M. G. Lattanzi
6.0	June 1996	S. T. Holfeltz
7.0	June 1998	O. L. Lupie & E. P. Nelan
8.0	June 1999	E. P. Nelan and R. B. Makidon
9.0	June 2000	E. P. Nelan and R. B. Makidon
10.0	June 2001	E. P. Nelan and R. B. Makidon

Send comments or corrections to:
Hubble Division
Space Telescope Science Institute
3700 San Martin Drive
Baltimore, Maryland 21218
E-mail: help@stsci.edu

Acknowledgments

The STScI FGS Program is run by the FGS Team within the Observatory Science Group. Currently, the team consists of Ed Nelan (Group Lead) and the invaluable members Diana Jong and Russ Makidon.

Many dedicated colleagues have contributed time and expertise to the STScI FGS Astrometry Program over so many years. (and in fact, *were* the FGS Astrometry Program). We wish to express our sincerest gratitude for their essential support of this program (in the hope it continues through many more years): Linda Abramowicz-Reed and Kevin Chisolm at BFGoodrich, the members of the Space Telescope Astrometry Team, especially Otto Franz and Larry Wasserman at Lowell Observatory, Fritz Benedict and Barbara McArthur with the University of Texas at Austin, and Denise Taylor, Sherie Holfeltz, and John Hershey at STScI. We also wish to thank Merle Reinhart, Vicki Balzano, and George Chapman with the commanding and implementation teams at STScI for their careful shepherding of our astrometry science and calibrations.

STScI would also like to thank BFGoodrich, in particular Kevin Chisholm and Linda Abramowicz-Reed for their invaluable assistance during the adjustment of the Articulating Mirror Assembly (AMA) to re-optimize both FGS1r and FGS2r. And not least, we would like to acknowledge that Chris Ftaclas originated and developed the conceptual basis of the AMA.

We would also like to thank Susan Rose and Steve Hulbert at STScI for their invaluable help with the preparation and publication of this Instrument Handbook. Without their patience and guidance, this Handbook could not have come together.

Finally, we thank Alain Fresneau for establishing the astrometry program at STScI.

Table of Contents

Acknowledgments iii

Chapter 1: Introduction 1

Purpose 2
Instrument Handbook Layout 2
The FGS as a Science Instrument 3
Technical Overview 4
The Instrument 4
Spectral Response 5
The S-Curve: The FGS's Interferogram 5
FGS1r and the AMA 5
Field of View 6
Modes of Operation 7
Planning and Analyzing FGS Observations 9
Writing an FGS Proposal 9
Data Reduction 9
FGS2r 9
HST's 2nd Replacement FGS 9

Chapter 2: FGS Instrument Design 11

The Optical Train 11
The Star Selectors 12
The Interferometer 13
FGS Detectors 17
HST's Spherical Aberration 17
The FGS Interferometric Response 18
The Ideal S-Curve 18
Actual S-Curves 19
The FGS1r Articulated Mirror Assembly 22

FGS Aperture and Filters 23
FOV and Detector Coordinates 23
Filters and Spectral Coverage 25
FGS Calibrations 27

Chapter 3: FGS Science Guide 29
The Unique Capabilities of the FGS 29
Position Mode: Precision Astrometry 30
Transfer Mode: Binary Stars and Extended Objects 31
Observing Binaries: The FGS vs. WFPC2 31
Transfer Mode Performance 33
Combining FGS Modes: Determining Stellar Masses 35
Angular Diameters 36
Relative Photometry 37
Moving Target Observations 39
Summary of FGS Performance 39
Special Topics Bibliography 40
STScI General Publications 40
Position Mode Observations 40
Transfer Mode Observations 40
Miscellaneous Observations 41
Web Resources 41

Chapter 4: Observing with the FGS 43
Position Mode Overview 43
The Position Mode Visit 43
The Position Mode Exposure 44
Planning Position Mode Observations 45
Target Selection Criteria 45
Filters 46
Background 48
Position Mode Exposure Time Calculations 49
Exposure Strategies for Special Cases 50
Sources Against a Bright Background 51
Crowded Field Sources 52

Position Mode Observing Strategies 52
Summary of Position Mode Error Sources 52
Drift and Exposure Sequencing 53
Cross Filter Observations 54
Transfer Mode Overview 55
The FGS Response to a Binary 55
The Transfer Mode Exposure 57
Planning a Transfer Mode Observation 58
Target Selection Criteria 58
Transfer Mode Filter and Color Effects 59
Signal-to-Noise 60
Transfer Mode Exposure Time Calculations 61
Transfer Mode Observing Strategies 63
Summary of Transfer Mode Error Sources 63
Drift Correction 63
Temporal Variability of the S-Curve 63
Faint Targets and Background Subtraction 64
Empirical Roll Angle Determination 65
Exposure Strategies for Special Cases: Moving Targets ... 65

Chapter 5: FGS Calibration Program 67
Position Mode Calibrations and Error Sources 67
Position Mode Exposure Level Calibrations 69
Position Mode Visit Level Calibrations 73
Position Mode Epoch-Level Calibrations 75
Transfer Mode Calibrations and Error Sources 76
Linking Transfer and Position Mode Observations 82
Cycle 10 Calibration and Monitoring Program 83
Active FGS1r Calibration and Monitoring Programs 83
Special Calibrations 83

Chapter 6: Writing a Phase II Proposal 85
Phase II Proposals: Introduction 85
Required Information 85
STScI Resources for Phase II Proposal Preparation 86
Instrument Configuration 87
Optional Parameters for FGS Exposures 88

Special Requirements 90
Visit-Level Special Requirements 91
Exposure-Level Special Requirements 92
Overheads 93
Position Mode Overheads 93
Transfer Mode Overhead 94
Proposal Logsheet Examples 95
1. Parallax Program with Position Mode 95
2. Bright Binary with Transfer Mode 99
3. Mass Determination: Transfer and Position Mode 102
4. Faint Binary with Transfer Mode: Special Background and Roll Angle Measurements 104

Chapter 7: FGS Astrometry Data Processing 109
Data Processing Overview 109
Exposure-Level Processing 110
Initial Pipeline Processing 110
Observing Mode Dependent Processing 111
Visit-Level Processing 113
Position Mode 113
Transfer Mode 114
Epoch-Level Processing 115
Parallax, Proper Motion, and Reflex Motion 115
Binary Stars and Orbital Elements 116

Appendix 1: Target Acquisition and Tracking 121
FGS Control 121
Target Acquisition and Position Mode Tracking 122
Slew to the Target 122
Search 123
CoarseTrack 124
FineLock 124
Transfer Mode Acquisition and Scanning 127
Visit Level Control 127

Appendix 2: FGS1r Performance Summary 129
FGS1r's First Three Years in Orbit 129
Angular Resolution Test 132
Test Results: The Data 133
Test Results: Binary Star Analysis 135
FGS1r's Angular Resolution: Conclusions 136
FGS1r: Final AMA Adjustment 136

Glossary of Terms 137

List of Figures 143

List of Tables 145

Index 147

CHAPTER 1:
Introduction

In this chapter . . .

Purpose / 2
Instrument Handbook Layout / 2
The FGS as a Science Instrument / 3
Technical Overview / 4
Planning and Analyzing FGS Observations / 9

The precision pointing required of the Hubble Space Telescope (HST) motivated the design of the Fine Guidance Sensors (FGS). These large field of view (FOV) white light interferometers are able to track the positions of luminous objects with ~1 millisecond of arc (mas) precision. In addition, the FGS can scan an object to obtain its interferogram with sub-mas sampling. These capabilities enable the FGS to perform as a high-precision astrometer and a high angular resolution science instrument which can be applied to a variety of objectives, including:

- relative astrometry with an accuracy approaching 0.2 mas for targets with V < 16.8;
- detection of close binary systems down to ~8 mas, and characterization of visual orbits for systems with separations as small as 12 mas;
- measuring the angular size of extended objects;
- 40 Hz relative photometry (e.g., flares, occultations) with milli-magnitude accuracy.

The purpose of this Handbook is to provide information needed to propose for HST/FGS observations (Phase I), to design Phase II programs for accepted FGS proposals (in conjunction with the Phase II Proposal Instructions), and to describe the FGS in detail.

Purpose

The *FGS Instrument Handbook* is the basic reference manual for observing with the FGS. It describes the FGS design, properties, performance, operation, and calibration. The Handbook is maintained by the Observatory Support Group at STScI, who designed this document to serve three purposes:

- To help potential FGS users decide whether the instrument is suitable for their goals, and to provide instrument-specific information for preparing Phase I observing proposals with the FGS.
- To provide instrument-specific information and observing strategies relevant to the design of Phase II FGS proposals (in conjunction with the Phase II Proposal Instructions).
- To provide technical information about the FGS and FGS observations.

The *HST Data Handbook* provides complementary information about the analysis and reduction of FGS data, and should be used in conjunction with this Instrument Handbook. In addition, we recommend visiting the FGS World Wide Web pages for frequent updates on performance, calibration results, and methods of data reduction and analysis. These pages can be found at:

`http://www.stsci.edu/instruments/fgs/`

Instrument Handbook Layout

To guide the proposer through the FGS's capabilities and help optimize the scientific use of the instrument, we have produced the *FGS Instrument Handbook*, the layout of which is as follows:

- Chapter 1: Introduction, describes the layout of the *FGS Instrument Handbook* and gives a brief overview of the instrument and its capabilities as a science instrument.
- Chapter 2: FGS Instrument Design, details the design of the FGS. Specific attention is given to the optical path and the effect of optical misalignments on FGS observations. The interferometric Transfer Function is described in detail, along with effects which degrade Transfer Function morphology. Descriptions of apertures and filters are also presented here.

- Chapter 3: FGS Science Guide, serves as a guide to the scientific programs which most effectively exploit FGS capabilities. The advantages offered by the FGS are described together with suitable strategies to achieve necessary scientific objectives. A representative list of publications utilizing the FGS for scientific observations is included for reference.
- Chapter 4: Observing with the FGS, describes the detailed characteristics of the two FGS observing modes - Position Mode and Transfer Mode - as well as the observational configurations and calibration requirements which maximize the science return for each mode.
- Chapter 5: FGS Calibration Program, describes sources of FGS errors, associated calibrations, and residual errors for Position and Transfer Mode observations. A discussion of calibration plans for the upcoming Cycle is also included.
- Chapter 6: Writing a Phase II Proposal, serves as a practical guide to the preparation of Phase II proposals, and as such is relevant to those researchers who have been allocated HST observing time.
- Chapter 7: FGS Astrometry Data Processing, briefly describes the FGS astrometry data processing pipeline and analysis tools. The various corrections for both Position and Transfer Mode observations are described along with the sequence in which they are applied.

In addition to the above chapters, we also provide two appendices:

- Appendix 1: Target Acquisition and Tracking, describes the acquisition of targets in both Position and Transfer Modes. The target acquisition scenario may have implications for observations of moving targets or targets in crowded fields.
- Appendix 2: FGS1r Performance Summary, describes the evolution of FGS1rFGS1r during its first three years in orbit and the adjustment of the AMA to improve performance in this instrument.

The FGS as a Science Instrument

The FGS has two modes of operation: Position Mode and Transfer Mode. In Position Mode the FGS locks onto and tracks a star's interferometric fringes to precisely determine its location in the FGS FOV. By sequentially observing other stars in a similar fashion, the relative angular positions of luminous objects are measured with a *per-observation* precision of about 1 mas over a magnitude range of $3.0 < V < 16.8$. This mode is used for relative astrometry, i.e., for measuring parallax, proper

motion, and reflex motion. Multi-epoch programs achieve accuracies approaching 0.2 mas.

In Transfer Mode an object is scanned to obtain its interferogram with sub-mas sampling. Using the fringes of a point source as a reference, the composite fringe pattern of a non-point source is deconvolved to determine the angular separation, position angle, and relative brightness of the components of multiple-star systems or the angular diameters of resolved targets (Mira variables, asteroids, etc.).

As a science instrument, the FGS is a sub-milliarcsecond astrometer and a high angular resolution interferometer. Some of the investigations well suited for the FGS are listed here and discussed in detail in Chapter 3:

- ***Relative astrometry*** (position, parallax, proper motion, reflex motion) with *single-measurement* accuracies of about 1 milliarcsecond (mas). Multi-epoch observing programs can determine parallaxes with accuracies approaching 0.2 mas.
- ***High-angular resolution observing***:
  - detect duplicity or structure down to 8 mas
  - derive visual orbits for binaries as close as 12 mas.
- ***Absolute masses and luminosities***:
  - The absolute masses and luminosities of the components of a multiple-star system can be determined by measuring the system's parallax while deriving visual orbits and the brightnesses of the stars.
- ***Measurement of the angular diameters*** of non-point source objects down to about 8 mas.
- ***40Hz 1–2% long-term relative photometry***:
  - Long-term studies or detection of variable stars.
- ***40Hz milli-magnitude relative photometry over orbital timescales.***
  - Light curves for stellar occultations, flare stars, etc.

Technical Overview

The Instrument

The FGS is a white-light shearing interferometer. It differs from the long-baseline Michelson Stellar Interferometer in that the angle of the incoming beam with respect to the HST's optical axis is measured from the tilt of the collimated wavefront presented to the "Koesters prism" rather

than from the difference in the path length of *two* individual beams gathered by separate apertures. Thus, the FGS is a *single aperture* (single telescope) interferometer, well suited for operations aboard HST. The FGS is a two dimensional interferometer; it scans or tracks an object's fringes in two orthogonal directions simultaneously. As a science instrument, the FGS can observe targets as bright as V=3 and as faint as V=17.5 (dark counts dominate for V>18 targets).

Spectral Response

The FGS employs photomultiplier tubes (PMTs) for detectors. The PMTs—four per FGS—are an end-illuminated 13-stage venetian blind dynode design with an S-20 photocathode. The PMT sensitivity is effectively monotonic over a bandpass from 4000 to 7000A, with an ~18% efficiency at the blue end which diminishes to ~2% at the red end.

Each FGS contains a filter wheel fitted with 5 slots. FGS1r contains three wide-band filters, F550W, F583W (sometimes called CLEAR), F605W, a 5-magnitude Neutral Density attenuator (F5ND), and a 2/3 pupil stop, referred to as the PUPIL. Not all filters are supported by standard calibrations. Transmission curves of the filters and recommendations for observing modes are given in Chapters 2 and 4 respectively.

The S-Curve: The FGS's Interferogram

The FGS interferometer consists of a polarizing orthogonal beam splitter and two Koesters prisms. The Koesters prism, discussed in chapter 2, is sensitive to the *tilt* of the incoming wavefront. Two beams emerge from each prism with relative intensities correlated to the tilt of the input wavefront. The relation between the input beam tilt and the normalized difference of the intensities of the emergent beams, measured by pairs of photomultiplier tubes, defines the fringe visibility function, referred to as the "S-Curve". Figure 1.1 shows the fringe from a point source. To sense the tilt in two dimensions, each FGS contains two Koesters prisms oriented orthogonally with respect to one another. A more detailed discussion is given in Chapter 2.

FGS1r and the AMA

During the Second Servicing Mission in March 1997 the original FGS1 was replaced by FGS1r. This new instrument was improved over the original design by the re-mounting of a flat mirror onto a mechanism capable of tip/tilt articulation. This mechanism, referred to as the *Articulated Mirror Assembly*, or AMA, allows for precise in-flight alignment of the interferometer with respect to HST's OTA. This assured

optimal performance from FGS1r since the degrading effects of HST's spherically aberrated primary mirror would be minimized (the COSTAR did not correct the aberration for the FGSs). This topic is discussed in detail in Chapter 2.

Figure 1.1: FGS Interferometric Response (the "S-Curve")

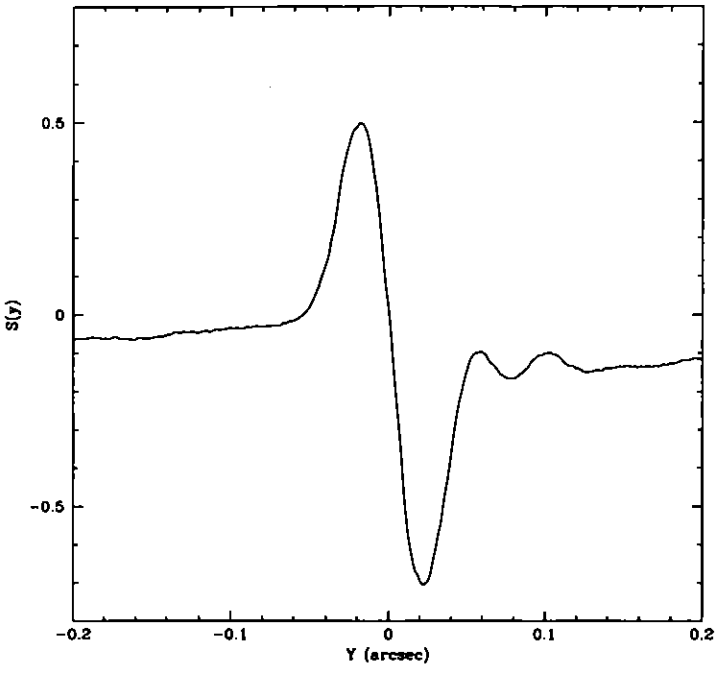

Field of View

The total *field of view* (FOV) of an FGS is a quarter annulus at the outer perimeter of the HST focal plane with inner and outer radii of 10 and 14 arcmin respectively. The total area (on the sky) subtended by the FOV is ~ 69 square arcmintues. The entire FOV is accessible to the interferometer, but only a 5 x 5 arcsec aperture, called the *Instantaneous Field of View* (IFOV), samples the sky at any one time. A dual component Star Selector Servo system (called SSA and SSB) in each FGS moves the IFOV to a desired position in the FOV. The action of the Star Selectors is described in detail in Chapter 2, along with a more detailed technical description of the instrument. Figure 1.2 shows a schematic representation of the FGSs relative to the HST focal plane.

Figure 1.2: FGSs in the HST Focal Plane (Projected onto the Sky)

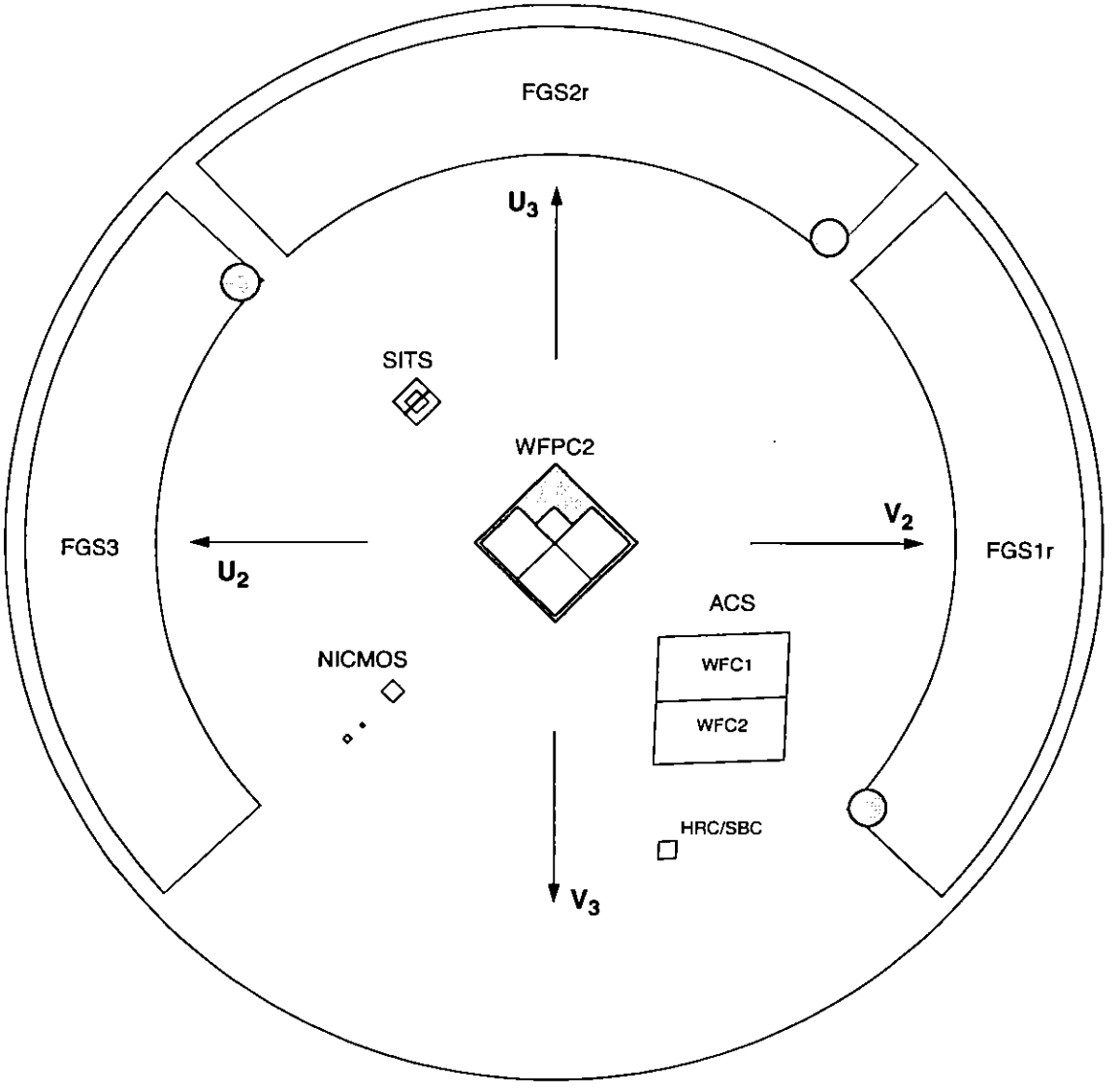

Modes of Operation

The FGS has two modes of operation: Position Mode and Transfer Mode.

Position Mode

The FGS Position Mode is used for relative astrometry, i.e. parallax, proper motion, reflex motion and position studies. In Position Mode, the

HST pointing is held fixed while selected FGS targets are sequentially observed (fringes are acquired and tracked, see appendix A1) for a period of time ($2 < t < 120$ sec) to measure their relative positions in the FOV. Two-dimensional positional and photometric data are continuously recorded every 25 msec (40 Hz). The raw data are composed of a Star Selector encoder angles (which are converted to FGS X and Y detector coordinates during ground processing) and photomultiplier (PMT) counts. Figure 1.3 is a schematic of the FGS FOV and IFOV. The figure shows how Star Selectors A and B uniquely position the IFOV anywhere in the FGS FOV.

Transfer Mode

In Transfer Mode, the FGS obtains an object's interferograms in two orthogonal directions by scanning the Instantaneous Field of View (IFOV) across the target (typically in 1" scan lengths). Transfer Mode observing is conceptually equivalent to imaging an object with sub-milliarcsecond pixels. This allows the FGS to detect and resolve structure on scales smaller than HST's diffraction limit, making it ideal for detecting binary systems with separations as small as 8 mas with ~ 1 mas precision.

Figure 1.3: FGS Star Selector Geometry

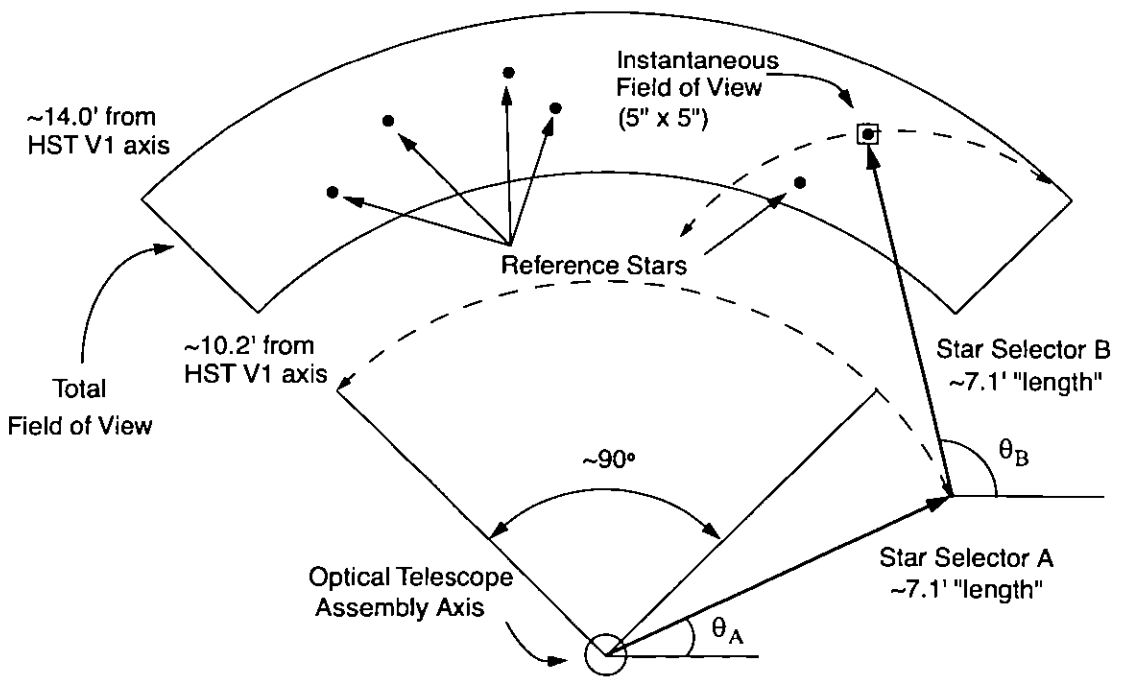

Planning and Analyzing FGS Observations

Writing an FGS Proposal

Chapters 3 and 6 are of particular use in designing and implementing an FGS proposal. Chapter 3 provides information on a variety of scientific programs which exploit the unique astrometric capabilities of the FGS. Chapter 6 provides guidelines on how to design the Phase II proposal. In Chapter 6 we provide examples of observing strategies and identify special situations where further discussions with STScI are recommended.

Data Reduction

The *HST Data Handbook* provides a detailed description of the FGS data and related data reduction. Chapters 5 and 7 in this Instrument Handbook contain useful summaries of that information. Chapter 5 provides a discussion of the accuracies and sources of errors associated with FGS data in addition to a detailed description of the calibration program planned for the upcoming Cycle. Chapter 7 describes the set of software tools which are available to observers to reduce, analyze and interpret FGS data. Please check the FGS web pages for details on these tools.

FGS2r

HST's 2nd Replacement FGS

After the second servicing mission (SM2) the original FGS1 was returned for refurbishment to its manufacturer, Raytheon Optical Systems Inc. (ROSI, currently BFGoodrich Space Flight Systems). Its (worn out) star selector shaft bearings were replaced and, like FGS1r, an AMA was installed. During the December 1999 servicing mission (SM3a) this repaired unit, redesignated as FGS2r, replaced the original, mechanically worn FGS2. As part of the orbital verification activities ROSI engineers, using observations of the standard star Upgren69, adjusted the AMA to align FGS2r's internal optics with the OTA to optimize the instrument's interferometric response.

With two AMA optimized FGSs now on board HST, the question of whether FGS1r or FGS2r should be designated as the science instrument might arise. The amplitude and morphology of both the FGS1r and FGS2r

S-curves vary with location in the FOV due to "beam walk", for which the AMA can not compensate (discussed in chapter 2). But FGS1r demonstrates optimal fringe visibility and morphology along *both its x and y axis simultaneously* at the center of its FOV, while FGS2r's x and y axis S-curves are not *simultaneously* optimal anywhere in its FOV. Therefore, FGS1r has significantly better angular resolution and remains the clear choice as the science instrument (FGS1r's performance as an astrometer is not impaired by the FOV dependent fringes).

There is also the consideration of the orientation of an FGS's FOV in HST's focal plane. For efficient astrometric determination of parallaxes, targets and reference stars are observed at times of maximum parallax factor. Due to HST sun angle constraints, FGS1r's orientation at such times is more favorable than that of FGS2r.

STScI does not regard FGS2r as a science instrument and has no plans to calibrate it as such. It has been calibrated only to the level needed for reliable performance as a guider. It will be monitored over time to verify that these calibrations remain within tolerance as the instrument desorbs water from its graphite epoxy composites.

CHAPTER 2:

FGS Instrument Design

In this chapter . . .

The Optical Train / 11
FGS Detectors / 17
HST's Spherical Aberration / 17
The FGS Interferometric Response / 18
The FGS1r Articulated Mirror Assembly / 22
FGS Aperture and Filters / 23
FGS Calibrations / 27

This chapter details the design of the FGS. The optical path, detectors, interferometric response, and the effect of optical misalignments and HST's spherical aberration on FGS performance are discussed in detail. Description of the apertures and available filters are provided.

The Optical Train

Each FGS comprises two orthogonal white-light, shearing interferometers, their associated optical and mechanical elements, and four S-20 photo-multiplier tubes (PMTs). For clarity, we divide the FGS optical train into two sections: the star selection mechanism and the interferometer.

The Star Selectors

A schematic view of the FGS optical train is shown in Figure 2.1 on page 13. Light from the HST Optical Telescope Assembly (OTA) is intercepted by a plane pickoff mirror in front of the HST focal plane and directed into the FGS. The beam is collimated and compressed (by a factor of ~60) by an *aspheric collimating mirror,* and guided to the optical elements of the Star Selector A (SSA) servo assembly. This assembly of two mirrors and a five element refractive corrector group can be commanded to rotate about the telescope's optical axis. The corrector group compensates for designed optical aberrations induced by both the asphere and the HST Optical Telescope Assembly (OTA). The asphere contributes astigmatism, spherical aberration and coma to the incident beam. Aberrations from the OTA's Ritchey-Chretien design include astigmatism and field curvature.

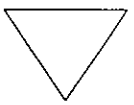

The FGS design does not correct for the unexpected spherical aberration from the telescope's misfigured primary mirror.

After the SSA assembly, the beam passes through a field stop (not shown) to minimize scattered light and narrow the field of view. The four mirrors of the Star Selector B (SSB) assembly intercept and re-direct the beam to a fold flat mirror and through the filter wheel assembly. From there, the Articulating Mirror Assembly (AMA) reflects the beam onto the Polarizing Beam Splitter. Like the SSA, the SSB assembly rotates about a vector parallel to the telescope's optical axis. Together the SSA and SSB assemblies allow for the transmission to the polarizing beam splitter only those photons originating from a narrow region in the total FGS field of view. This area, called the *Instantaneous Field of View* (IFOV), is a 5 x 5 arcsec patch of sky, the position of which is uniquely determined by the rotation angles of both the SSA and SSB. The IFOV can be brought to any location in the full FOV and its position can be determined with sub-milliarcsecond precision (see Figure 1.3 on page 8).

The AMA is an enhancement to the original FGS design. It allows for in-flight alignment of the collimated beam onto the polarizing beam splitter and therefore the Koesters prisms. Given HST's spherically aberrated OTA, this is an important capability, the benefits of which will be discussed in subsequent chapters.

Figure 2.1: FGS1r Optical Train Schematic

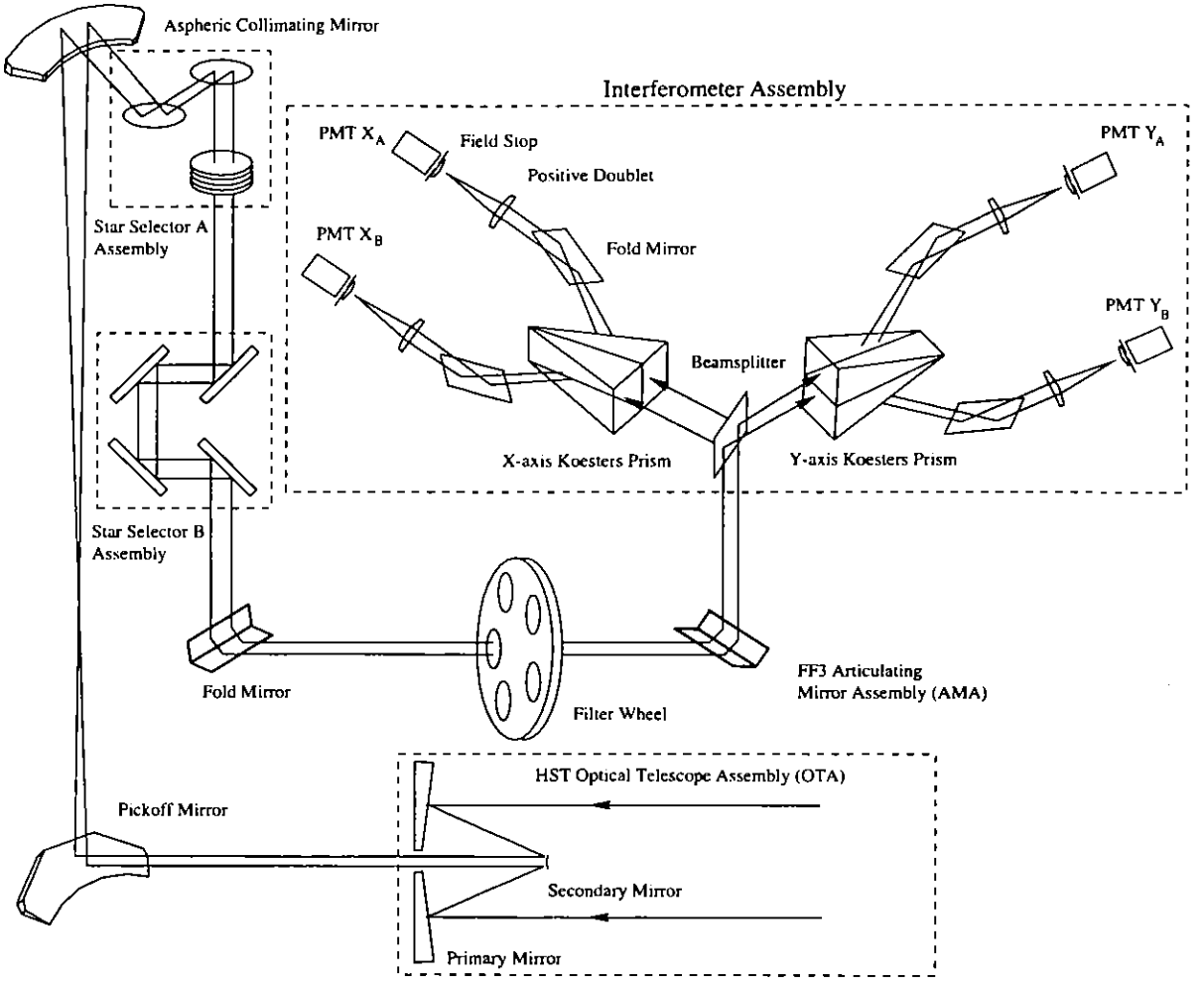

The Interferometer

The interferometer consists of a polarizing beam splitter followed by two Koesters prisms. The polarizing beam splitter divides the incoming unpolarized light into two plane polarized beams with orthogonal polarizations, each having roughly half the incident intensity. The splitter then directs each beam to a Koesters prism and its associated optics, field stops, and photomultiplier tubes. Figure 2.2 on page 14 illustrates the light path between the Koesters prism and the PMTs.

The Koesters prisms are constructed of two halves of fused silica joined together along a coated surface which acts as a dielectric beam splitter. The dielectric layer performs an equal intensity division of the beam, reflecting half and transmitting half, imparting a 90 degree phase lag in the transmitted beam. This division and phase shift gives the Koesters prism its

interferometric properties: the beam reflected from one side of the prism interferes constructively or destructively with the beam transmitted from the other side. The degree of interference between the two beams is directly related to the angle, or tilt, between the incoming wavefront's propagation vector and the plane of the dielectric surface.

Each Koesters prism emits two exit beams whose relative intensities depend on the tilt of the incident wavefront. Each beam is focussed by a positive doublet onto a field stop assembly (which narrows the IFOV to 5 x 5 arcsec). The focussed beams are recollimated by field lenses (after the field stop) and illuminate the photomultiplier tubes (PMT). The PMT electronics integrate the photon counts over 25 millisecond intervals.

The Koesters prism is sensitive to the angle of the incoming wavefront as *projected* onto its dielectric surface. To measure the *true* (non-projected) direction of the source, each FGS has two Koesters prisms oriented perpendicular to one another (and therefore a total of 4 PMTs).

Figure 2.2: Light Path from Koesters Prisms to the PMTs

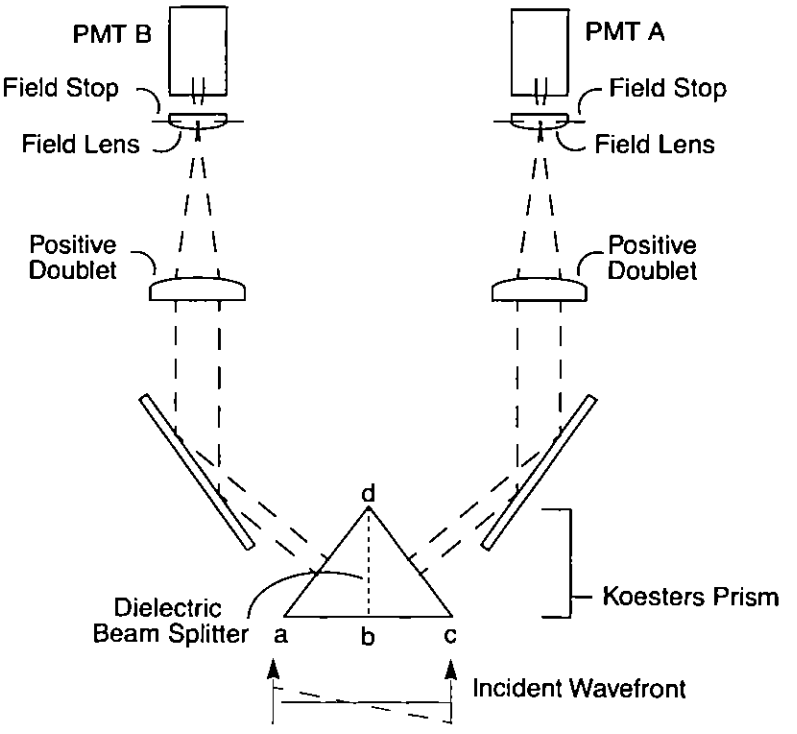

Small rotations of the star selector A and B assemblies alter the direction of the target's collimated beam, and hence the tilt of the incident wavefront with respect to the Koesters prisms. Figure 2.3 on page 16 is a simplified illustration of Koesters prism interferometry. As the wavefront rotates about point b, the relative phase of the transmitted and reflected

beams change as a function of angle α. When the wavefront's propagation vector is parallel to the plane of the dielectric surface (b-d) a condition of *interferometric null* results, and the relative intensities of the two emergent beams will ideally be equal. When α is not zero, the intensities of the left and right output beams will be unequal and the PMTs will record different photon counts.

Figure 2.3: The Koesters Prism: Constructive and Destructive Interference.

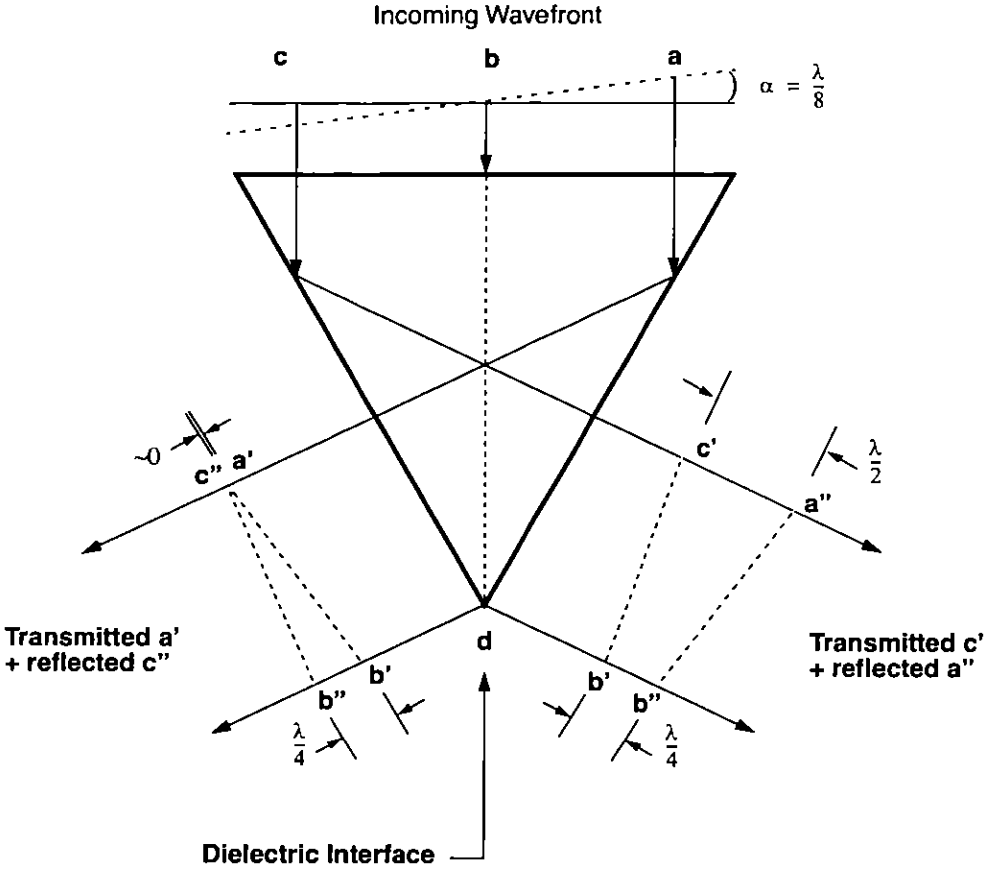

This case shows the interference within the Koesters Prism for a wavefront with a tilt α such that the ray entering the prism at point *a* is advanced by λ/4 with respect to the ray entering at point *c*. The rays *a'* and *c'* are transmitted though the dielectric surface and are retarded by λ/4 in the process. Rays *c"* and *a"* are reflected by the dielectric and suffer no change in phase. Rays *c'* and *a"* are interferometrically recombined and exit the prism on the right hand side. Similarly, rays *a'* and *c"* are recombined and exit to the left. The intensity of each exit ray depends upon the phase difference of recombined reflected and transmitted rays.

The rays exiting the prism at its apex will always consist of components with 90 degree phase difference (because the reflected and transmitted components initially had zero phase difference, but the dielectric retarded the transmitted wave by λ/4). Therefore, at the apex, constructive and destructive interference occur at the same rate and the two exit rays have equal intensity. In the example shown here, the intensity of the rays exiting the left face of the prism increases as one moves along the face, away from the apex, in the direction of increasing constructive interference (the recombined beams *a'* and *c"* have zero phase difference). On the right face of the prism, destructive interference increases away from the apex (*a"* and *c'* are out of phase by 180 deg), so the intensity of these rays diminishes along the face. Therefore the intensity of the left hand beam is greater than that of the right hand beam. The tilt α in this example corresponds to a peak of the S-curve. Rotating the wavefront about point *b* by 2α in a clockwise direction would produce the other peak of the S-curve.

FGS Detectors

The FGS PMTs (four per FGS) are end-illuminated, 13 stage venetian blind dynode S-20 photon-counting detectors with an effective photocathode area of about 4 mm. The A and B channels for each FGS interferometric axis operate independently. The PMTs are sensitive over a bandpass of 4000-7000A, with an efficiency of ~ 18% at the blue and diminishing linearly to about 2% at the red end.

The FGS1r dark counts for each channel are given in Table 2.1 on page 17.

Table 2.1: FGS1r Dark Counts

PMT	counts/second[a]	stdev
A_X	240	±72
B_X	134	±43
A_Y	200	±59
B_Y	300	±72

a. Values based on an average of 40Hz PMT counts and associated standard deviations.

HST's Spherical Aberration

The interferometric response of the Koesters prism arises from the difference in optical path lengths of photons entering one side of the prism to those entering the other side (and therefore to the tilt of the wavefront). A photon transmitted by the dielectric surface within the prism is re-combined with one which has been reflected by the surface. Both of these photons were incident on the prism's entrance face at points equidistant from, but on opposite sides of, the dielectric surface. The degree to which they constructively or destructively interfere depends solely on their difference in phase, which by design, should depend only upon the wavefront tilt. Any optical aberration in the incident beam that does not alter the phase difference of the recombining beams will not affect the interferometric performance of the FGS. Such aberrations are considered to be *symmetric*.

No correction for the HST's spherical aberration is incorporated in the original or refurbished FGSs. Though the Koesters prisms are not sensitive to symmetric aberrations (e.g., spherical aberration), small misalignments in the internal FGS optical train shift the location of the beam's axis of tilt ("b" in Figure 2.2 on page 14 and in Figure 2.3 on page 16) effectively

breaking the symmetry of the OTA's spherical aberration. This introduces an error in the phase difference of the re-combining photons and degrades the interferometric response.

With HST's 0.23 microns of spherical aberration, a decentering of the wavefront by only 0.25 mm will decrease the modulation of the S-Curve to 75% of its perfectly aligned value. If the telescope were not spherically aberrated (i.e., if the wavefront were planar) misalignments up to five times this size would hardly be noticeable. The impact of HST spherical aberration and the improved performance of FGS1r are discussed in the next sections.

The FGS Interferometric Response

FGS interferometry relates the *wavefront tilt* to the normalized difference of intensity between the two beams emerging from the Koesters prism (see Figure 2.3 on page 16). As the tilt varies over small angles (as when the IFOV scans the target), this normalized intensity difference defines the interferogram, or "S-Curve", given by the relation,

$$S_x = (A_x - B_x) / (A_x + B_x),$$

where A_x and B_x are the photon counts from PMT_{XA} and PMT_{XB} respectively accumulated over 25 milliseconds intervals when the IFOV is at location x. The Y-axis S-Curve is defined in an analogous manner. Figure 1.1 on page 6 shows an S-Curve resulting from several co-added scans of a point source.

Because the FGS is a white light, broad bandpass interferometer, its S-Curve is essentially a single fringe interferogram. The spectral incoherence of white light causes the higher order fringes to be strongly damped. Because the S-Curve is a normalized function, its amplitude is not sensitive to the target's magnitude provided the background and dark contributions to the input beam are relatively small. However, as fainter targets are observed (i.e., $V \geq 14.5$), the S-Curve's amplitude will be reduced (background and dark counts contributions are not coherent with light from the target). Usually the effect of dark + background is easily calibrated and therefore does not compromise the instrument's scientific performance in either Position or Transfer Mode.

The Ideal S-Curve

The intensity of each beam exiting the Koesters prism is the integral of the intensity of each ray along the entire half-face of the prism. When the IFOV is more than 100 milliarcseconds (mas) from the location of the interferometric null, the PMTs of a given channel record nearly equal

intensities since the re-combining beams are essentially incoherent over such large optical path differences (the photons constructively and destructively interfere at approximately the same rate). Closer to the interferometric null (at about +/- 40 mas from the null), a signal emerges as the Koesters prism produces exit beams of different relative intensities.

Maximum fringe visibility of the ideal S-Curve min/max extremas is 0.7, occurring at about –20 and +20 mas for the positive and negative fringe maxima, respectively. Thus the "peak-to-peak" amplitude is 1.4. An ideal S-curve is inverse symmetric about the central "zero point crossing". This crossing occurs when the wavefront's propagation vector is normal to the Koesters prism entrance face, a condition referred to as interferometric null (jargon derived from guide star tracking or Position Mode observing for when a target's fine error signal has been nulled out).

Actual S-Curves

HST's Spherical Aberration

The characteristics of real S-Curves depend on several factors: the quality and fabrication of the internal optics, the relative sensitivity of the PMTs, the alignment of the internal optics, the filter in use, the color of the target, and the effect of the spherically aberrated HST primary mirror. Some of the effects can be removed during processing and calibration, while others limit the performance of the instrument.

Referring back to Figure 2.3 on page 16, if the tilt axis is of the incident beam is not at point 'b,' the beam is said to be *decentered* with respect to the Koesters prism. Given the presence of spherical aberration from the HST's misfigured primary mirror, the wavefront presented to the Koesters prism is not flat but has curvature. This greatly amplifies the effects of misalignments in the FGS optical train. A decentered spherically aberrated beam introduces a phase error between the re-combining transmitted and reflected beams, resulting in degraded S-Curve characteristics. The interferometric response (in filter F583W) of the 3 original FGSs are shown in Figure 2.4 on page 20. Decenter emerges as morphological deformations and reduced modulation of the fringes. Of the original three FGSs, FGS3 was the only instrument with sufficient fringe visibility to perform as an astrometric science instrument.

Figure 2.4: Full Aperture S-Curves of the Original FGSs

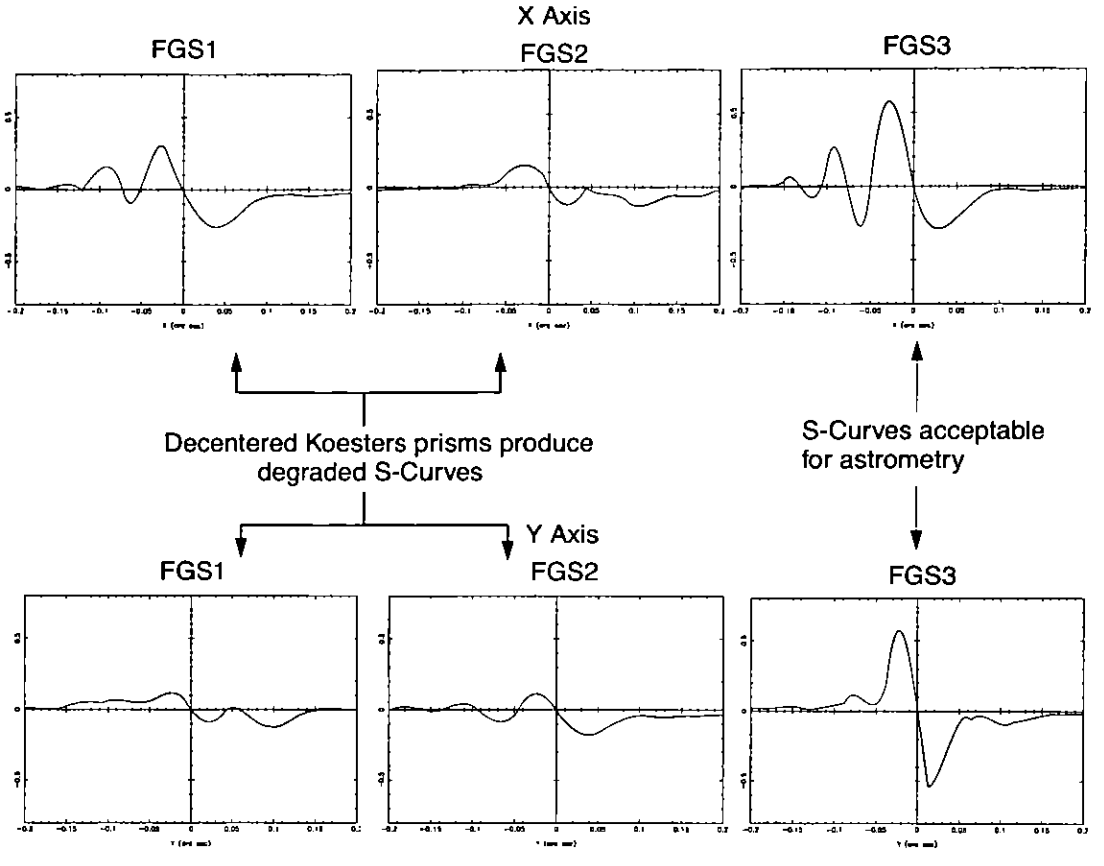

The degrading effects due to the misalignment of an FGS with the spherically aberrated OTA can be reduced by masking out the outer perimeter of the HST primary mirror. This eliminates the photons with the largest phase error. The 2/3 PUPIL stop accomplishes this and restores the S-Curves to a level which allows the FGS to track guide stars anywhere in the FOV. Unfortunately, it also blocks 50% of the target's photons, so nearly a magnitude of the HST Guide Star Catalog is lost. Figure 2.5 on page 21 shows the improvement of the S-Curve signature with the 2/3 PUPIL in place relative to the full aperture for the three FGSs. The PUPIL has been used for HST guiding since launch.

Figure 2.5: Improved S-Curves for Original FGSs when Pupil is in Place

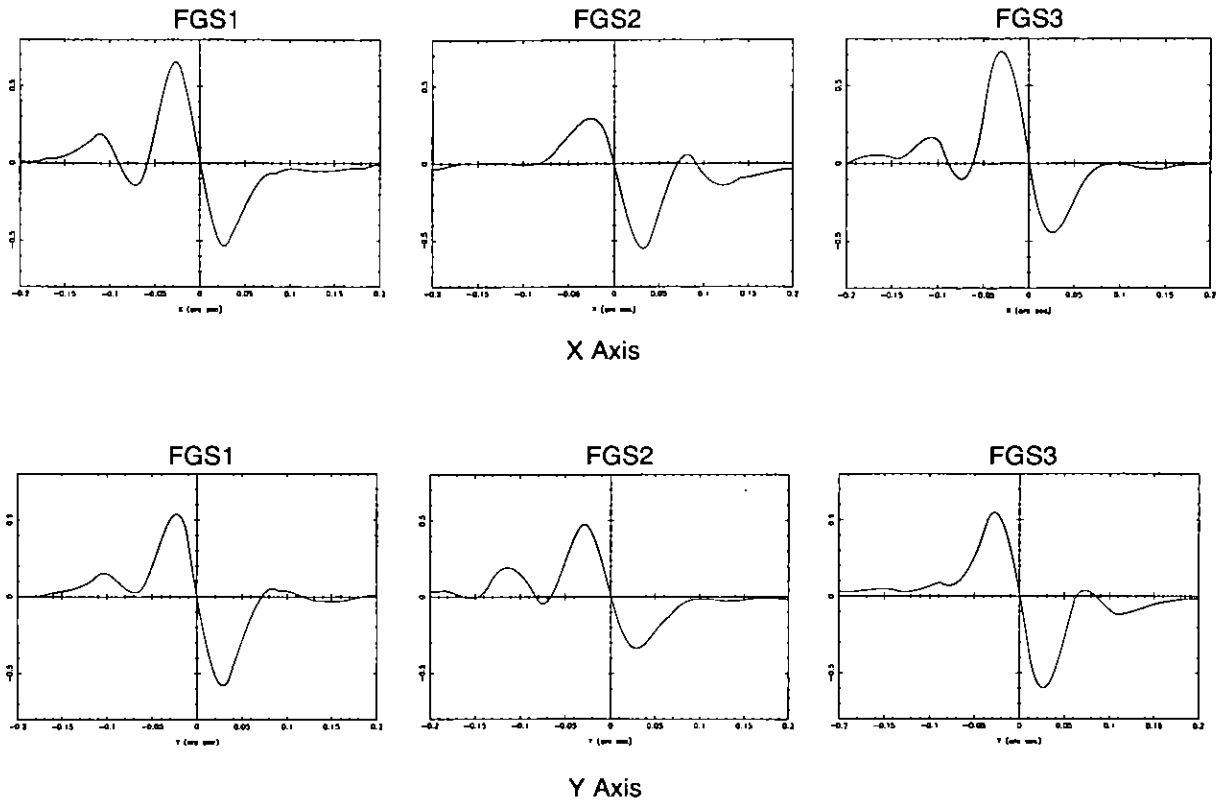

Field Dependence and Temporal Stability of the S-Curves

The Star Selectors center the beam on the face of the Koesters prisms while varying the tilt of the wavefront. Errors in the alignment of either the SSA or SSB with respect to the Koesters prisms will decenter the beam on the face of the prisms. Since the servos rotate over large sky angles to bring the IFOV to different positions in the Field of View, misalignments of these elements result in field-dependent S-curves. For this reason, Transfer Mode observations should be restricted to the center of the FGS FOV, the only location supported by observatory calibrations.

The S-Curve measurements in the original three FGSs indicated large decenters of the Koesters prisms in FGS1 and FGS2 and field dependency in FGS3. FGS1r also shows field dependence, as can be seen for three positions across the FGS1r FOV in Figure 2.6 on page 22 (however, note that its x,y fringes are near ideal at the FOV center).

Temporal stability of S-Curves is also a concern. Monitoring of the FGS3 S-Curves along the X-axis showed the instrument suffered from variability of such amplitude that it could not be used to reliably resolve binary systems with projected X-axis separations less than ~ 20 mas. Conversely, FGS1r is far more stable. Its interferometric fringes show

much less temporal variation, allowing the observer to confidently distinguish the difference between a point-source and a binary star system with a separation of 8 mas. This, in part, prompted the switch to FGS1r as the Astrometer for Cycle 8 and beyond.

Figure 2.6: FGS1r S-Curves in Full Aperture Across the Pickle

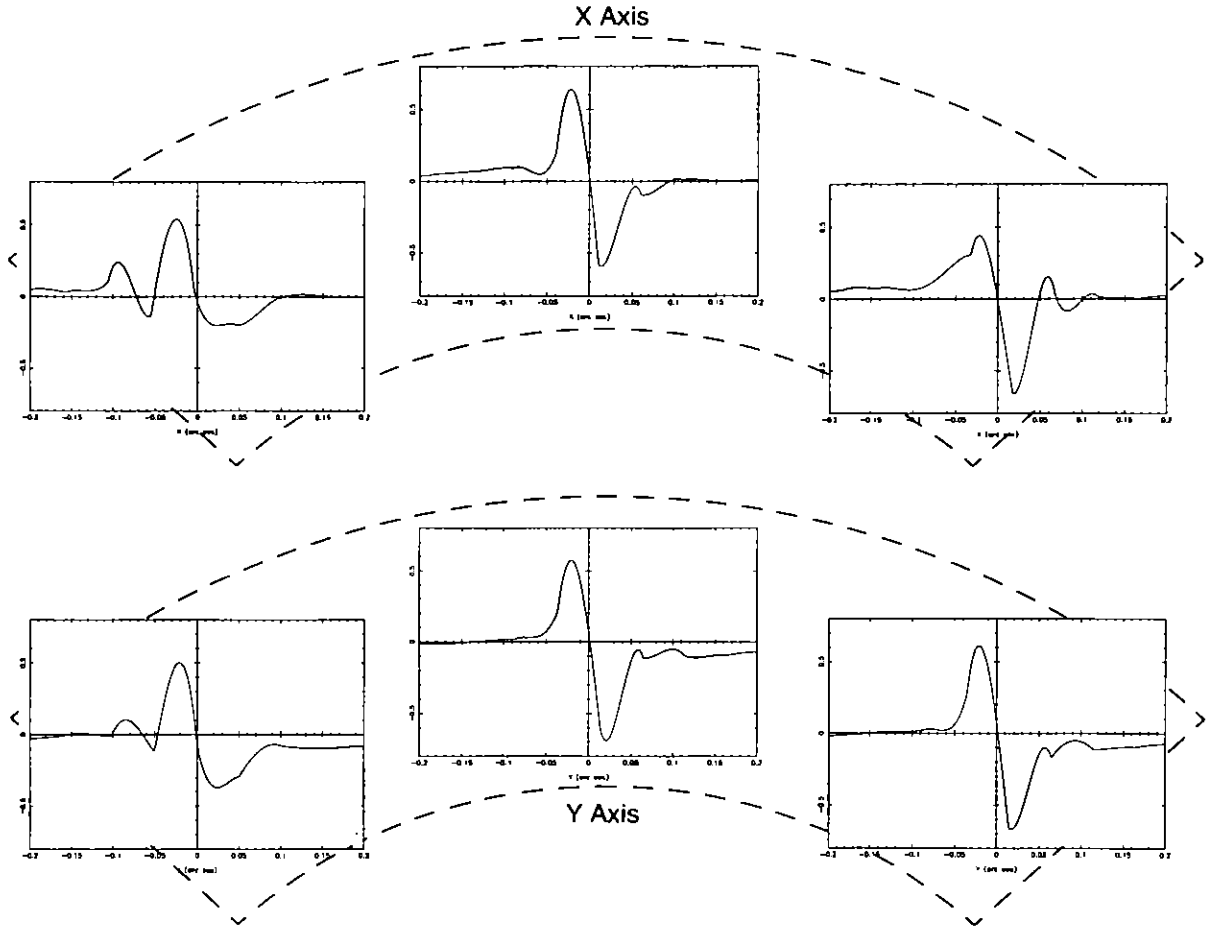

The FGS1r Articulated Mirror Assembly

FGS1r has been improved over the original FGS design by the insertion of the articulating mirror assembly (AMA) designed and built by Raytheon (formerly Hughes Danbury Optical Systems, currently BFGoodrich Space Flight Systems). A static fold flat mirror (FF3 in Figure 2.1 on page 13) in FGS1r was mounted on a mechanism capable of tip/tilt articulation. This Articulating Mirror Assembly (AMA) allows for in-orbit re-alignment of

the wavefront at the face of the Koesters prism. An adjustable AMA has proven to be an important capability since, given HST's spherical aberration, even a small misalignment degrades the interferometric performance of the FGS. On orbit testing and adjustment of the AMA were completed during FGS1r's first year in orbit. A high angular resolution performance test executed in May 1998 demonstrated the superiority of FGS1r over FGS3 as a science instrument. Therefore, FGS1r has been designated the Astrometer and has replaced FGS3 in this capacity. Information on the FGS1r calibration program can be found in Chapter 5 of this handbook.

The AMA has been adjusted to yield near-perfect S-Curves at the center of the FGS1r FOV, and an optimum compromise results for the remainder of the FOV. The variation of S-Curve characteristics across the FOV arises from "beam walk" at the Koesters prisms as the star selectors rotate to bring the IFOV to different locations in the FGS FOV. This field dependence does not necessarily impair FGS1r's performance as a science instrument, but it does restrict Transfer Mode observations to the center of the FOV since it is the only location calibrated for that mode (Position Mode is calibrated for the entire FOV).

FGS Aperture and Filters

FOV and Detector Coordinates

Figure 1.2 on page 7 shows the HST focal plane positions of the FGSs as projected onto the sky. Figure 2.7 on page 25 is similar, but includes the addition of two sets of axes: the FGS detector coordinate axes, and the POSTARG coordinate axes (used in the Phase II proposal instructions to express target offsets).

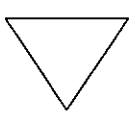

The detector reference frame and the POS TARG reference frames differ from each other and from the Vehicle Coordinates V2,V3 (or U2,U3).

Each FGS FOV covers approximately 69 square arcmin, extending radially from 10 arcmin to 14 arcmin from the HST's boresight and axially 83.3 degrees on the inner arc and 85 on its outer arc. The IFOV determined by the star selector assemblies and field stops is far smaller, covering only 5 x 5 arcsec. Its location within the pickle depends upon the Star Selector A and B rotation angles. To observe stars, the star selector assemblies must be

rotated to bring the IFOV to the target. This procedure is called *slewing* the IFOV.

The (X,Y) location of the IFOV in the pickle is calculated from the Star Selector Encoder Angles using calibrated transformation coefficients. Each FGS has its own detector space coordinate system, the $(X,Y)_{DET}$ axes, as shown in Figure 2.7. FGS2 and FGS3 are nominally oriented at 90 and 180 degrees with respect to FGS1r, but small angular deviations are present (accounted for in flight software control and data reduction processing). The FGS detector reference frame is used throughout the pipeline processing. The POS TARG coordinate axes, $(X,Y)_{POS}$, should be used to express offsets to target positions in the Phase II proposal (Special Requirements column). See Chapter 5: Writing a Phase II Proposal for more details.

The *approximate* U2,U3 coordinates for the aperture reference position (default placement of a target) for each FGS and the angle from the +U3 axis to the $+Y_{DET}$ and $+Y_{POS}$ Axis are given in Table 2.2 on page 24. The angles are measured from +U3 to +Y in the direction of +U2 (or counterclockwise in Figure 2.7). Note that the FGS internal detector coordinate reference frame and the POS TARG reference frame have opposite parities along their respective X-axes.

Table 2.2: Approximate Reference Positions of each FGS in the HST Focal Plane

Aperture	U2 (arcsec)	U3 (arcsec)	Angle (from +U3 axis)
FGS1r	-723	+10	~270
FGS2r	0	+729	~0
FGS3	+726	+6	~90

Figure 2.7: FGS Proposal System and Detector Coordinate Frames

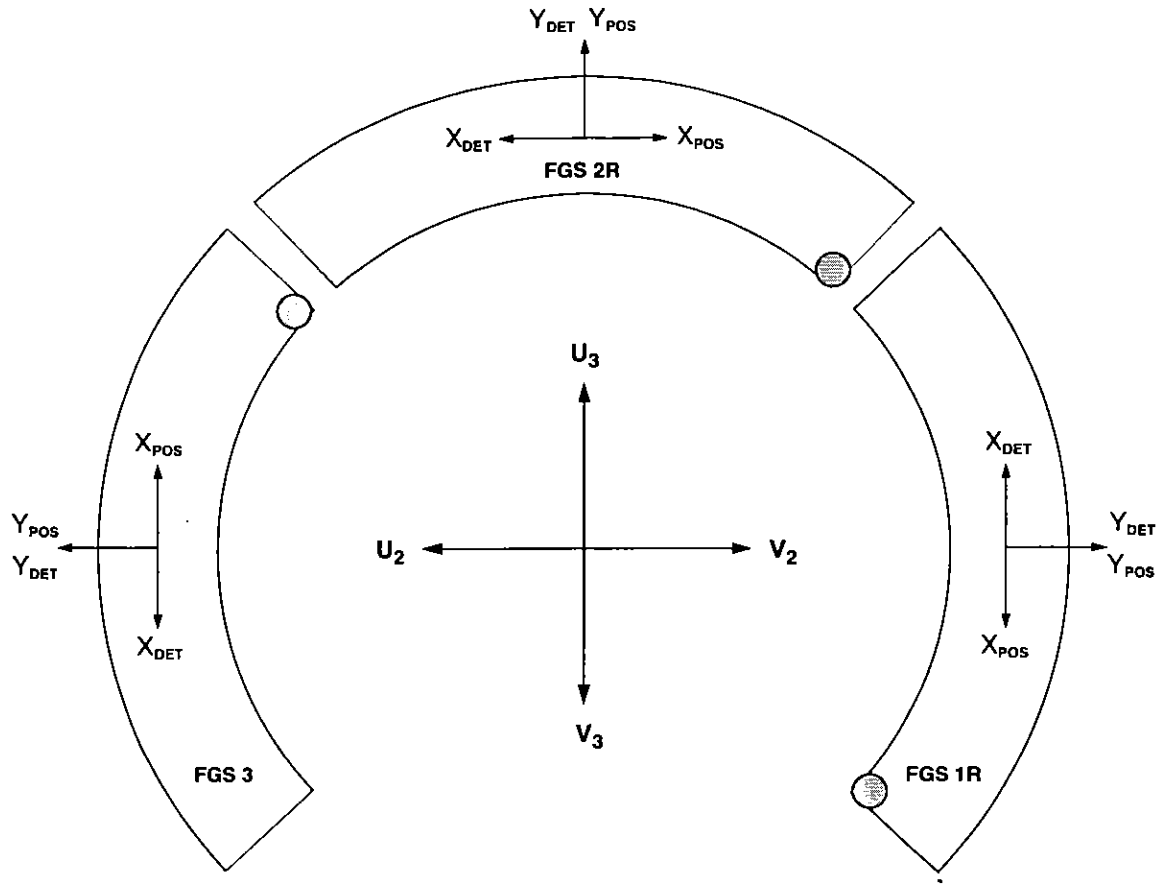

Filters and Spectral Coverage

Filter Bandpasses

The filter wheel preceding the dielectric beam splitter in each FGS contains five 42mm diameter slots. Four of these slots house filters—F550W, F583W, F605W and F5ND—while the fifth slot houses the PUPIL stop. This stop helps restore the S-Curve morphology throughout the FOV of each FGS by blocking out the outer 1/3 perimeter of the spherically aberrated primary mirror. The filter selection for each FGS, their central wavelengths, and widths are listed in Table 2.3 on page 26. The transmission curves (filters and PUPIL) are given in Figure 2.8. The PMT efficiency is given in Figure 2.9 on page 27.

Figure 2.8: FGS1r Filter Transmission

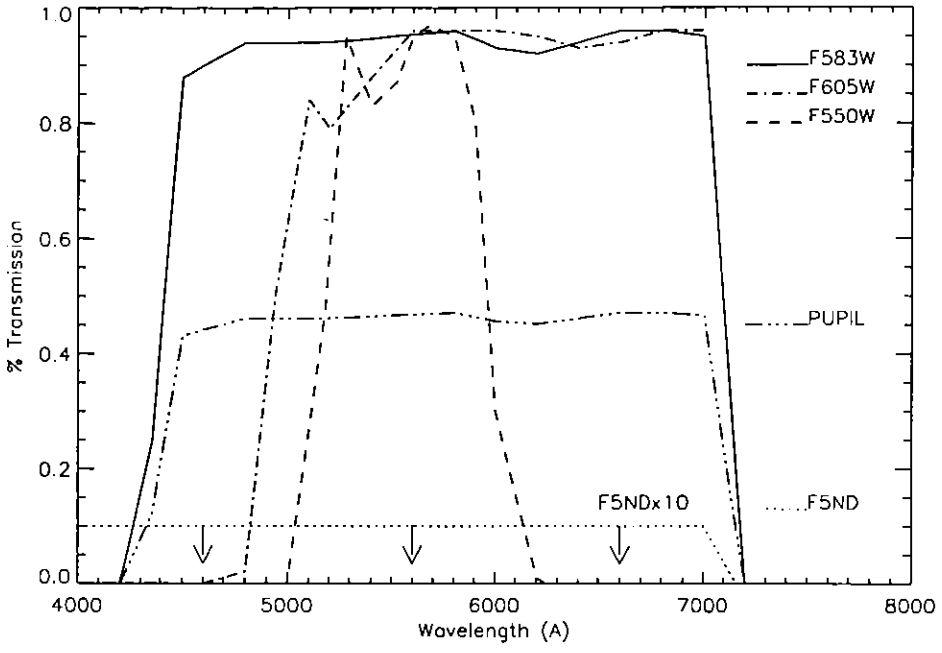

Table 2.3: Available Filters

Filter	Central Wavelength Å	Spectral Range Å	FWHM Å	FGS
F583W	5830	4600–7000	2340	1,1R,2,3
F605W	6050	4800–7000	1900	1,1R,2
PUPIL	5830	4600–7000	2340	1,1R,2,3
F550W	5500	5100–5875	750	1,1R,2,3
F650W	6500	6200–6900	750	3
F5ND	5830	4600–7000	2340	1,1R,2,3

Figure 2.9: PMT Efficiency

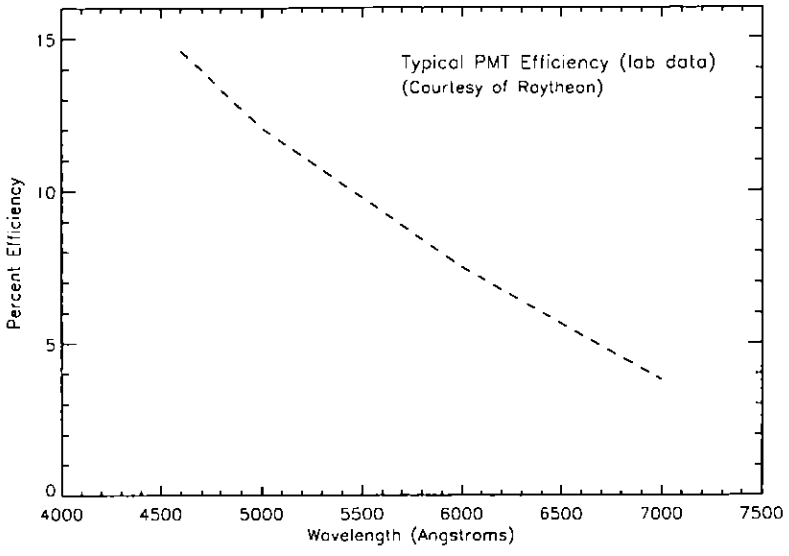

FGS Calibrations

For the most part, the calibration requirements of the current Cycle's GO science programs will be supported by STScI. For Position Mode observations, this includes the optical field angle distortion (OFAD) calibration, cross-filter effects, lateral color effects, and the routine monitoring of the changes in distortion and scale across the FOV.

For Transfer Mode, STScI will calibrate the interferograms (S-Curves) as a function of a star's spectral color. In addition, the S-Curves will be monitored for temporal stability.

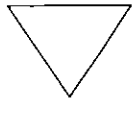

Only the center of the FGS1r FOV will be calibrated for Transfer Mode observations.

CHAPTER 3:

FGS Science Guide

In this chapter . . .

The Unique Capabilities of the FGS / 29
Position Mode: Precision Astrometry / 30
Transfer Mode: Binary Stars and Extended Objects / 31
Combining FGS Modes: Determining Stellar Masses / 35
Angular Diameters / 36
Relative Photometry / 37
Moving Target Observations / 39
Summary of FGS Performance / 39
Special Topics Bibliography / 40

This chapter serves as a brief guide to the scientific programs which most effectively exploit the FGS's capabilities. The advantages offered by the FGS are described in this chapter. A representative list of publications making use of FGS science and calibration data is included. Suitable strategies to achieve scientific objectives are outlined in Chapter 4.

The Unique Capabilities of the FGS

As a science instrument the FGS offers unique capabilities not presently available by other means in space or on the ground. Its unique design and ability to sample large areas of the sky with milliarcescond (mas) accuracy or better gives the FGS advantages over all current or planned interferometers.

The FGS has two observing modes, Position and Transfer mode. In Position mode the FGS measures the relative positions of luminous objects within its Field of View (FOV) with a *per-observation* accuracy of ~ 1 mas

for targets with $3.0 < V < 16.8$. Multi-epoch programs can achieve relative astrometric measurements with accuracies approaching to 0.2 mas.

In Transfer Mode the FGS is used as a high angular resolution observer, able to detect structure on scales as small as 8 mas. It can measure the separation (with ~1 mas accuracy), position angle, and the relative brightness of the components of a binary system down to ~10 mas for cases where $\Delta V < 1.5$. For systems with a component magnitude difference of $2.0 < \Delta m < 4.0$, the resolution is limited to 20 mas.

By using a "combined mode" observing strategy, employing both Position Mode (for parallax, proper motion, and reflex motion) and Transfer Mode (for determination of a binary's visual orbit and relative brightnesses of the components), it is possible to derive the total and fractional masses of a binary system, and thus the mass-luminosity relationship for the components.

Alternatively, if a double lined spectroscopic system is resolvable by the FGS, then the combination of radial velocity data with Transfer Mode observations can yield the system's parallax and therefore the physical size of the orbit, along with the absolute mass and luminosity of each component.

In this chapter, we offer a brief discussion of some of the science topics most conducive to investigation with the FGS.

Position Mode: Precision Astrometry

A Position Mode visit consists of sequentially measuring the positions of stars in the FGS FOV while maintaining a fixed HST pointing. This is accomplished by slewing the FGS Instantaneous Field of View (IFOV, see Figure 1.3 on page 8) from star to star in the reference field. acquiring each in FineLock (fringe tracking) for a short time (2 to 100 sec). This yields the relative positions of the observed stars to a precision of ~1 milliarcsecond (mas).

With only three epochs of observations at times of maximum parallax factor (a total of six HST orbits), the FGS can measure an object's relative parallax and proper motion with an accuracy of about 0.5 mas. Several multi-epoch observing programs have resulted in measurements accurate to ~0.2 mas. Unlike techniques which rely upon photometric centroids, the accuracy of FGS measurements are not degraded when observing variable stars or binary systems. And techniques which must accumulate data over several parallactic epochs would have greater difficulty detecting comparably high frequency reflex motions (if present).

Transfer Mode: Binary Stars and Extended Objects

In Transfer Mode, the FGS scans its IFOV across a target to generate a time-tagged (40 hz) mapping between the position of the IFOV (in both X and Y) and counts in the four PMTs. These data are used to construct the interferogram, or transfer function, of the target via the relation

$$S_x = (A_x - B_x) / (A_x + B_x)$$

as described in chapter 2. The data from multiple scans are cross correlated and co-added to obtain a high SNR transfer function.

In essence, Transfer Mode observing is conceptually equivalent to sampling an object's PSF with milliarcsecond pixels. This enables the FGS to resolve structure on scales finer than HST's diffraction limit, making it ideal for studying close binary systems and/or extended objects.

The transfer function of a multiple star system is a normalized linear superposition of the S-Curves of the individual stars, with each S-curve scaled and shifted by the relative brightness and angular separation of the components. If the components are widely separated (> ~60 mas), two S-Curves are clearly observed in the transfer function, as illustrated in the left panel of Figure 3.1. Smaller separations result in merged S-Curves with modulation and morphology differing significantly from that of a single star. Figure 4.3 on page 56 illustrates these points.

By using point source S-curves from the calibration library one can deconvolve the composite observed transfer function of a binary star into component S-Curves (done by either Fourier Transforms or semi-automated model fitting) to determine the separation, position angle, and relative brightness of the components. If enough epochs of data are available, the time-tagged position angles and angular separations can be used to construct the apparent relative orbit, from which one can derive the parameters P, a, i, ω and Ω which define the true relative orbit. Note that the semi-major axis is an angular quantity; to convert it to a physical length, one must know the object's distance (which can be obtained from parallax measurements).

Observing Binaries: The FGS vs. WFPC2

The FGS, while capable of very-high angular resolution observations, is not an "imaging" instrument like HST's cameras. However, the ability to sample the S-curve with milliarcsecond resolution allows the FGS to resolve structure on scales too fine for the cameras. To illustrate, we present a comparison between binary observations with HST's Planetary Camera (PC) and with FGS1r in Figure 3.1. The image at left is a PC snapshot image of the Wolf-Rayet + OB binary WR 146 (Niemela et al. 1998). To the right is a simulated FGS1r "image" of this binary shown at the same

scale. With the 0.042" pixels of the PC, the binary pair is clearly resolved. Based on point-spread function (PSF) photometry, Niemela et al. publish a separation of 168 ±31 mas for this pair. In comparison, an analysis of the FGS "observation" of the binary yields a separation of 168 ±1 mas, a far more accurate result.

Figure 3.1: Comparison: PC Observation v. FGS Observation

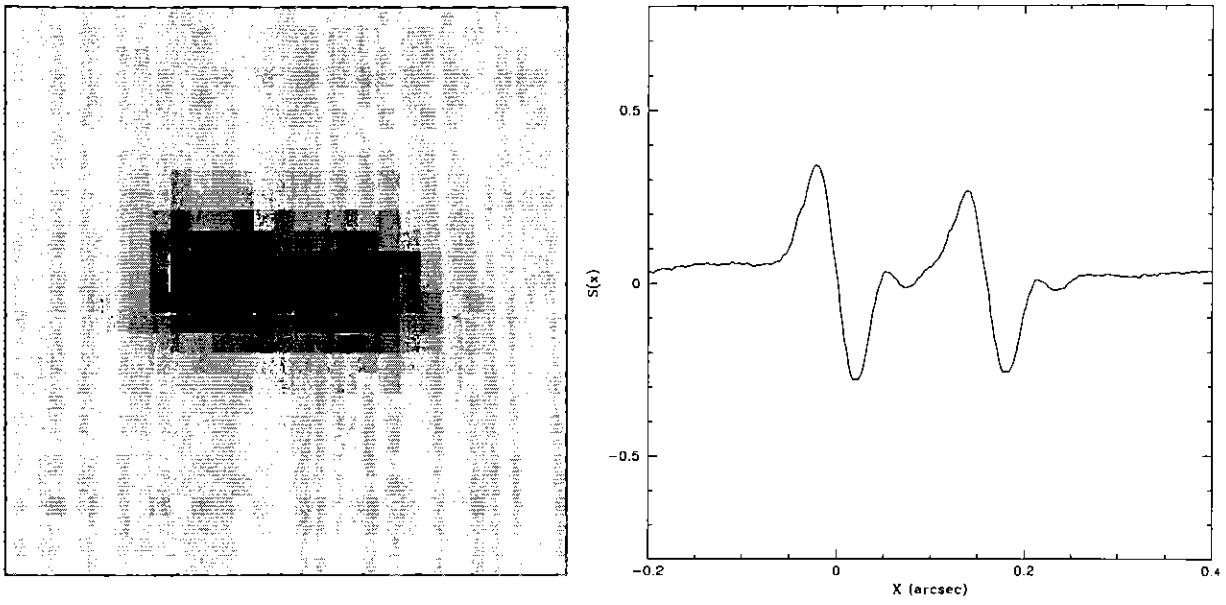

Though a vigorous PC observing strategy involving multiple exposures and image recombination techniques (i.e, "drizzling") might improve the resolution of the binary, the accuracy of the measured separation would not match that achievable with the FGS. In addition, the total exposure time of such a PC program might exceed that of the FGS observation. Most importantly, the FGS can *just as easily detect the components and accurately measure their separations for binaries as close as 20 mas*, a feat not possible with HST's cameras regardless of the observing strategy.

In Figure 3.2, we show a TinyTIM simulation of a PC image of a 70 mas binary and an FGS observation of the same simulated pair. Note the PC image suggests - by it's shape - that the observed binary is not a point source. However, it would be difficult to determine an accurate component separation or brightness ratio from this image. This is not a problem for the FGS, where both components are easily resolved, and an accurate separation and mass ratio can be determined.

Figure 3.2: Simulated PC Observations v. FGS Observations of a 70mas Binary

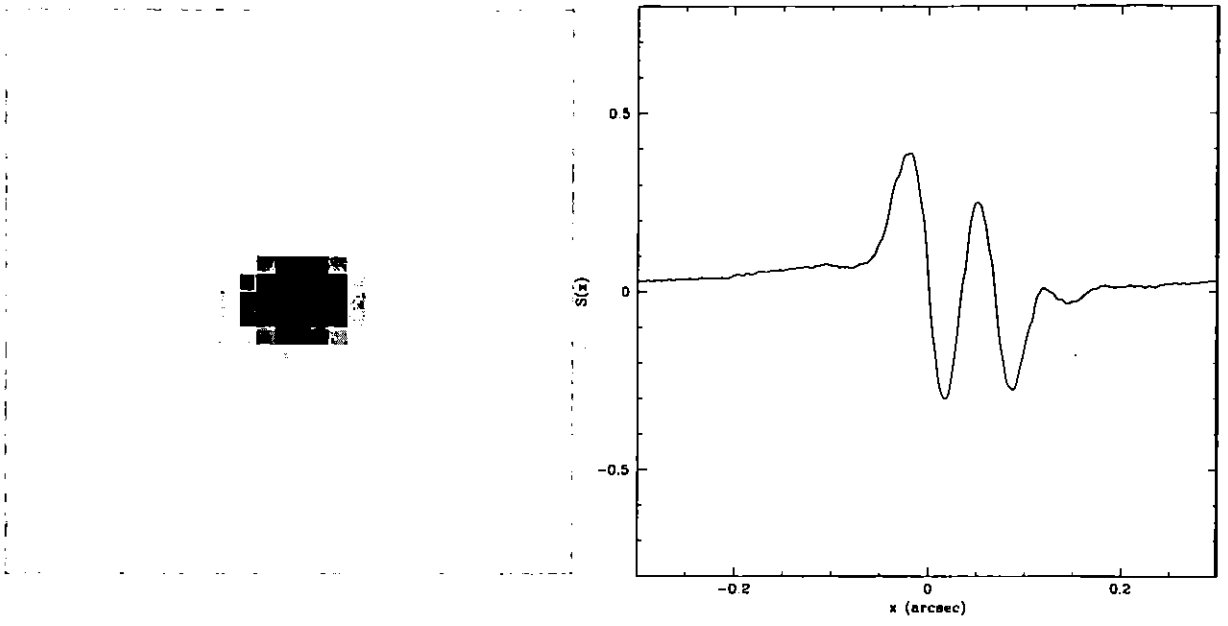

Transfer Mode Performance

The most relevant way to express the FGS Transfer Mode performance is through its ability to detect and to resolve components of a multiple component system. Figure 3.3 on page 34 is a plot of the *predicted* parameter space defined by the separation in milliarcseconds and the relative brightness of the components of a binary system. The shaded areas are the domains of success in resolving binary systems for both FGS3 and FGS1r. The extension of FGS1r into the smaller separation parameter space is attributed to an optimized S-Curve achieved by proper adjustment of the articulating mirror assembly (see Chapter 2 for more details), and to the fact that its fringes are highly stable in time. (FGS3, by comparison, suffers a persistent random variability of its x-axis fringe which precludes it from reliably studying binary systems with separations less than about 20 mas.) These data originate from simulations and are supported by a special assessment test run aboard the spacecraft in May 1998 as well as GO science data (see Appendix 2 for more details).

Figure 3.3: Comparison of FGS1r and FGS3 Transfer Mode Performance

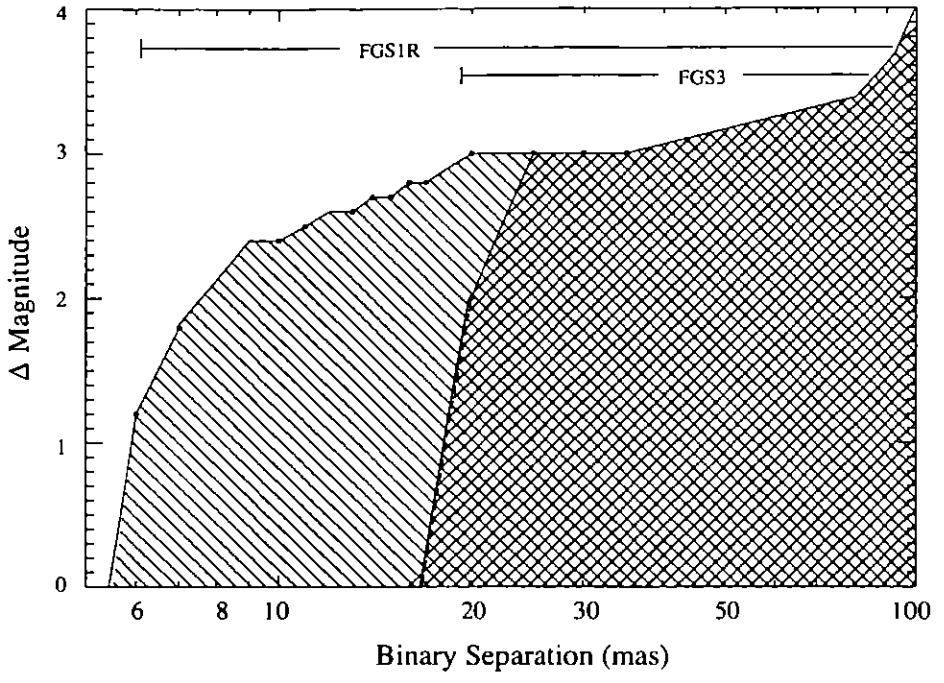

Table 3.1 on page 34 contains the expected resolution limits for FGS1r. Columns 1 and 2 show the separation and accuracy for a single measurement, column 3 details the relative brightness limit needed to achieve that precision, and the last column is the total apparent magnitude of the system. The table should be read in the following way: a separation of 10 mas is measurable if the system is 13.0 magnitudes or brighter and the magnitude difference of the components (Δm) is less than 1.0. For the same separation, as the magnitude difference increases, the apparent magnitude of the system must decrease.

Table 3.1: FGS1r TRANSFER Mode Performance: Binary Star

Separation (mas)	Estimated Accuracy (mas)	ΔMag	V
7[a]	-	1.0	13.0
10	1	1.0	13.0
15	2	2.0	14.5
20	1	2.5	13.0
20	3	3.0	15.0
50	2	3.5	15.0

a. This represents detection of non-singularity. Reliable measurements of the angular separation might not be achievable. Check the web pages for updates.

Combining FGS Modes: Determining Stellar Masses

Stellar mass determination is essential for many astronomical studies: star formation, stellar evolution, calibrating the mass/luminosity function, determining the incidence of stellar duplicity, and the identification of the low-mass end of the main sequence, for example.

The *combination* of Position Mode *and* Transfer Mode observations is an effective means to derive a full orbital solution of a binary system. Wide-angle astrometry from a multi-epoch Position Mode program can be used to measure the parallax, proper motion and reflex motion of a binary system. High angular resolution Transfer Mode observations can be used to determine the relative orbit and differential photometry of the components. Figure 3.4 on page 36 illustrates the benefit of this technique as applied to the low mass binary system Wolf 1062 (Benedict et al. 2001). The small inner orbit of the primary star was determined from Position Mode measurements of the primary's position relative to reference field stars. The large orbit of the secondary low mass companion was derived from Transfer Mode observations of the binary, which at each epoch yields the system separation and position angle. Combining these data allows one to locate the system barycenter and thereby compute the relative mass of each component. And with the parallax known (from the Position Mode data), the total system mass, and hence the mass of each component, can be determined.

Figure 3.4: Relative Orbit of the Low-Mass Binary System Wolf 1062 AB

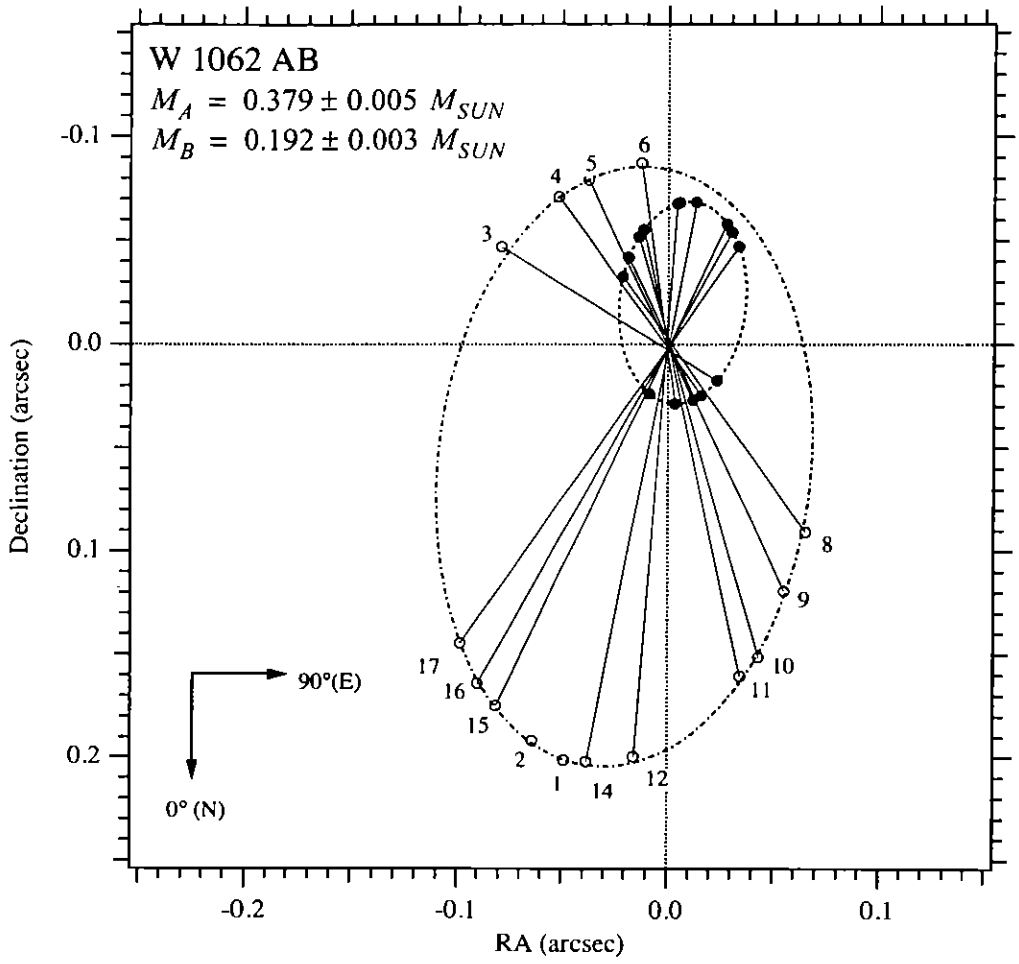

Figure courtesy of G. Fritz Benedict, University of Texas at Austin

Angular Diameters

The FGS has been used (Lattanzi et al. 1997) to determine the angular diameters of non-point sources. The example given in Figure 3.5 shows the Transfer Function of a Mira-type variable superposed on the S-Curve of a point source (both observed with FGS3). The extended source - a disk of 78±2 mas - is clearly distinguishable from a point source. In addition to stellar discs, other objects which might be (or have been) resolved by the FGS include galactic nuclei, asteroids, and planetary moons.

Figure 3.5: Mira-type variable with a resolved circumstellar disk

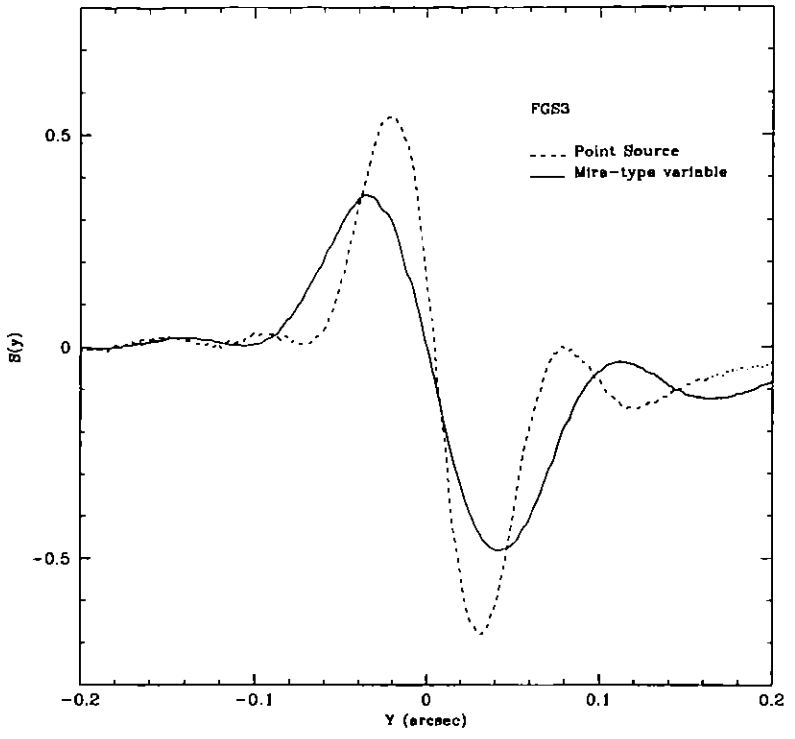

Relative Photometry

While observing in Position Mode, FGS3 serendipitously observed the outburst of a flare on the nearby star Proxima Centauri (Figure 3.6, see Benedict et al. 1998). The FGS has also been used to measure the relative flux of a star during an occultation of that star by the Neptunian moon Triton (Figure 3.7), and the data were subsequently used to examine the thermal structure of Triton's atmosphere (see Elliot et al. 1998 and Elliot et al. 2000).

The absolute FGS photometric response of FGS 3 has been stable at the 2% level over the past eight years (L. Reed, BFGoodrich). FGS1r is expected to be as stable or better. For relative photometry on time scales of orbits, the FGS has been shown to be stable at the 1 milli-magnitude level, thus affording an opportunity for 0.1–0.2% time series photometry.

Figure 3.6: Flare Outburst of Proxima Centauri as Observed with FGS3

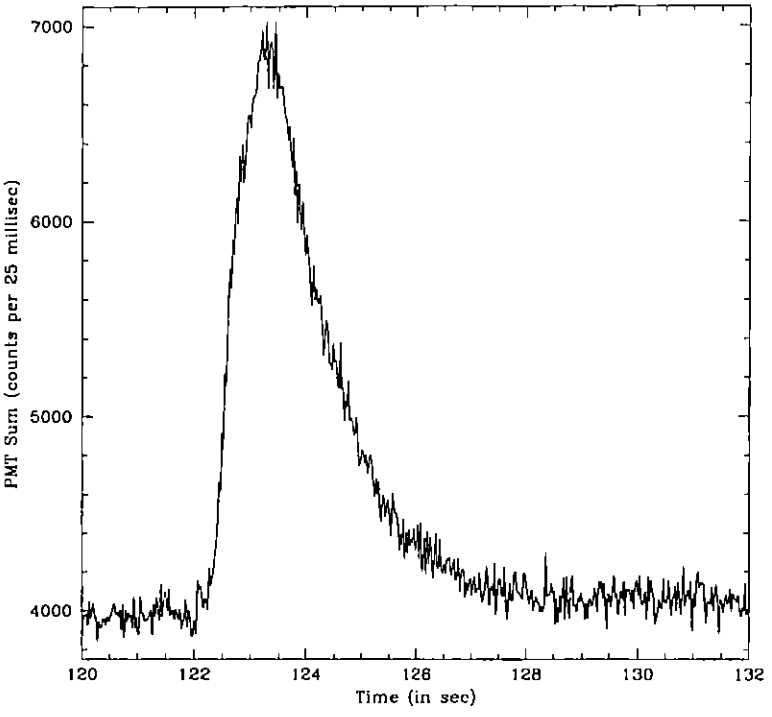

Figure 3.7: Triton Occultation of the Star TR180 as Observed by FGS 3

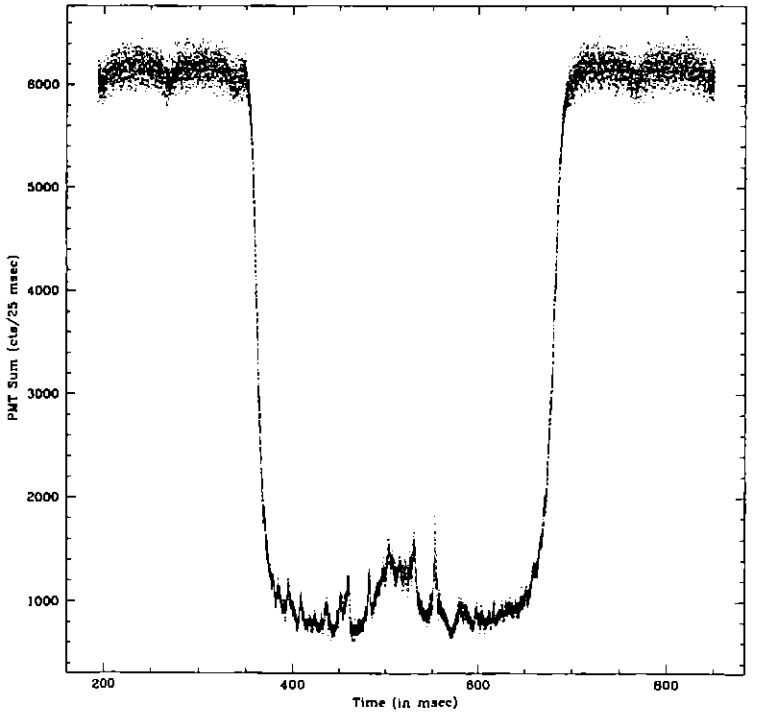

Moving Target Observations

The FGS is suitable for the observation of solar system objects in both Position and Transfer modes. The technique to acquire the data is not as straightforward as standard HST moving target observations, but in cases where the target is not moving too rapidly, the observation is certainly feasible. We note that the FGS has been used in previous Cycles to observe Main Belt asteroids, both in Position Mode and in Transfer Mode. More detail on moving target observations can be found in Chapter 4.

Summary of FGS Performance

In Position Mode, the FGS offers capabilities not achievable by other HST instrument or by the current generation of ground-based interferometers. These capabilities include:

- a large field of view (69 arcmin^2).
- large dynamic range.
- a *per-observation* precision of ~ 1 mas for V < 16.8.
- multi-epoch astrometry accurate to ~ 0.2 mas.

Similarly, the FGS Transfer Mode offers:

- 7 to 10 mas resolution down to V = 14.5, with wider separations observable to V = 16.8.
- the ability to determine relative separation and position angle of a binary system's components, and hence the apparent relative orbit of the system.

Additionally, mixed-mode observations - employing both Position Mode and Transfer Mode - allow the user to combine parallax, proper motion, and relative orbit information to derive the true orbit of a multiple-star system and a determination of stellar masses.

The FGS's two observing modes make it possible for the instrument to resolve structure in objects too faint for other interferometers and on scales too small for any imaging device, while simultaneously measuring the distance to that object. It is anticipated the FGS will be the sole occupant of this niche until the arrival of the long baseline interferometer in space, such as the Space Interferometry Mission (SIM), expected to launch in 2009.

Special Topics Bibliography

STScI General Publications

- Soderblom, D., ed. *Hubble Space Telescope Phase 2 Proposal Instructions for Cycle 10*, Version 10.0.2, STScI, 2001.
- Voit, M. ed. *HST Data Handbook*, Version 3.0 Volume I. STScI, 1997.

Position Mode Observations

- Benedict, G. F. et al., "Interferometric Astrometry of the Detached White Dwarf - M Dwarf Binary Feige 24 Using HST Fine Guidance Sensor 3: White Dwarf Radius and Component Mass Estimates", 2000, AJ, 119, 2382.
- McArthur, B. E. et al., "Astrometry with Hubble Space Telescope Fine Guidance Sensor 3: The Parallax of the Cataclysmic Variable RW Triangulum", 1999, *ApJ*, 520, L59.
- Harrison, Thomas E. et al., "Hubble Space Telescope Fine Guidance Sensor Astrometric Parallaxes for Three Dwarf Novae: SS Aurigae, SS Cygni, and U Geminorum", 1999, *ApJ*, 515, L93.

Transfer Mode Observations

- Benedict, G.F. et al., "Precise Masses for Wolf 1062 AB from Hubble Space Telescope Interferometric Astrometry and MCDonald Observatory Radial Velocities", 2001, *AJ*, 121.1607.
- Henry, T. J. et al., "The Luminosity Relation at the End of the Main Sequence (0.08 - 0.20 M_solar)",1999, *ApJ*, 512, 864.
- Gies, D. R. et al., "The O-type Binary 15 Monocerotis Nears Periastron," 1997, *ApJ*, 475, L49.
- Lattanzi, M.G., et al., "Interferometric Angular Diameters of Mira Variables with the Hubble Space Telescope", 1997, *ApJ*, 485, 328.
- Simon, M., S.T. Holfeltz, and L.G. Taff, "Measurement of T Tauri Binaries Using the Hubble Space Telescope Fine Guidance Sensors", 1996, *ApJ*, 469, 980.

Miscellaneous Observations

- Elliot, J. L. et al., "Global Warming on Triton," *Nature*, 393, 765, 1998.

Web Resources

Many additional documents, including Instrument Science Reports and ST Analysis Newsletters are available through the FGS web page:

`http://www.stsci.edu/instruments/fgs/`

CHAPTER 4:

Observing with the FGS

In this chapter . . .

Position Mode Overview / 43
Planning Position Mode Observations / 45
Position Mode Observing Strategies / 52
Transfer Mode Overview / 55
Planning a Transfer Mode Observation / 58
Transfer Mode Observing Strategies / 63

Position and Transfer Modes each have distinct calibration requirements and observing strategies. This chapter describes the detailed characteristics of the two observing modes and the observational configurations which maximize science return.

Position Mode Overview

The Position Mode Visit

A Position Mode *visit* yields measurements of the location of objects in the FGS's total field of view (FOV), and hence their relative angular positions. The objects are observed sequentially according to the sequence of exposure lines in the proposal. The target list of a typical Position Mode visit consists of the science object(s) and reference stars used to define the local reference frame. A subset of the targets, referred to as check stars, should be observed several times during the course of the visit to track any

spurious motion of the FGS's FOV on the plane of the sky (e.g., thermally induced drift or OTA focus changes). The changes in the positions of the check stars are used to model the drift as a function of time so that its contaminating effect can be eliminated from the astrometry.

An FGS astrometry visit begins when the HST computer - the 486 - commands the Star Selector Servos to place the IFOV at the predicted location of the first star specified in the visit (as per Phase II proposal). Control is transferred to the Fine Guidance Electronics (FGE) microprocessor, which commands the FGS to acquire and track the target (Search, CoarseTrack, and FineLock). Later, at a specific spacecraft clock time, after the exposure time + overhead has expired, the 486 resumes control of the FGS, terminates the FineLock tracking of the object and slews the IFOV to the expected location of the next star in the sequence. This process repeats until the FGS has completed all exposures in the visit. The spacecraft's pointing is held fixed on the sky under the control of the guiding FGSs for the entire visit unless otherwise instructed by the Phase II proposal. The status flags, photometry and instantaneous location of the IFOV is recorded every 25 msec (40 Hz).

The Position Mode Exposure

During a Position Mode exposure the object is tracked in FineLock (see Appendix I). After the target is acquired by the Search and CoarseTrack procedures, FineLock begins with a WalkDown, a series of steps of the IFOV toward the CoarseTrack photocenter. At each step, the IFOV is held fixed for a period defined by FESTIME (Fine Error Signal averaging time) while the PMT data are integrated to compute the Fine Error Signal (FES, the instantaneous value of the S-Curve) on each axis. Once the FES on both axes have exceeded a pre-set threshold, FineLock tracking begins. The star selectors are continuously adjusted after every FESTIME to re-position the IFOV in an attempt to zero out the FES during the next integration period. The objective is to present the Koesters prism a wavefront with zero tilt.

The defining parameters of an exposure are the target magnitude, the filter, the FESTIME and the exposure time. These topics are discussed in the following sections.

Planning Position Mode Observations

Target Selection Criteria

When targets are selected for FGS Position Mode observations, several options and requirements should be considered. These options are described below.

Brightness

The bright limit for FGS1r is V = 8.0 without the neutral density filter in place. With the F5ND filter, objects of V = 3.0 or fainter can be observed. The faint limit is V ~ 17.0.

Near Neighbors

FGS target acquisition in Position Mode will be unreliable if the target has a neighbor of comparable or greater brightness within a radius of 10 arcsec. In essence, the FGS's IFOV - a 5" x 5" box - expects to encounter the target star within the search radius. Companions of similar brightness within this search radius may be mistakenly acquired instead of the target. However, for magnitude differences $\Delta m > 1$, companions within ~ 6" will not affect the acquisition of the brighter target. Note that binary stars with component separations less than about 0.5" can be successfully acquired in Position mode, regardless of the Δm. Refer to the discussion under "Exposure Strategies for Special Cases" on page 50 for further details regarding the acquisition of binary systems in Position mode.

Target Field

The target field consists of the science target and reference stars. Observations of the reference stars will be used to define the local reference frame for relative astrometry. Since the optical field angle distortions are calibrated most accurately in the central region of the FOV, the pointing of the spacecraft (via POS_TARG commands - see Chapter 6 for more details) should be specified to place the target field (as much as possible) in this area.

If the visit also includes Transfer Mode observations of an object, the spacecraft pointing should be chosen to place the object at the FOV center, as this is the only location calibrated for Transfer Mode. If the target field geometry requires the Transfer Mode observations be executed at other locations in the FOV, special calibrations will be needed. Proposers should consult STScI's Help Desk for assistance.

Reference Stars

Ideally, reference stars should have the following characteristics:

- Have magnitudes in the range $8 < V < 15$ to avoid the need for an F5ND cross-filter calibration and to minimize exposure times.
- Be geometrically distributed around the target.
- Have at least 10 arcsec distance between one another and from the science target to avoid acquisition of the wrong object.
- Should fall within the FOV for all HST orientations specified in the proposal.

Check Stars

Check stars, which are a subset of the target list, are observed several times over the course of an orbit (visit). Two or more check stars, distributed across the field, provide the information needed to characterize the drift of the FGS's FOV on the sky (which is typically about 4 mas over the course of the visit). Each check star should be observed at least three times. The best check stars are brighter than 14th magnitude to minimize exposure time, and should include the science object for the highest accuracy astrometry.

Filters

Table 4.1 is a listing of the FGS1r filters, their calibration status and applicable brightness restrictions. (Refer back to Figure 2.8 on page 26 for the filter transmissions as a function of wavelength.)

Table 4.1: Filters for which FGS1r will be Calibrated for Cycle 8

Filter	Calibration Status	Comments	Target Brightness Restrictions
F583W	Full	"Clear" filter; OFAD calibration filter; Position Mode Stability Monitor	$V \geq 8.0$
F5ND	Limited	Pos Mode Cross Filter calibration with F583W; limited to selected locations within the FOV.	Required for targets w/ $3.0 < V < 8.0$;
PUPIL	No	Not calibrated	$V > 7.5$
F605W	No	Not calibrated	$V > 8.0$
F550W	No	Not calibrated	$V > 7.5$

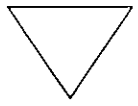

Only the F583W filter will be calibrated for Position Mode for the full FGS FOV. Filter F5ND will be calibrated only at selected locations within the FOV

PUPIL Not Recommended for Position Mode

Occupying the fifth slot on the wheel is the PUPIL. It is not a filter but rather a 2/3 pupil stop. Use of the PUPIL significantly reduces the degrading effect of spherical aberration (which does not necessarily improve Position Mode performance) but collaterally alters the field dependence of the distortions. Consequently, the OFAD calibration for the F583W filter cannot be applied to PUPIL observations. In addition, PUPIL observing attenuates the object's apparent brightness by nearly a full magnitude, which sets the faint limiting magnitude at about V=16 while making observations of stars fainter than V = 14.5 excessively time consuming.

FESTIME and Signal-to-Noise

Photon statistics dominates the noise in the measured position of stars fainter than V ~ 13.0. To track fainter objects, the Fine Error Signal must be integrated for longer periods. Table 4.1 on page 48 lists the default FESTIMES for various target magnitudes. The default FESTIMES, determined from the Phase II target magnitude, are appropriate for most observations, and are set to ensure that photon noise, when converted into the Noise Equivalent Angle (NEA), does not exceed a predefined angular error threshold. The NEA is given by the relation

$$NEA = \left(\frac{1}{1.51 \times 10^{7}}\right) \cdot \frac{\sqrt{0.5 \cdot C + B}}{0.5 \cdot C \cdot \sqrt{t}} \cdot$$

The NEA is used by the proposal processing system (RPS2) to set the default FESTIME time. The parameter C is the total count rate expected from the target summed over all four PMTs, B is the background count rate, and t is the FESTIME. The NEA is plotted as a function of magnitude and FESTIME in Figure 4.1 on page 48. C as a function of filter and magnitude for FGS1r is given by:

$$C = 20776 \times \text{f-factor} \times 10^{-0.4(V-13)}$$

The constant *f-factor* is a function of the filter and the target's spectral color. Table 4.3 on page 49 provides the *f-factor* for each combination of

filter and color. The default FES times used by the proposal processing software for Position Mode measurements are listed in Table 4.1.

Table 4.2: Default FES Times

V Magnitude	FESTIME (seconds)
8–12	0.025
13	0.050
14	0.1
15	0.4
16	1.6
17	3.2

Figure 4.1: Default FESTIME as a Function of V Magnitude for F583W FGS1r: NEA as a Function of Magnitude and FESTIME

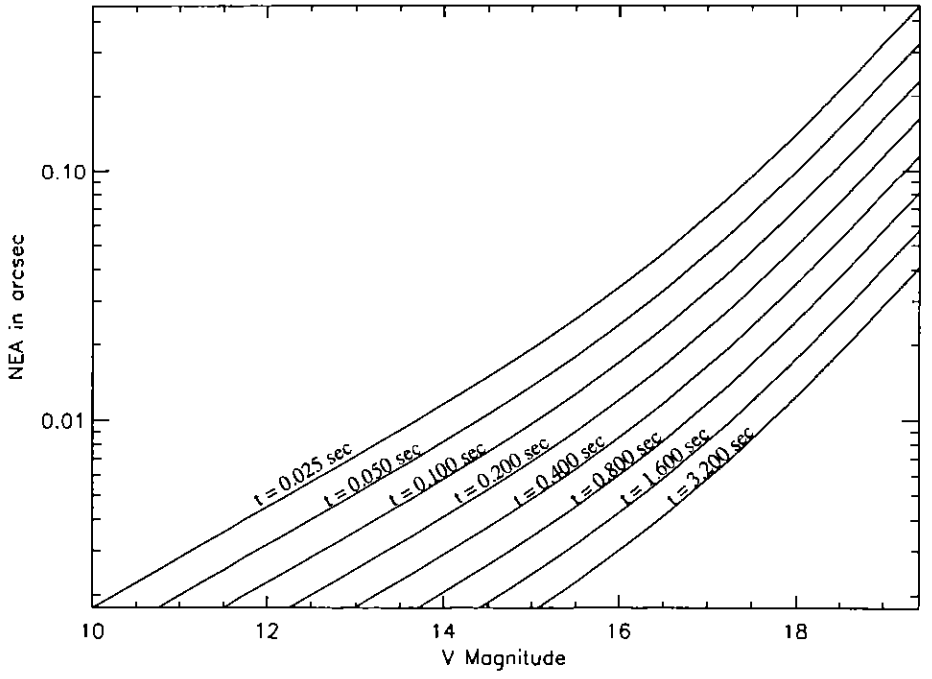

Background

Background noise includes cosmic ray events, particle bombardment during passages through the South Atlantic Anomaly (SAA), and scattered light falling in the 5 x 5″ IFOV. Cosmic ray events are suppressed by special circuitry and the FGS is prohibited from operating while transiting regions of heaviest impact from the SAA. Table 4.4 gives the average

Table 4.3: F-factor Transmission Estimator for Combination of Filter and Color

Filter	B-V			
	+1.78	+0.60	+0.040	–0.24
F583W	1.000	1.000	1.000	1.000
PUPIL	0.491	0.491	0.491	0.491
F5ND	0.010	0.010	0.010	0.010
F550W	0.356	0.354	0.331	0.331
F605W	0.860	0.700	0.624	0.575

background + dark counts for FGS1r in 0.025 seconds. If the background counts for a specific observation is needed for the analysis of the data, it can be obtained from the photometry acquired during the slew of the IFOV to (or away from) the target position. These data extracted by the FGS pipeline package CALFGSA from the FITS files that input are cleaned of spikes from "interloping stars" and can be used to estimate the background levels during post-observation data reduction.

Table 4.4: FGS1r: Background + Dark

FGS1r PMT	Average Background + Dark Counts per 0.025 sec
Ax	5.7
Ay	3.2
Bx	4.9
By	7.7

Position Mode Exposure Time Calculations

The exposure time is the minimum time that an object will be tracked in FineLock. Based the rate at which the measured location (or centroid) of a star converges (from analysis of FGS1r data) Table 4.5 lists the recommended exposure times as a function of target magnitude. We note that:

- Exposures should be as short as possible to allow for more individual observations during the visit, but should be longer than HST's mid-frequency oscillations (~10 seconds).

- Usually, Position Mode observations yield an additional 10 to 20 seconds of FineLock data in excess of the exposure time specified in the phase2 proposal (a result of unused overheads). Hence, specifying a 10 second exposure results in 20 to 30 seconds of FineLock data.

Table 4.5: Recommended FGS1r Exposure Times

Magnitude	*phase2 exposure time* **(in sec)**
8–14	10
15-17	25

Exposure Strategies for Special Cases

Observing Binaries and Extended Sources in Position Mode

Multiple or extended sources in the FGS's IFOV will result in a reduction of the amplitude of the observed interferometric fringes (relative to that of a point source). This occurs because light from multiple sources in the IFOV do not interact coherently (the observed rays originate from different angles on the sky). Therefore, multiple point source fringes will be superimposed upon one another, each scaled by the relative brightness of the source and shifted by its relative angular displacement on the sky. The result is a composite Transfer Function with reduced fringe visibility.

The fringe visibility reduction for the brighter component of a binary system with an angular separation along the X or Y axis greater than about 80 mas (i.e., when the individual S-Curves are fully separate) is given by:

$$F_r = \frac{f_a}{(f_a + f_b)}$$

where f_a and f_b are the intensities of the brighter and fainter components, respectively. A similar expression, but with l_b in the numerator, is appropriate for the faint star S-curve (see Figure 4.3 for examples).

For projected angular separations less that 80 mas, the Transfer Function will be a blend of the merged point source S-Curves. The resultant fringe visibility will depend on the relative brightness and the angular separation of the components (i.e., F_r is more difficult to predict).

Even significant loss of fringe visibility does not pre-dispose the object from being successfully observed in Position Mode. To be acquired in FineLock, an object's *Fine Error Signal* (see Appendix1) must exceed a fringe detection threshold (see Figure 1.2). The threshold is set on the basis of the target's V magnitude, as entered in the proposal, to accommodate the acquisition of faint targets. (The fainter the target the more effectively the

background and dark counts reduce the fringe amplitude, hence lower detection thresholds must be applied.) If the GO were to state the V magnitude of a binary system or extended source to be sufficiently faint, (regardless of its true value), then the observed fringes will exceed the (lower) detection threshold, and the FGS will successfully acquire the object. However, if a false magnitude is specified, one should also manually set the FESTIME (an optional parameter) to the value appropriate to the object's true magnitude. Otherwise, the observation's overheads will be excessively long.

Some binary systems are not *reliably* observed in Position Mode, even with the adjustment to the fringe detection threshold. Objects in this category include those with components exhibiting small magnitude differences ($\Delta m < 1$) and angular separations greater than 60 mas but less than 800 mas (as projected along an interferometric axis). In these cases, either star may be acquired. There have been cases where one component was acquired on the X-axis while the other was acquired on the Y-axis. Such data are still useful, but care must be applied in the post- observation data processing.

There is a class of binary stars which *cannot* be observed in Position Mode. In a FineLock acquisition (see Appendix A1), the WalkDown to FineLock is a finite length path (approximately 0.810") beginning at a point which is "backed off" a fixed distance from the object's photocenter. If the fringes of both stars lie outside this path, then neither will be encountered and the FineLock acquisition will fail. The condition for such a *failure* is the following,

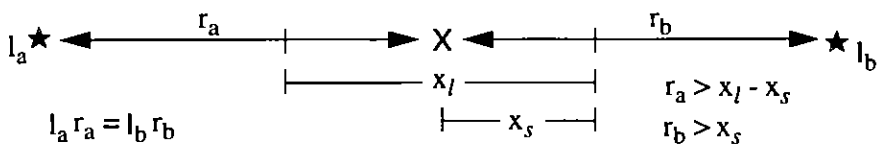

where X is the location of the system's photocenter, r_a and r_b are the distances from the photocenter to the fringes of the components "a" and "b" respectively, l_a and l_b are the flux from each component, x_s is the starting position of the WalkDown, and x_l is the length of the WalkDown. If the position of the binary along either the X or Y axis is known to meet this failure requirement, Position Mode observations of this system should not be attempted.

It is recommended that a proposer contact the STScI Help Desk for assistance with Position mode observations of binary systems.

Sources Against a Bright Background

For sources against bright backgrounds, the fringe visibility function is reduced by $I / (I + B)$ where I is the point source flux and B is the

background flux. The proposer should contact the STScI Help Desk for assistance with such observations.

Crowded Field Sources

Crowded fields create two problems for FGS observations:

- A nearby star (< 10 arcsec away) of similar magnitude could be acquired during the search phase.
- The background brightness in the 5 x 5 arcsec aperture may be increased by the presence of numerous faint stars or nebulosity.

The proposer should consult the STScI Help Desk for assistance with such observations.

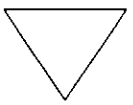

Proposers should document—in the proposal—the logic for selecting a FESTIME or entering a false apparent magnitude of a target.

Position Mode Observing Strategies

Measurement errors can be minimized by carefully structuring the order of exposures in a visit. This section describes strategies which maximize science return.

Summary of Position Mode Error Sources

The reduction of a Position Mode data set requires several corrections and calibrations:

- ***Exposure Level:***
  - Background determination.
  - Star Selector encoder positions (7 LSB).
  - PMT response.
  - Optical Field Angle Distortion calibration.
  - Differential velocity aberration.
  - Lateral color aberration.
- *Visit Level:*
  - Vehicle jitter.

- Drift of FGS's FOV.
- Cross filter (F583W v. F5ND, if used).

• *Program Level:*

- Plate solutions (4 or 6 parameter fits).
- Plate scale.

Each of the corrections and calibrations are briefly discussed in Chapter 5, and are thoroughly reviewed in the *HST Data Handbook*. Many of the corrections specified on the list are determined by analysis of individual observations and removed later in the data reduction processing, (e.g., jitter data is retrieved from the guide star telemetry and removed from the target data). Calibrations, such as the plate scale, the OFAD, lateral color, and cross filter effect are derived from STScI calibration programs. A potentially dominant source of error, the FOV drift (time scale of several minutes), must be measured during the visit, and to that end, the sequence of exposures must be carefully arranged.

Drift and Exposure Sequencing

Stars observed more than once per visit ("check stars") are typically seen to drift across the FGS by ~ 2 to 6 mas when two FGSs guide the telescope (or ~ 5 to 20 mas with only one FGS guiding). Because astrometry observations execute sequentially, the errors in the measured angular separations between objects increase as the time between the measurements lengthens. If uncorrected, this drift will overwhelm the astrometry error budget.

Whatever causes the position of an object to "drift" in the astrometer's FOV affects the guiding FGSs as well. The apparent motion of the guide stars are interpreted as "errors" by the pointing control system and are "corrected" by a small vehicle maneuver. The astrometry FGS witnesses the pointing change. Therefore, the check star motion will have a contribution from all three FGSs.

When only one FGS is used for guiding, the telescope is not roll-constrained, and large motions in the astrometric FGS - up to 10 mas - are not uncommon. Nevertheless, this drift can be successfully removed from the astrometry data, provided the proposal specifies an adequate check star sequence. The more check star observations, the more precise the drift correction. Check stars can be reference or science targets. Ideally, both rotation and translation corrections should be applied to the data, implying the use of at least two check stars with at least three measurements each.

The need to observe check stars can be in conflict with other aspects defining an optimal observing strategy, so compromises will be necessary. Overall an optimal Position Mode visit is scripted to:

- Define a check star strategy which will be robust against FOV drift.
- Maximize the number of reference stars observed.
- Maximize the number of observations of each object.

For example, a visit could contain 10–35 exposures, provided the overheads are minimized and exposure times are less than 20 seconds. A sample geometry is given in Figure 4.2, where the science target is represented by the central object.

Figure 4.2: A Sample Visit Geometry

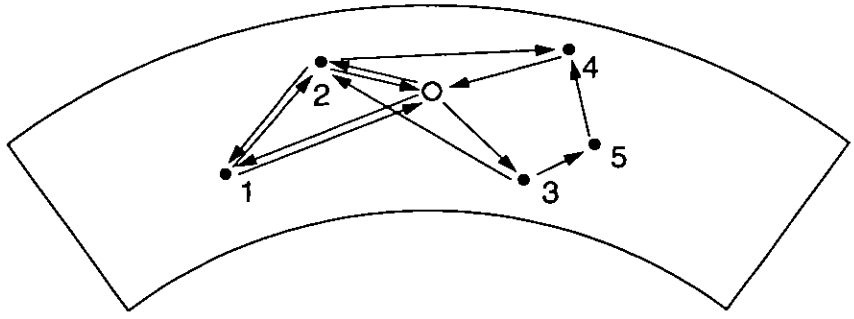

For the geometry specified above, the exposures may be sequenced as follows:

```
 1 - 2 - target - 3 - 2 - 4 - target - 3 - 5 - 4 - target -->
--> 2 - 1 - target - 3 - 5 - 4 - target - 2 - 1 - target.
```

Additional examples expressed in proposal logsheet syntax are given in Chapter 6.

Cross Filter Observations

Targets brighter than V = 8 cannot be observed with the F583W. The F5ND attenuator must be used for such observations. If the visit includes observations of fainter objects with the F583W, a cross-filter correction will be needed for the data reduction. For FGS3, the F583W/F5ND cross-filter effect was found to be astrometrically large (~ 7 mas) and varied with location in the FOV. This effect as been calibrated at the center of FGS1r's FOV by STScI calibration programs. If needed at other locations in the FOV, special calibrations by the proposer might be required.

Moving Target Observation Strategy

In Position Mode, the FGS can track a bright target ($V \leq 14.0$) whose motion is less than ~0.1 arcsec per second. However, planning the observation requires extreme precision: the moving target must be accurately located, to within 10 arcsec, in the IFOV at the start of the

exposure, implying a very accurate ephemeris. Transfer Mode observations of moving targets are discussed in the next section.

Transfer Mode Overview

The FGS Response to a Binary

If the source is a double star, then its wavefront has two components, each incoherent with respect to the other. Two propagation vectors characterize this wavefront and the angle between them is directly related to the angular separation of the stars on the sky. As the FGS's IFOV scans across the object, each component of the wavefront can be thought of as generating its own interferogram (or "S-Curve"), whose modulation is diminished by the non-interfering "background" contributed by the other component. The resulting relationship between the position of the IFOV to the normalized difference of the PMTs depends on the separation of the stars and their relative brightnesses. *The composite interferogram of a multiple system is the linear superposition of the fringes from the individual components, scaled by their relative brightness and shifted with respect to one another by their separation on the sky.* Given this, the fringe pattern of a binary system, whose components have an angular separation α (as projected along the X-axis) and fluxes f_a and f_b, is given by

$$S_{binary}(x) = l_1 S_{single}(x) + l_2 S_{single}(x+\alpha),$$

where:

$$l_1 = \frac{f_a}{f_a + f_b}$$

$$l_2 = \frac{f_b}{f_a + f_b}.$$

Figure 4.3 on page 56 shows the changes in the observed FGS1r interferogram due to binary systems of varied separations and magnitude differences. In Figure 4.3a we display the interferogram of a wide binary pair with component separations and magnitude differences of (200 mas, 1.0) respectively. Figure 4.3b is an example of a system with the same separation, but with a magnitude difference of $\Delta m = 2.0$. The binary system in Figure 4.3c has a smaller separation and magnitude difference (50 mas and 0.5 respectively), while in Figure 4.3d increases the magnitude difference to $\Delta m = 2.0$ for a component separation of 50 mas.

Figure 4.3: .Binary S-Curves Generated from FGS1r X-Axis Data

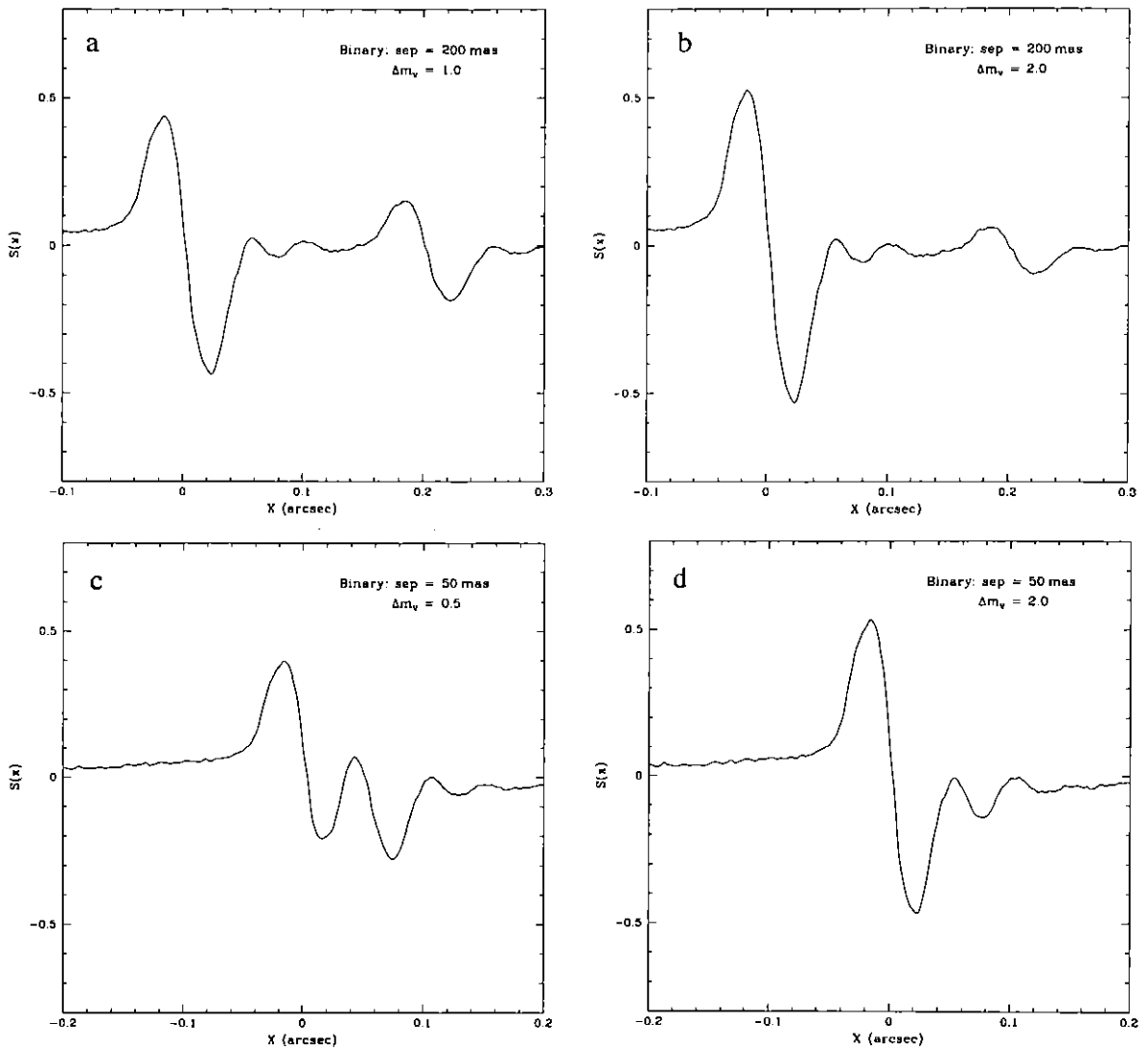

If the angular separation of the stars is greater than the width of the S-Curve, two distinct S-Curves are apparent, but the modulation of each will be diminished relative to that of a single star by an amount depending on the relative flux from each star (see Figure 4.3a and also Figure 3.1). On the other hand, if the angular separation is small, the S-Curves will be superimposed, and the morphology of the resulting blend complicated (as in Figure 4.3d). In either case, the composite S-Curve can be deconvolved using reference S-Curves from point sources, provided the angular separations are not too small and the magnitude difference is not too large. To be more precise, fitting the observed double star S-Curve with two appropriately weighted, linearly superimposed reference S-Curves from single stars leads to the determination of the angular separation, position

angle, and magnitude difference of the binary's components. The modulation, morphology, and temporal stability of the point-source calibration S-Curves determine the resolving power of the FGS. For FGS1r, this is about 7 mas for $\Delta m < 1.0$.

The Transfer Mode Exposure

Rather than tracking the fringe as in Position Mode observation, the IFOV is scanned across the object along a 45 degree path (with respect to the FGS detector axes) in a Transfer Mode exposure. Every 25 milliseconds, star selector angles and data from the four PMTs are recorded. From these data, the fringes of the object can be reconstructed. The number of scans and the length of each scan are derived from the Phase II proposal.

For each target, the step size and scan length must be adjusted as necessary to accomplish the goals of the observation

- ***Step Size:*** The *step-size* refers to the angular distance covered by the IFOV along an axis during a 25 millisecond interval. The default step-size is 1.0 mas. Higher resolution is achievable using step sizes as fine as 0.3 mas. However, such a small step size may prohibitively increase the total time to complete a scan, and as a result of least significant bit (LSB) constraints and vehicle jitter, the effective resolution may not be better than 1.0 mas. The goal is to execute as many scans as possible, with the smallest StepSize (0.6 or 1.0 mas), to achieve the highest S/N ratio.
- ***Scan Length:*** The required scan length is depends on the geometry of the target. A minimum of scan length of 0.3" is needed to fully sample the fringes of a point source along with a sufficient segment of the wings to either side. For binary systems, the scan length should be *at least* as wide as the component separation plus 0.3".

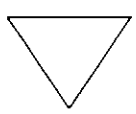

The point-source calibration S-Curves are obtained only at the center of the FGS1r FOV. Other locations in the FOV are not routinely calibrated.

Planning a Transfer Mode Observation

Target Selection Criteria

Other than the brightness restrictions specified in Table 4.6 on page 59 there are several additional considerations when selecting targets for Transfer Mode observations.

- ***Position in the FOV:*** The morphology of the fringe varies considerably with position in the FOV, as shown for FGS1r in Figure 2.6. As explained in Chapter 2, this field dependence is the manifestation of small misalignment between the star selector optics and the Koesters prism which is greatly magnified by HST's spherical aberration. To obtain the highest quality data with the best resolution, all Transfer Mode observations should be obtained at the AMA optimized position at the center of the FOV. *Under normal circumstances, STScI will provide reference S-Curve calibrations only at the center of the Field of View.*
- ***Color:*** The FGS's interferometric response is moderately sensitive to the spectral color of the target. The FGS calibration library contains interferograms from point-source objects with a variety of (B-V) colors. The GO is encouraged to inspect this library to ascertain whether a suitable reference (δ(B-V) < 0.3) is available for data analysis. If not, the FGS group should be alerted, and efforts will be made to enhance the library. The color calibrations available in the FGS library are listed in Chapter 5. Up-to-date additions can be found on the FGS web site:

  http://www.stsci.edu/instruments/fgs/

- ***Minimum Scan Length:*** In order for Transfer Mode observations to achieve the highest possible signal-to-noise, the length of the scan should be as short as possible (to allow for more scans in the allotted time). The minimum scan length is determined by the expected angular separation of the components of the binary being observed plus the recommended minimum size (for a point source) of 0.3", or,

  $$\text{Min Scan Length (arcsec)} = 0.7 + 2x,$$

  where the value x is the largest anticipated angular separation of the binary along either axis.

- ***Maximum Scan Length:*** When considering the maximum scan length, three concerns should be addressed:

- Masking by the field stops becomes relevant when the FOV is moved beyond 2 arcsec from the photocenter. False interferometric features become prevalent.
- Beyond 2.5 arcsec from the photocenter, the intensity of the target's light drops off considerably, resulting in poor signal-to-noise photometry.
- Maximum commandable scan length is 6.7".

- ***Target Orientation:*** If the approximate position angle of the non-point source is known, then specifying an orientation for the observation may be advantageous. If possible, (for wide binaries) avoid the situation where the projected angular separation along one of the axes is less than 20 mas. Specific orientations are achieved by rolling the HST to an off-nominal roll attitude or by scheduling an observation at a time when the nominal roll is suitable. It should be noted however that special orientations are considered as special scheduling requirements which affect schedulability.
- ***Target Field:*** The Search and CoarseTrack acquisition are vulnerable to acquiring the wrong object if the field is too crowded (with neighbors of comparable brightness within 8 arcsec of the target). Hence, the problem addressed in "Crowded Field Sources" on page 52 for Position Mode observations applies equally to Transfer Mode observations.

Transfer Mode Filter and Color Effects

Table 4.6 on page 59 is a summary of the available filters and associated restrictions governing their use.

Table 4.6: FGS1r Transfer Mode Filters to be Calibrated During Cycle 8

Filter	Calibration Status at Pickle Center	Comments	Target Brightness Restrictions
F583W	Full	Monitoring of Reference Standard star Upgren69 and single epoch color calibrations as required by the GO proposal pool.	Recommended for V > 8.0; Not permitted for V < 8.0
F5ND	Single-epoch color calibrations as needed	None.	Required for V < 8.0; Not recommended for V > 8.0
PUPIL	Single-epoch color calibrations as needed	Reduces the flux to half and loss of angular resolution.	Not permitted for V < 7.5
F605W	Single-epoch color calibrations as needed	None.	Not permitted for V < 8.0

Filter	Calibration Status at Pickle Center	Comments	Target Brightness Restrictions
F550W	Single-epoch color calibrations as needed	None.	Not permitted for V < 7.5

The S-Curve morphology and modulation have a wavelength dependence. Experience with FGS3 has shown that the color of the reference star should be within $\delta(B-V) = 0.1 - 0.2$ of the science target. We endeavor to maintain a library of single reference stars which accommodate the color requirements of the GO proposals in the Cycle. These color standards are usually observed once during the Cycle, while Upgren69 is observed every 6 months to monitor S-curve stability.

Signal-to-Noise

In essence, the "true" signal in a Transfer Mode observation of a binary system is the degree to which the observed Transfer Function differs from the S-curve of a point source. The signal-to-noise (S/N) required of an observation will depend upon the object being observed; a wide binary whose stars have a small magnitude difference and separation of 200 mas will be much easier to resolve than a pair with a larger magnitude difference and a separation of only 15 mas.

The "noise" in an observation has contributions from both statistical and systematic sources. Photon noise, uncertainty of the background levels, and spacecraft jitter comprise the statistical component. The temporal variability and spectral response of the S-curves dominate the systematic component (these are monitored and/or calibrated by STScI). Provided that at least 15 scans with a 1 mas step size are available, observations of bright stars (V < 13.0) suffer little from photon noise and uncertain background levels, and show only slight degradations from spacecraft jitter (with high S/N photometry, the segments of the data which are degraded by jitter are easily identified and removed from further consideration).

Maximizing the S/N for observations of fainter objects requires a measurement of the background level (see Chapter 6) and a larger number of scans to suppress the Possonian noise in the photometry of the co-added product. But with lower S/N photometry in a given scan, corruption from spacecraft jitter becomes more difficult to identify and eliminate. Therefore, the quality of Transfer Mode observations of targets fainter than V = 14.5 will become increasingly vulnerable to spacecraft jitter, no matter how many scans are executed.

Systematic "noise" cannot be mitigated by adjusting the observation's parameters (i.e., increasing the number of scans). To help evaluate the reliability of a measurement made in Transfer Mode, STScI monitors the

temporal stability and spectral response (in B-V) of FGS1r's interferograms. As discussed elsewhere, the FGS1r S-curves appear to be temporally stable to better than 1%, and the Cycle 10 calibration plan calls for observations of single stars of appropriate B-V to support the data reduction needs of the GOs (this calibration will be maintained in Cycle 11). This should minimize the loss of sensitivity due to systematic effects.

Transfer Mode Exposure Time Calculations

The step_size and number of scans determine the number of photometric measurements available for co-addition at any given location along the scan path. Typically, up to 50 scans with 1mas step_size are possible within a 53 minute observing window, (after accounting for overheads and assuming a scan length ~ 1.2 arcsec per axis). The step size and number of scans that should be specified are in part determined by the target's magnitude and angular extent and also by the need to allocate time within the visit to any other objectives, such as Position Mode observations of reference stars (to derive a parallax for the binary). The total exposure time for a Transfer Mode observation (excluding overheads) is:

$$T_{\exp} = \frac{ScanLength}{StepSize} \cdot (0.025\,\mathrm{sec} \cdot N_{scans})$$

where T_{exp} is the total exposure time in seconds, N_{scans} is the total number of scans, 0.025 is the seconds per step, ScanLength is the length of the scan *per axis* in arcsec, and StepSize is given in arcsec.

Photon noise is reduced by increasing the number of scans, N_{scans}, as displayed in Figure 4.4: FGS1r (F583W) S-Curves: Single and Co-Added, which demonstrates the benefits of binning and co-adding individual scans. Trade-offs between step size, length, and total duration of an exposure are unavoidable especially when considering visit-level effects such as HST jitter.

Figure 4.4: FGS1r (F583W) S-Curves: Single and Co-Added

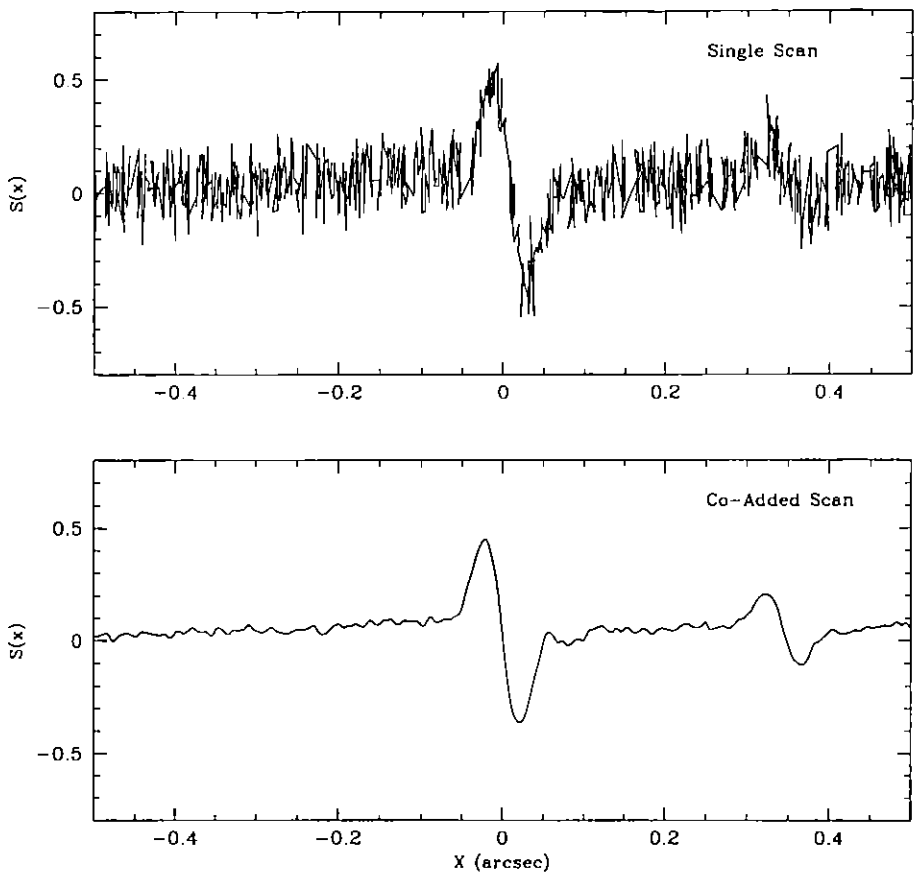

Simulations using actual data scaled by target magnitude are needed to relate the Transfer Function signal-to-noise (described in the previous section) to the resolving performance of the instrument. A robust exposure time algorithm is in development. In Table 4.7, we offer some guidelines on the minimum number of scans to use in a visit for various binary parameters.

Table 4.7: Suggested Minimum Number of Scans for Separations < 15 mas

V Mag	Δmag =0.0	Δmag =1.5	Δmag =3.0
5	18	20	NA
9	15	20	NA
12	15	25	NA
14	30	30	NA
15	35	NA	NA
16	35	NA	NA

Transfer Mode Observing Strategies

Summary of Transfer Mode Error Sources

The Transfer Mode corrections and calibrations are:

- *Exposure Level:*
  - Background subtraction.
  - Star Selector Encoder correction (7 LSB).
  - Cross-correlating and co-adding individual scans.
  - Availability of a suitable point-source reference S-Curve (color response).
- *Program Level:*
  - Roll dependence of the FGS plate scale.

Each of the corrections and calibrations are discussed briefly in Chapter 5 and more thoroughly in the *HST Data Handbook*. Those corrections that could result in an enhanced observation strategy are discussed here.

Drift Correction

As discussed in the Position Mode section, targets observed multiple times per Position Mode visit typically drift across the FGS by about 6 to 12 mas when two FGSs guide the telescope. This drift is also apparent in Transfer Mode observations, but the cross-correlation of S-Curves prior to binning and co-adding automatically removes the drift. Each single-scan S-Curve is shifted so that the particular features of the S-Curve used for the cross correlation coincides with that of the fiducial S-Curve. The reliability of implicitly removing the drift is only as good as the accuracy of the cross correlation procedure, which, for bright objects ($V < 14.5$) is accurate to < 1 mas. Analysis is underway to determine the procedure's accuracy for fainter objects.

Temporal Variability of the S-Curve

Measurements of the standard star Upgren69 over the lifetime of FGS3 indicated a 10 – 18% temporal variability of the S-Curve morphology. The amplitude of these changes have important consequences on the analysis of binary star observations when the separation of the components is less than 30 mas and the magnitude difference exceeds 1.6. These temporal changes also affect analyses of extended source observations. The cause of the

variability in FGS3 has not been determined. Monitoring of FGS1r has shown this instrument to be stable at the 2% level over periods of months. There does appear to be a slow evolution of the y-axis S-curve however, as shown in Figure 4.5. STScI will continue to monitor FGS1r's S-Curves so that this evolution can be calibrated and its effect on science data minimized.

Figure 4.5: Evolution of S-curve morphology along the FGS1r Y-axis

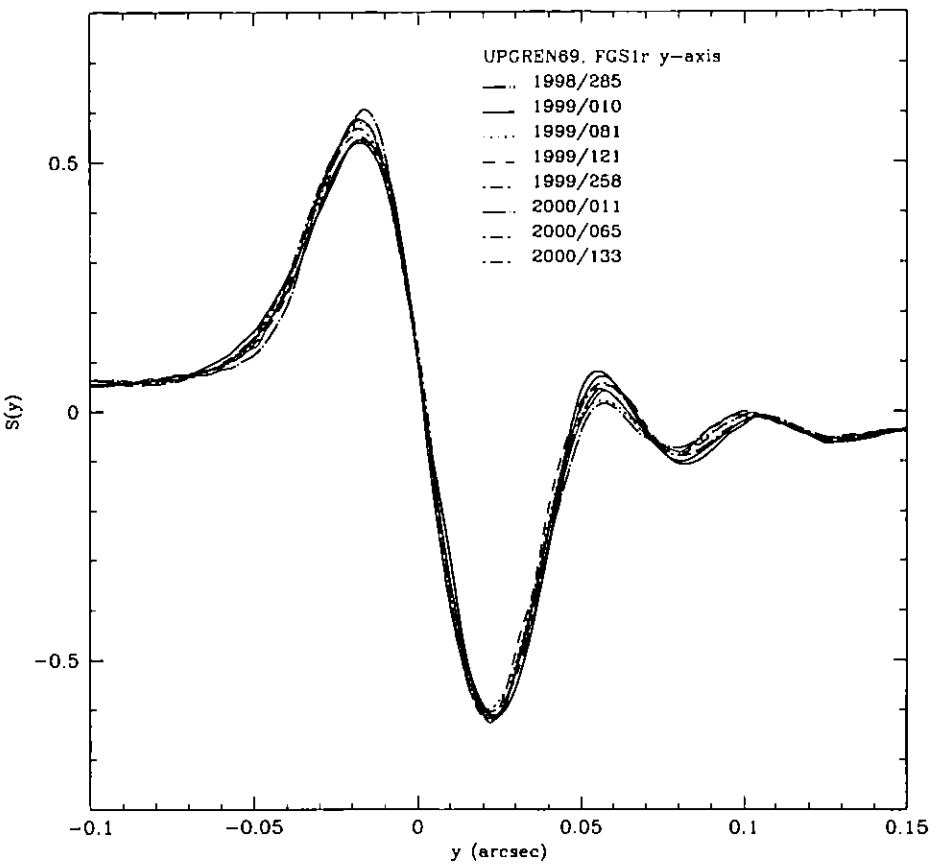

Faint Targets and Background Subtraction

For programs with targets brighter than V = 13.5, background is not an issue. For programs with fainter binaries, knowledge of the background is required. In order to obtain a background measurement, it is necessary that there be at least two targets in the observing sequence, separated by at least 60″. The background will be measured during the slew of the IFOV from one target to the next. If necessary, the proposer should specify a false target at some location in the FOV at least 60″ from the science object, and observe it in Position Mode for approximately 30 seconds with the same

filter as the target. Care must be taken to avoid observing "background" objects brighter than V = 8.0 with F583W.

Empirical Roll Angle Determination

The science data headers contain the commanded HST roll angle, not a measured angle. The errors that contribute to a difference between the commanded and actual roll include: the relative guide star positional error, the FGS-FGS alignment error, and errors in the predicted ephemeris. The actual roll angle is calculated from the guide star telemetry by the observatory monitoring system, and is reported in the STScI Observation Logs that accompany the science data. More information is available on the following web page:

`http://www.stsci.edu/instruments/observatory/`

The error in the calculated roll angle is estimated to be about 0.04 degrees. If a more accurate determination is needed, the position angle of the observed binary with respect to the local reference frame can be measured via Position Mode observations of the target and a reference star (or two reference stars if the target cannot be acquired in Position mode—see "Exposure Strategies for Special Cases" on page 50) should be included in the visit along with the Transfer Mode exposures. Please confer with STScI for help designing the visit and calculating the roll from Position Mode measurements.

Exposure Strategies for Special Cases: Moving Targets

For Transfer Mode observing, a moving target represents a special case. The flight software which enables HST to track a moving target has not been implemented for FGS observations. Nonetheless, the FGS is quite capable of acquiring a moving target provided that the object's angular speed is less than 80 mas/sec. However, during the observation, the scan path is not adjusted to accommodate for the object's motion. The target's fringe will be displaced in each subsequent scan until it moves completely out of the scan path. A method to work around this problem is to specify several observations of the object during the visit. For example:

1. The target should be observed in several short exposures rather than in one or two long exposures. The FGS would re-acquire the target with each new Search, CoarseTrack acquisition regardless of the target's motion. The target list should contain enough entries to cover the swath of sky traversed by the moving target, e.g., if the motion takes the object 10 arcsec across the FOV, then at least two sets of target coordinates should be specified.

2. The number of individual observations (entries in the exposure logsheet) and number of scans in an observation will be dictated by the object's angular speed.
3. Plan the observation when the target is moving its slowest, e.g., at opposition (if possible).
4. Take advantage of rolling the telescope to adjust the angle between the target motion vector and relevant FGS reference directions (please contact STScI for assistance).
5. Choose the exposure times to be as short as possible.

CHAPTER 5:

FGS Calibration Program

In this chapter . . .

Position Mode Calibrations and Error Sources / 67
Transfer Mode Calibrations and Error Sources / 76
Linking Transfer and Position Mode Observations / 82
Cycle 10 Calibration and Monitoring Program / 83

This chapter describes FGS error sources, associated calibrations, and residual errors for Position, Transfer, and mixed (Position + Transfer) observing modes. A discussion of the FGS 1R Cycle 10 calibration plan is included.

Position Mode Calibrations and Error Sources

FGS science data is processed at three distinct levels: the exposure, the visit, and the epoch. Each of these levels is subject to different sources of error. Table 5.1 on page 68 summarizes the accuracies of Position Mode calibrations. Most of the errors listed are statistical. Multi-epoch observations reduces the impact of these errors in the science data.

Table 5.1: FGS1r Position Mode Calibration and Error Source Summary

Type of Calibration Correction	**Pre-Calibration Error Extent**	*Calibration Error (mas)*	*Comments*
	Exposure Level Calibration Corrections:		
Average background and detector noise	–	–	Serendipitously acquired during the FGS IFOV servo slew to the target; ~215 cts/sec in each PMT; used to adjust for position centroid errors.
Star Selector Encoder fine bit errors	~1 mas	0.1	Correction applied in the SSA,B->X,Y conversion.
Centroid errors	Magnitude Dependent	~ 1, V < 14.5 ~ 2, V >16	Apply median filter.
Relative PMT sensitivity	–	–	Analysis removes PMT mismatch effect; used to adjust for position centroid errors.
Differential velocity aberration	± 30 mas (function of geometry)	0.1	Depends on HST velocity vector and target geometry, ephemeris errors and alignment calibration. Correction applied during post-observation processing.
Relative distortion across FOV (OFAD)	~ 500 mas	~1 mas	STScI calibration in filter F583W.
Lateral color correction	< 1 mas relative shift for δ(B-V) = 1	carried	No corrections applied. Calibration planned for FGS1r.
Cross filter calibration	~7 mas	< 0.5 center	Relative positional shifts are calibrated for filters F583W and F5ND at pickle center.
	Visit Level Calibration Corrections:		
HST jitter	2–4 mas: quiet; 10–50 mas: day/night	< 0.1 during quiescence.	Correction derived from guide star motion. Large jitter excursions could cause loss of lock or corrupt a data set; disqualify outliers.
Drift	5–20 mas: two GS FineLock. 12–60 mas: one GS + gyro roll control	< 0.5	Special observing strategy for check stars; Drift models derived from check star motion and applied to target data.
	Epoch-Level Calibration Corrections:		
Temporal evolution of OFAD and plate scale.	<100> mas/year	0.5 mas	Long-term stability monitor program: update OFAD coefficients and FGS star selector calibration.

Position Mode Exposure Level Calibrations

The corrections and calibrations described below are applied by the FGS Calibration Pipeline.

Star Selector Encoder Fine Bit Errors

The star selector rotation angles are read as 21 bit integers. The 7 least significant bits (LSBs) are read by an optical resolving device that was calibrated during the manufacturing process. The size of the calibrated correction is about 1 mas with a residual of about 0.1 mas. Errors in the 14 most significant bits (MSBs) are absorbed by the OFAD calibration.

Position Centroiding

The location of a star in the FOV during a Position Mode observation is determined by identifying the median of the 40 Hz SSA or SSB samples (while the target is being tracked in FineLock). The median measurement is robust against most spacecraft jitter, short-interval transients and telemetry dropouts. If *faint* targets ($V > 16.0$) are observed, the photometric noise results in a large noise equivalent angle. Spacecraft jitter and photometric noise contribute to the standard deviations about the median of up to 2 mas per axis for $V < 14.5$ and up to 3 mas per axis for $V > 15.0$. However, the repeatability of the centroid measurement (over smaller intervals of the exposure) is the true assessment of the precision of the measurement, typically 0.7 mas and 1.5 mas for targets where $V < 14.5$ and $V > 15.0$ respectively.

PMT Sensitivities and Position Centroid Adjustment

The effect of PMT sensitivity on FGS observations is discussed in Appendix 1. In order to accommodate the differences between the two PMTs along each axis, the FGE computes an average difference (DIFF) and average sum (SUM) of their photometric response to the star over the first few FESTIMES in the WalkDown. These values are used in the calculation of the Fine Error Signal. The results are accurate for bright ($V < 14.0$) objects but become unreliable for fainter targets, a result of the short integration period and increasingly noisy photon statistics. The pipeline gathers photometric data over the entire WalkDown (typically 80 times as many samples) to achieve a better signal-to-noise and more reliable values of DIFF and SUM. These are used to recompute the Fine Error Signal and adjust the (x,y) centroids in post-observation data reduction.

Differential Velocity Aberration

Differential velocity aberration arises as a result of small differences in the angle defined by the HST velocity vector and the line of sight to targets in the FGS FOV. The HST PCS guides for zero differential velocity aberration (DVA) at one position in the FOV. The positions of targets elsewhere in the FOV must be corrected for DVA. Calibration errors in the

relative alignment of the FGSs, catalog position errors of the guide stars, and ephemeris errors all contribute—though negligibly—to the errors in the differential velocity aberration correction. The actual adjustment to the target's positions can be as large as ± 30 mas (depending on the target and velocity vector geometry) but are corrected by post-observation data processing to an accuracy of ± 0.1 mas.

Optical Field Angle Distortion (OFAD) Calibration

Field angle distortion introduces errors in the measurement of the relative angular separation of stars at varied positions across the FGS FOV. The distortion errors originate from:

- Radial distortions induced by the Ritchey-Chretian design of the OTA.
- Manufacturing irregularities in the FGS/OTA optical train.
- The optical reader produces errors in the 14 most significant bits of the 21-bit Star Selector A and B encoder values.

The distortion is independent of target magnitude, color, or exposure time, and depends only on the location of the object in the FGS FOV. The Space Telescope Astrometry Science Team (STAT) has calibrated the optical field angle distortion (OFAD) in FGS3 and maintained this calibration (the OFAD has a slow time dependence). The data for calibrating FGS1r became available in December 2000 and the analysis of those observations is underway (by the STAT) at the time of this writing. However, using FGS3 to infer FGS1r potential distortion, we expect - on average - 500 mas distortion across the FOV. This effect is represented by two fifth-degree two-dimensional polynomials. Post-calibration residual errors are typically ±1 mas throughout most of the FOV. The FGS3 OFAD residuals are plotted in Figure 5.3 on page 72 for illustration. See the *HST Data Handbook* for additional information. The OFAD calibration of FGS1r is a part of the FGS calibration plan.

We expect smaller OFAD residuals for FGS1r (compared to FGS3) due to the design of the calibration test. The FGS3 data were acquired at a time when the roll of HST was restricted to be within 30 degrees of nominal for the date of the observations. The FGS1r test executed when the target field (M35) was close to the "anti-sun" position, i.e., when HST could be rolled over a full 360 degrees. Figure 5.1 on page 71 shows an overlay of the pointings used for the FGS3 calibration, while Figure 5.1 on page 71 shows the same for the FGS1r calibration. Clearly, the distortions should be more apparent in the FGS1r test, allowing for an optimal calibration (compared to the FGS3 test).

Figure 5.1: Overlay of the pointings used for the FGS3 OFAD calibration.

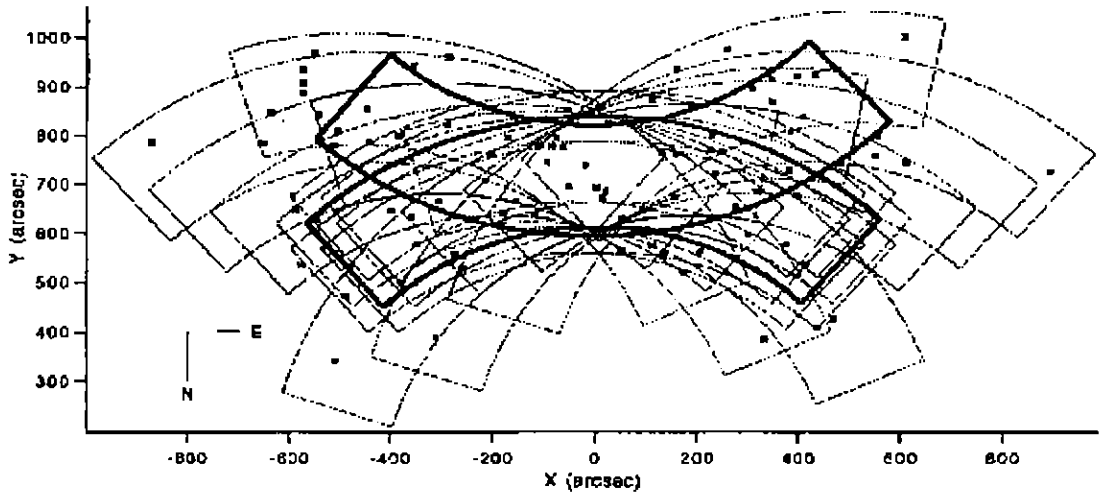

Figure 5.2: Overlay of pointings used for the FGS1r OFAD calibration

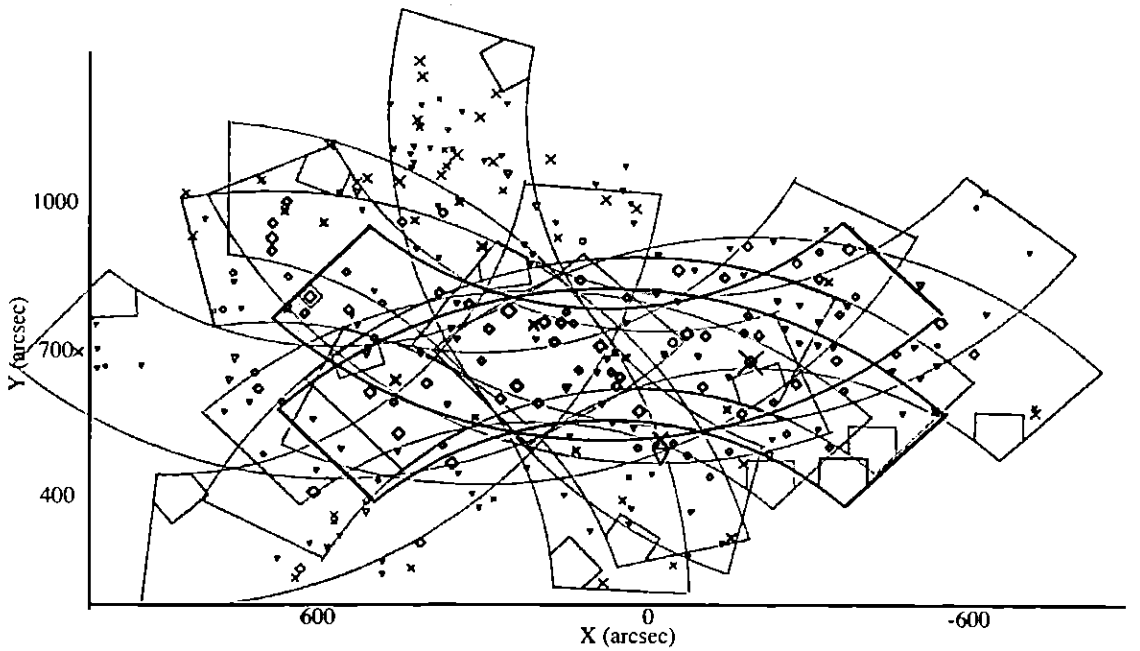

Figure 5.3: FGS3: Residuals of OFAD Calibration in the X-axis (top panel) and Y-axis (bottom panel).

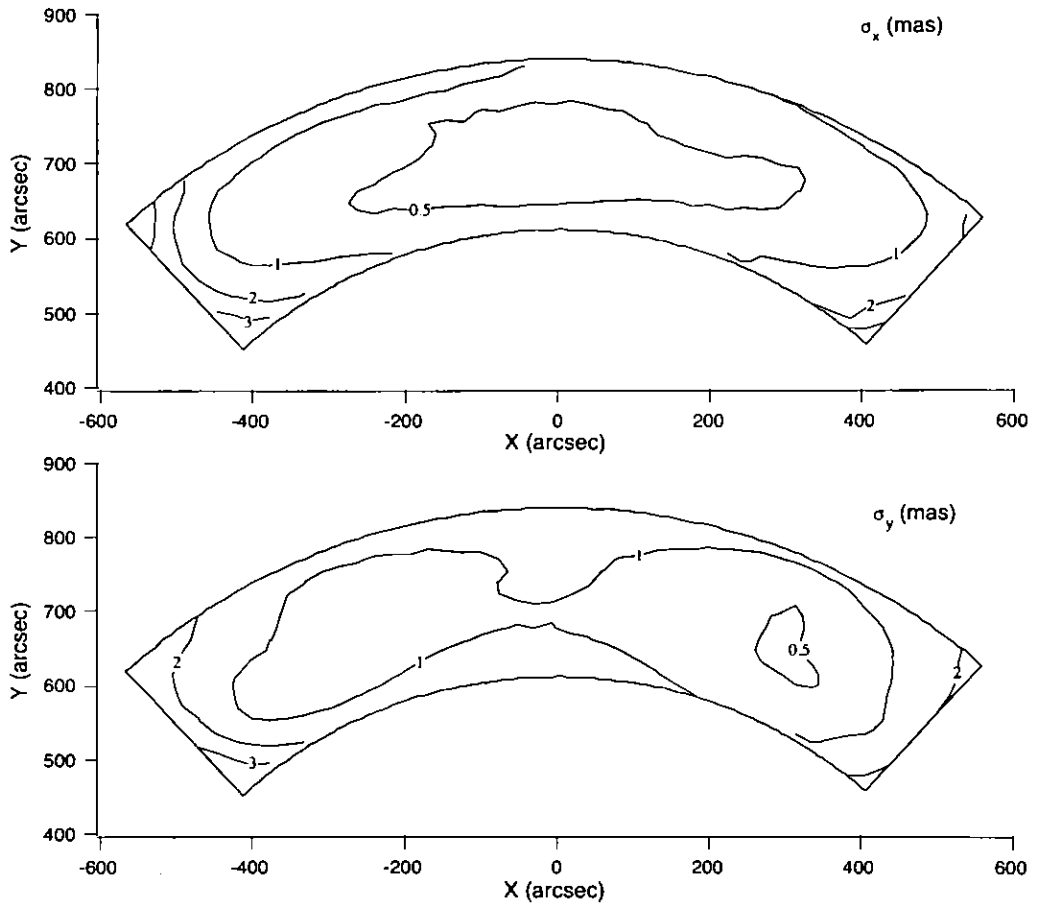

Figure courtesy of B. McArthur, University of Texas at Austin

Lateral Color

The five-element corrector group (see box in Figure 2.1) is a collection of refractive elements tasked with the removal of astigmatism and the final of the beam. It's refractive properties introduce subtle changes to angle of propagation of the beam to a degree which depends on the spectral color of the source. This change causes the apparent position of the star in the FOV to shift slightly, an effect referred to as *lateral color*. The positional error introduced by lateral color is thought to be relevant only when comparing the relative positions of two targets of extreme colors: a color difference of $\delta(B - V) = 1$ between two targets could introduce a ±1 mas positional error. An in-orbit assessment of lateral color associated with FGS1r was performed in December 2000, and the analysis is pending. Please check the FGS Web Site for more details.

Position Mode Visit Level Calibrations

Jitter

Significant enhancements to the HST pointing control system and the replacement of the original solar arrays have reduced quiescent vehicular jitter to 2–4 mas. Although small for most HST science applications, the jitter must be removed from astrometry data.

Since astrometric measurements are made sequentially, relating the measurements to one another requires a mapping of each measurement onto a fixed common reference that defines the visit. Guide star positional data, also telemetered at 40 Hz, are used to define jitter characteristics over the course of the visit. In this way, low frequency jitter (on time scales of minutes) can be removed from the target data.

High frequency, large-excursion jitter, most often a result of the transition to and from orbital day and night, ranges from 5 to 150 mas in amplitude and lasts for several seconds to several minutes. If particularly frenzied, the large jitter can cause total or temporary loss of lock of the guide stars. An example of the jitter during the onset of a day/night transition is shown in Figure 5.4 on page 74. The large vibrations increase the standard deviations of FineLock tracking in the three FGSs by up to a factor of eight over the pre-transition values. Fortunately, such instances are rare.

The overall residual from the "de-jittering" process is only ~ 0.1 mas, the small value testifying to the advantages of using a median filter in the centroid computation and to the excellent pointing of the HST.

Figure 5.4: FGS2 Guide Star Motion at the Onset of a Day/Night Transition

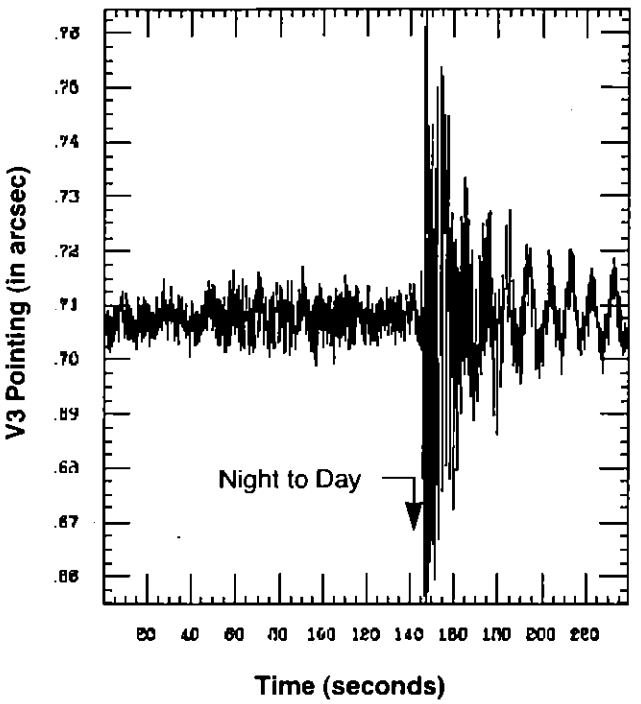

Drift

FGS drift was discussed in Chapter 7 with regards to observation strategy, i.e., the use of check stars to track apparent motion of the FOV during the visit so it can be removed during post-observation processing. There are two different classes of drift, depending on whether one or two FGSs guided the HST during the visit. With two FGSs guiding, drift is identified as a slow but correlated wander of the targets observed more than once during the visit. The amount of drift *appears* to be related to the intensity of the bright Earth entering the telescope during target occultations. Accordingly, the drift is highest for targets in HST's orbital plane (~ 10 mas) and lowest for those at high inclination (~ 2 mas).

When only one FGS is used to guide the telescope, the drift is typically 20 mas over the course of the visit. The single guide star controls the translational motion of the spacecraft while the HST roll axis is constrained by the gyros. Gyro-induced drift *around the dominant guide star* ranges from 0.5 to 5 mas/sec, and is typically of order 1 mas/sec. Note the gyro drift is a spacecraft roll, and does not represent the translational motion of a target at the FGS (which will typically be ~0.01mas/sec). Over the course of a visit, the roll drift error measured by the astrometer can build up to 40 mas or more (but is typically less than 20 mas).

Regardless of the size of the drift, it can be characterized and removed by applying a model to the check star motions, provided the visit includes a *robust* check star strategy: a check star observation every 5–6 minutes

(described in Chapter 7). At a minimum, two check stars measured three times each are needed to model translational and rotational drift.

Cross Filter Calibrations

For a target star (or any reference stars) brighter than V = 8.0 to be included as part of an FGS observation, it must be observed with the neutral density attenuator F5ND. As a result of the differing thicknesses of F583W and F5ND, and possibly a wedge effect between the two filters, the measured position of the bright target in the FOV will shift relative to the (fainter) reference stars. A cross-filter calibration is required to relate these observations, as relative positional shifts may be as high as 7 mas. Also, further evidence from FGS3 indicates these shifts are field dependent. If the effect is uncorrected, a false *parallax* will occur between the science and reference targets as the star field is observed at different orientations in the FOV. Since it would be prohibitive to calibrate the cross-filter effect as a function of field location, FGS1r cross-filter calibrations will be restricted to the center of the FOV. For reference, the uncertainty after the FGS3 cross-filter calibration is ~0.5 mas.

Position Mode Epoch-Level Calibrations

Plate Scale and Relative Distortion Stability

For FGS3, the plate scale and OFAD exhibits a temporal dependence on an average time scale of ~4 months and a size of several tens of milliarcseconds (predominately, a scale change). The evolution of the FGS3 OFAD revealed that the variability is probably due to the slow but continued outgassing (even after 10 years!) of the graphite epoxy structures in the FGS. A long-term stability monitoring test is executed bi-monthly to help measure and characterize the distortion and relative plate scale changes and thus update the OFAD. Post-calibration residuals are on average ± 1 mas along the X-axis and Y-axis. Better performance (of order ± 0.5 mas) is achieved in the central region of the FOV.

The FGS1r Position Mode stability was coarsely monitored during Cycle 7. Large scale changes in its S-Curve, attributed to outgassing effects, show that the instrument was unstable (for high accuracy astrometry) during its first year in orbit, as expected. In early 1998 the evolution slowed, and by April 1998 FGS1r's S-curves fully stabilized; a major prerequisite for the OFAD calibration was met.

The OFAD and lateral color calibrations were to have been performed during cycle 8 when the target field was at anti-sun and HST would not be roll constrained. Unfortunately this coincided with and was pre-empted by the Servicing Mission 3a. Rather than perform the calibrations under less favorable, roll-constrained conditions, STScI decided to defer the observations until December 2000, when the target field again has an anti-sun alignment.

The science data that has accumulated since the beginning of cycle 8 will be re-processed once the OFAD calibrations are in hand. Any temporal evolution since the beginning of cycle 8 can be back-calibrated away by use of the long term monitoring observations that have been executing all along. Check the FGS web pages for updates with regard to the OFAD calibrations.

Errors Associated with Plate Overlays

The errors associated with several of the corrections described above will not manifest themselves until data from individual visits are compared. The most dominant source of Position Mode error are the OFAD and changes in the plate-scale. The derivation of a plate scale solution is described in the *HST Data Handbook*. In general, for regions near the center of the pickle, residuals are smaller than 1 mas if the reference star field is adequately populated.

Transfer Mode Calibrations and Error Sources

Table 5.2 summarizes Transfer Mode sources of error and associated calibrations. Each entry is described in the subsections below.

Table 5.2: FGS1r Transfer Mode Calibrations and Error-Source Summary

Correction	Pre-Calibration Error Extent	Calibration Error (mas)	Comments
Background and detector noise	-	-	Serendipitously acquired during the FGS servo slew to the target;~215 cts/sec in each PMT.
HST jitter	2–4 mas: quiet; 10–50: day/night	< 0.1 during quiescence	Correction applied during data co-addition
Drift	5–20 mas: 2 guide star FineLock. 12–60: 1 guide star plus gyro roll control	< 0.5	Cross correlation of S-Curve scans during post observation data processing removes drift errors.
S-Curve temporal variability	~2% in FGS1r	limits resolution	Monitor standard star (Upgren69).
S-Curve wavelength dependence	~2%	limits resolution	Use calibration point source (i.e., an unresolved star) of appropriate (B-V) color.

A Transfer Mode observation contains multiple scans of a target. To obtain optimal S/N values, the individual scans are cross-correlated, binned, and co-added. The reliability of this process is dominated by

spacecraft jitter for targets with V < 13.5, and by photometric noise for targets fainter than this.

Background and Dark Subtraction

Targets fainter than V ~ 14.5 are increasingly affected by dark and background counts which reduce the amplitude of the S-Curve (see Chapter 7). Provided the dark and background measurements are available (see Chapter 6), the analysis of the Transfer Mode data will not be significantly impaired.

PMT Sensitivity Differences

Although individual PMT sensitivities in an FGS differ, these differences do not introduce a significant source of error in Transfer Mode observations. Differences in the PMT response manifest themselves as a bias (offset) of the S-Curve. This bias is present in the calibration standard star S-Curves (the single stars) as well, and so the effect is neutralized when deconvolving the science target Transfer Function into its component single S-Curves (provided the spectral colors of the science and reference targets are well matched).

Jitter

Typically, quiescent vehicular jitter is about 2–4 mas in amplitude on timescales of minutes. Large-excursion jitter—a result of the transition to and from orbital day and night—ranges from 15 to 150 mas in amplitude may last from seconds to minutes. Spacecraft jitter is removed by eliminating corrupted scans or segments of scans from the co-addition process. For illustration, Figure 5.5 shows the effects of jitter on the FGS1r interferogram (single scan).

Figure 5.5: Effects of Jitter on an FGS1r S-Curve (single scan)

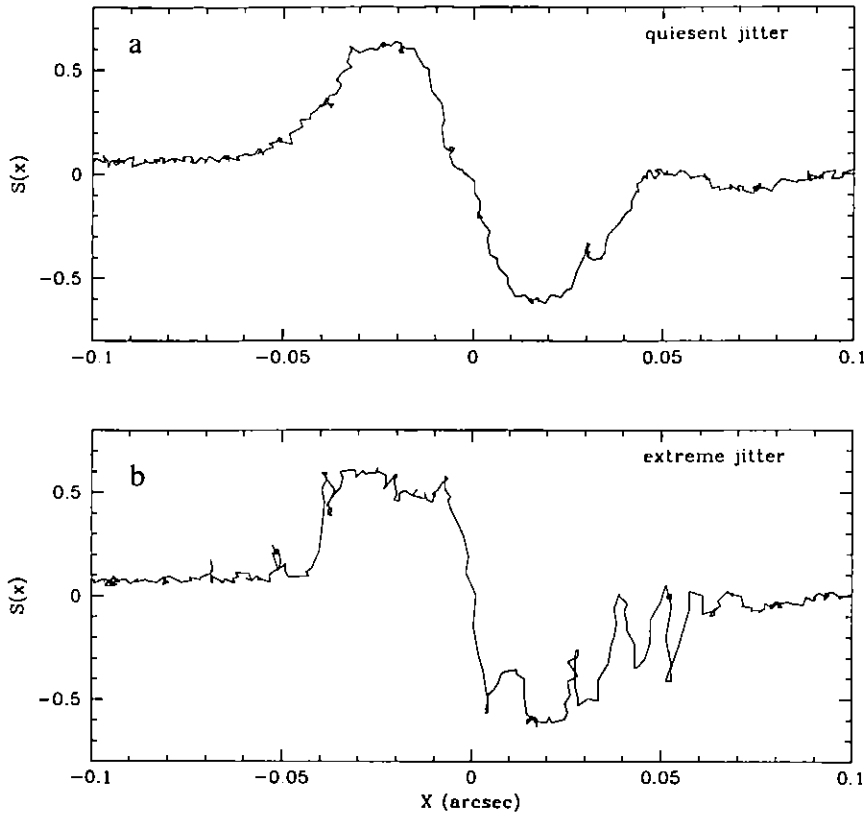

The quiescent scan (Figure 5.5a) shows features due to jitter - like the jump in S(y) around 0.03 arcsec - which can be filtered out during post-observation processing. Unfortunately, the extreme effects of vehicle jitter on the S-Curve shown in Figure 5.5b cannot be corrected for. Scans such as this would be deleted from further consideration in the analysis. Note the small variations in the S-Curve's wings seen near the extreme edges of the plot (i.e., ±0.08 arcsec) are due to photometric noise (the data presented in this example are from an observation of a bright V=9 star).

Drift

Drift was defined in Chapter 7, and its application to Position Mode observations has been discussed earlier in this chapter. Drift is also apparent in Transfer Mode observations but its removal from the raw data is straightforward; the cross-correlation of S-Curves, prior to binning and co-adding, automatically accounts for drift. Each individual S-Curve is shifted so that the particular feature of the S-Curve used for the cross correlation coincides with that of the fiducial S-Curve. However, the reliability of implicitly removing the drift is only as good as the accuracy of the cross correlation procedure.

For bright stars with $V < 13$, FGS drift is estimated to degrade the resolution of Transfer Mode observations by about 0.5 mas. For fainter

stars, the degradation is worse. If an observation of a faint star (V > 15) was subject to typical drift (10 to 12 mas), then the estimated loss of angular resolution would be ~ 2 mas.

Instrumental Stability

Analysis of observations of resolved objects (i.e, binary systems or extended sources) involves the de-convolution of the observed transfer function using reference S-Curves of point sources. The repeatability, or temporal stability, of point-source S-Curves has a direct effect on the reliability (or accuracy) of the scientific result. FGS3 continued to demonstrate a variability of ~ 15% in its X-axis S-Curve (as determined from repeated observations of a standard star). This effectively rendered FGS3 unreliable for observing close (separations < 20 mas) binary systems. However, FGS1r has demonstrated repeatability at the 2% level, implying reliable measurements of binary systems down to 7 mas.

Figure 5.6 on page 80 illustrates FGS3's persistent variability and FGS1r's stability over comparable timescales. Figure 5.6a shows FGS3's inherent variability in the S-Curves of the same point source over a 102-day span in 1997. Note this intrinsic variability in the instrument is indistinguishable from its interferometric response to a 15 mas binary with $\Delta m = 0.5$ mag (when compared with a point-source, as shown in Figure 5.6c). In contrast, the stability of FGS1r (Figure 5.6b) easily permits detection of the 15 mas binary system (Figure 5.6d) when compared to a point-source. We note the "difference" seen in Figure 5.6d are due to *systematic* changes in the observed interferogram (i.e., the object is resolved), not random effects.

As was discussed in chapter 4, FGS1r has shown a slow "evolution" of its y-axis S-curve. This should not compromise the reliability of this instrument for observing close binary systems; STScI will continue to observe calibration standards in each cycle as needed so that GOs have access to calibration data appropriate of a given epoch.

Figure 5.6: Temporal Stability: FGS3 v. FGS1r

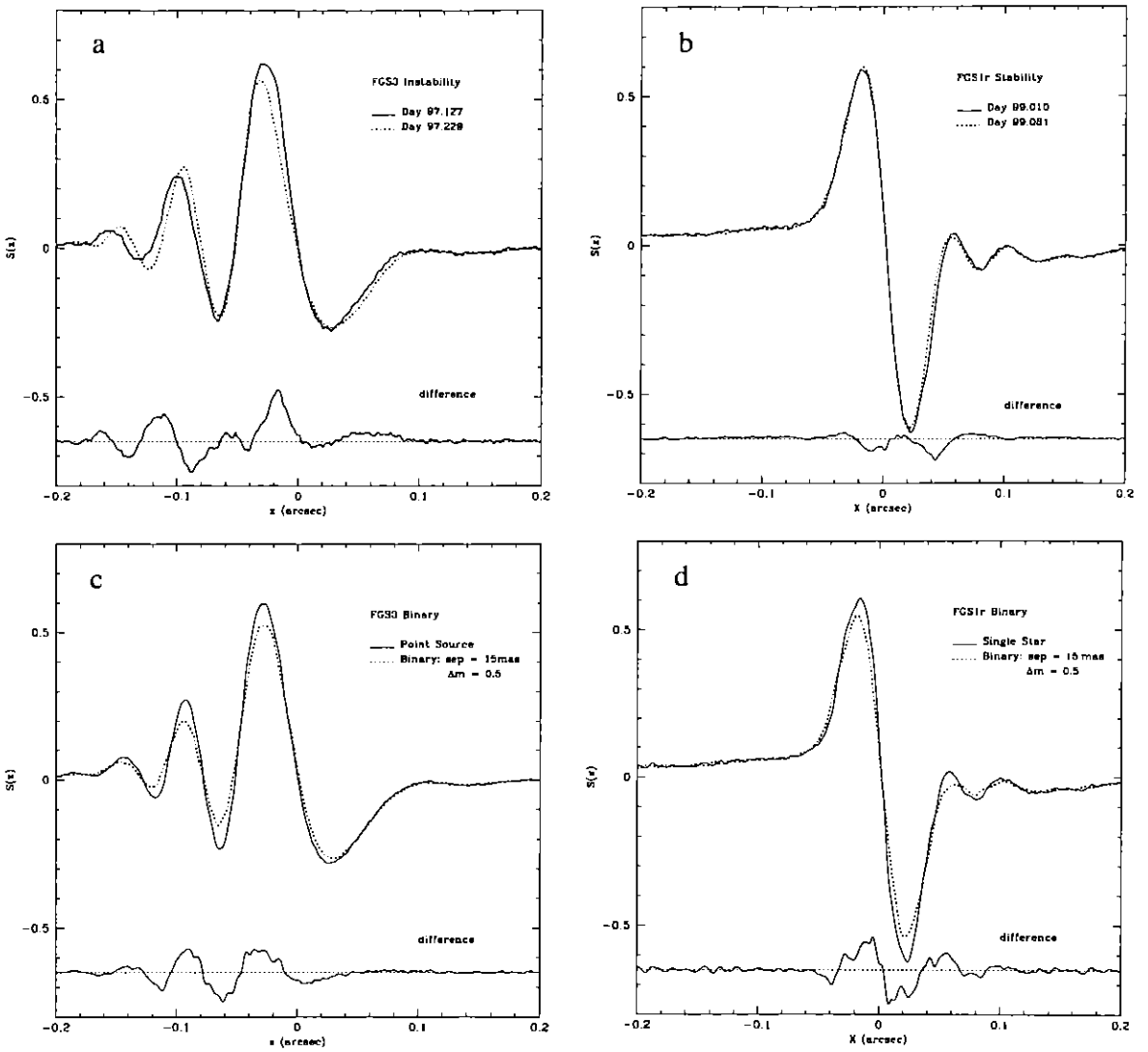

Interferometric Response and Source Color

The morphology and amplitude of the S-Curve is sensitive to the spectral color of the source. Experience with FGS3 has shown the point-source reference S-Curve should match the color of the target to within $\delta(B - V) = 0.3$ for proper analysis of close binaries (with

separations < 80 mas). FGS1r will be calibrated appropriately to meet the needs of the GO science program.

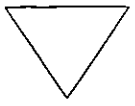

The point-source calibration S-Curves are obtained only at the center of the FGS1r FOV. Other locations in the FOV are not routinely calibrated.

The current FGS1r reference star color library is given in the following table.

Table 5.3: FGS1r Transfer Mode - F583W Observed Reference Star Colors

Reference Target	*V*	*B-V*	*Observed Filters*
HD 38666 (Mu Col)	5.15	-0.25	F5ND
NGC 188 UMK 69 (Upgren69)	9.60	0.50	F583W
HD233877	9.52	1.37	F583W
SA0185689	9.61	1.59	F583W

Transfer Mode Scale as a Function of HST Roll Angle

Testing of FGS1r during its commissioning in Cycle 7 revealed that the measured separation and position angle of the stars in a binary system is sensitive to the system's orientation relative to the interferometer axis and hence the HST roll angle. Over time, as a system is observed at a variety of HST roll angles, this introduces systematic errors into the derivation of the binary's apparent orbit. The error in the measured separation of the stars can be as large as ~ 1% of the true projected separations, so measurements of wide binaries are affected more than those of close systems. The effect is believed to be due to a small rotation error of the Koesters prism(s) about the normal to its entrance face.

During Cycle 9 a wide binary (KUI 83, component separation ~0.3") was observed with FGS1r in Transfer mode at three different HST roll angles (V3roll = 25, 43, 60 degrees). The measured total separation of the components was constant to about 1 mas, indicating that the scale is not dependent upon vehicle roll, in contradiction to the Cycle 7 results. STScI will monitor this aspect of FGS1r's performance, but at a low frequency (approximately every 2 to 3 years).

Linking Transfer and Position Mode Observations

It is possible to use the FGS in both Transfer and Position Mode during a given observing session (visit). As was mentioned in "Combining FGS Modes: Determining Stellar Masses" on page 35, by using Transfer Mode observations to determine a binary system's true relative orbit, and using Position Mode observations of nearby reference stars (and perhaps the binary as well) to determine the binary's parallax, the system's total mass can be derived. Furthermore, if the data are of sufficient quality, i.e., if the uncertainty in the position of each component with respect to the reference stars is small compared to the semi-major axis of the binary's orbit, then the motion of each component about the system's barycenter can be determined. From this information, the mass ratio, and hence the mass to luminosity ratio of each of the two stars, can be calculated.

Investigations of an extended source, such as a giant star, can also benefit from a combination of Transfer and Position Mode observations. If the FGS in Transfer Mode can resolve the disk and measure its angular size, and nearby stars are measured in Position Mode to derive the object's parallax, then the physical size of the disk can be determined.

In order to achieve these scientific objectives, the Transfer Mode data must be related to the Position Mode data. If the binary is observable in Position Mode, then it is straightforward to determine the offsets between the Position Mode reference frame and Transfer Mode positions. If the binary cannot be observed in Position Mode, then the task of relating the Transfer data to the Position data is more complex.

Linking a Transfer Mode observation of a binary system to Position Mode observations of reference stars in the same visit requires that the x,y coordinates of each of the binary's components, derived from analysis of the Transfer function, be mapped onto the same x,y coordinate system as the Position Mode observations (the visit level "plate"). This implies that all pertinent corrections and calibrations applied to Position Mode data must be applied to the Transfer Mode centroids, i.e., visit-level corrections for low frequency oscillations of the spacecraft's pointing, FOV drift, the OFAD, and the differential velocity aberration. The level of difficulty in accomplishing this task depends on the structure of the binary (i.e., the separation of the components and their relative brightness).

More information on analysis techniques can be found in the *HST Data Handbook*.

Cycle 10 Calibration and Monitoring Program

A short summary is given for each FGS1r calibration and monitoring observation included the Cycle 10 calibration plan. For specific information, please refer to the STScI FGS web page (under the topic "FGS and Calibration Plans") and to the HST Schedule and Program Information web page:

`http://presto.stsci.edu/public/propinfo.html`

Active FGS1r Calibration and Monitoring Programs

- Prop 8847: Long Term Monitoring of FGS1r in Position Mode
  - The open cluster M35 will be observed six times per year to evaluate the stability of the FOV, plate scale, and optical field angle distortions (OFAD) in FGS1r. Products will include calibration database parameters which remove these effects in science data.
- Prop 8898: Calibrating FGS1r's Interferometric Response as a Function of Spectral Color
  - Unresolved stars of a variety of (B - V) colors will be observed in Transfer Mode to calibrate the effect of color on a point-source S-Curve. In addition, each object will be observed in Position Mode to help calibrate the POS/TRANS offset as a function of color. These data will provide the GO with a library of appropriate point-source templates. This proposal also monitors the temporal stability of the S-curves since the target list includes stars that have been observed in Cycles 8 and 9.
- Prop 8899: Calibrating FGS1r Plate Scale in Position Mode
  - At least two stars from the Hipparcos Catalog, simultaneously present in the FGS1r FOV, will be observed in Position Mode along with reference field stars to determine the absolute plate scale of FGS1r to about 10^{-6}. (Note that the OFAD calibration does not solve for scale.)

Special Calibrations

The Cycle 11 calibration program will be defined a few months after the Phase II deadline for approved programs. It is expected that the same calibrations outlined here for recent cycles and the current Cycle 10 plan will be maintained for Cycle 11.

It is the intention of STScI to develop a calibration program that most effectively balances the needs of the community for obtaining excellent science results from the instrument with the limited resources available(e.g., a nominal limit of 10% time available for calibration). Common uses of the instrument will be fully calibrated.

In special circumstances proposers may wish to request additional orbits for the purpose of calibration. These can be proposed in two ways and should be for calibrations that are not likely to be in the core calibration programs. An example of a non-core calibration would be one that needs to reach precision levels well in excess of those outlined in Tables 5.1 and 5.2.

The first type of special calibration would simply request additional orbits within a GO program for the purpose of calibrating the science data to be obtained (see section 4.3 of the CP). In this case the extra calibration would only need to be justified on the basis of the expected science return of the GO's program.

The second type of special calibration would be performed as a general service to the community via Calibration Proposals (section 3.7 of CP). In this case the calibration observations should again be outside the core responsibilities of the FGS group to perform, and furthermore should be directed at supporting general enhancement of FGS capabilities with the expectation of separately negotiated deliverables if time is granted.

Proposers interested in obtaining either type of special calibration should consult with Instrument Scientists from the FGS Group via questions to the Help Desk at least 14 days before the proposal deadline in order to ascertain if the proposed calibrations would be done at STScI in the default program.

Observations obtained for calibration programs will generally be flagged as non-proprietary.

CHAPTER 6:

Writing a Phase II Proposal

In this chapter . . .

Phase II Proposals: Introduction / 85
Instrument Configuration / 87
Special Requirements / 90
Overheads / 93
Proposal Logsheet Examples / 95

This chapter is a practical guide to the preparation of Phase II proposals, and as such is relevant to those researchers who have been allocated HST observing time. For details or more general information, we refer the reader to the *HST Call for Proposals* and *Phase II Proposal Instructions*.

Phase II Proposals: Introduction

Required Information

The information required for Phase II proposals are:

- Precise target information: positions accurate to ± 3″, and V magnitude. Including $(B - V)$ color is strongly recommended, although not required in the proposal. The color, if available, is very important for two reasons: 1) archival identification; and 2) to help the FGS Instrument Scientist determine if the standard calibrations are appropriate for the proposal (especially if Transfer Mode is being used).

- Configuration and scheduling instructions for each exposure and visit, expressed in the specified proposal syntax.
- The relationship between the visits: scheduling, relative orientations, etc.
- Justification for special scheduling or configuration requirements.

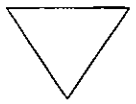

Important: A clear explanation for: 1) the use of special requirements; 2) the special design of a logsheet; or 3) the calculation of an exposure time, orient angle, or target offset, etc., will help STScI during the review and verification process. Text can be included in the "Additional Comments" section of the proposal or in the justification for real-time and special requirements. If an action is critical for the successful implementation of an exposure line, a short one-line comment (in the comments syntax) should be placed on individual exposure lines.

STScI Resources for Phase II Proposal Preparation

- ***RPS2:*** The Remote Proposal Submission-2, is the STScI interactive graphical software interface. RPS2 provides proposal preparation tools and several verification and error-checking phases: proposal syntax, operational feasibility, and schedulability. Proposers are strongly encouraged to make full use of this friendly and helpful software. The software is available on the World Wide Web at:

  `http://presto.stsci.edu/public/rps2home.html`

- ***Program Status:*** For proposal status, scheduling (visit level) information, weekly calendars, recent proposal listings (in RPS2 syntax and in a formatted listing), please consult the STScI web pages "Observing with HST":

  `http://www.stsci.edu/observing/resources.html`

- ***Contact Scientist:*** After HST observing time has been allocated by the TAC, a Contact Scientist may be assigned to the proposal. The objective of the Contact Scientist is to ensure the scientific return of the observing program is maximized.

Instrument Configuration

This section is designed to complement the section on FGS instrument parameters contained in the Phase II Proposal Instructions. Table 6.1 summarizes the FGS instrument parameters.

Table 6.1: FGS Instrument Parameters

Config	Aperture	Sp_Element	Opmode	Optional_Parameters
FGS	PRIME (=1) 1, 2, 3 (FGS1=FGS1r)	F5ND F550W F583W F605W(FGS1r,FGS3) F650W (FGS 2) PUPIL	POS	ACQ-DIST, ACQ-MODE, COUNT, FESTIME, NULL, LOCK
			TRANS	ACQ-DIST, ACQ-MODE, SCANS, STEP-SIZE

Aperture

The aperture must be defined as either Prime or "1" on the logsheet. One FGS is designated as the astrometer: FGS1r is designated for Cycle 8 and beyond. For illustrations of the FGS1r field of view in the HST focal plane, refer to Chapter 1.

Spectral Element

"Spectral Element" refers to filters, etc. chosen for the observation. For FGS1r, the available filters are: F583W, F5ND, PUPIL, F605W, and F550W. Only one filter can be in place for an exposure, though multiple filters can be used during a visit (check that calibrations are available for the configuration). Recommendations for specific mode and filter combinations are discussed in Chapters 5 and 7. Table 6.2 presents a summary of the calibrated modes and filter configurations.

Table 6.2: Summary of Calibrated Mode and Filter Combination

Mode	Filter	Status	Comments
Position Mode:	F583W	Calibrated across entire FOV	OFAD in F583W only
	F5ND	Calibrated at the center of the FOV	Cross-filter calibration with F583W
Transfer Mode:	F583W; Others as needed	• All calibrations at FOV center • Select reference S-Curves from library of standard stars • If needed, propose for calibration time to observe a reference standard star at the same epoch as the science visit (see Chapter 7).	Availability of standard stars with appropriate spectral energy distributions, i.e., colors of reference star and science target should differ by no more than $\delta(B\text{-}V) \sim 0.3$

Mode

Two operation modes are available: Position Mode (POS) for measuring relative astrometric positions of targets in the FGS FOV and Transfer Mode (TRANS) for obtaining high resolution interferometry.

Optional Parameters for FGS Exposures

A program is customized by specifying optional parameters for each exposure. Table 6.3 and Table 6.4 list the optional parameters, default values, and recommended settings for Position and Transfer Modes, respectively.

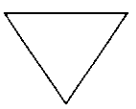

Many of the optional parameters have** default values. **In such cases, the entry for that optional parameters may be omitted. If an observer wishes to** override the default value, **the parameter and its value must be specified.

Table 6.3: Position Mode Optional Parameters

Optional Parameter	Allowed Values	Comments and Recommendations
ACQ-DIST	DEF (default=15), 0.0 to 90.0 Units: arcsec	Determines the size (in arcseconds) of the search region. For ACQ-MODE=SEARCH, ACQ-DIST is the maximum radius of the search spiral. *Recommendation*: Although Search radii up to 90 arcsec are allowed, larger values *must be used with caution*, i.e., the larger the search radius, the more potential to acquire a spurious nearby star. If the target coordinates are expressed with respect to the Guide Star System, the default value of 15 arcsec (radius) should be sufficient to find the target. Typically the target is found with 0.3 to 1.0 arcsec. *Reference:* Appendix 1: Target Acquisition
ACQ-MODE	SEARCH (default) Units: None	Determines the strategy for locating the target. The Search Phase is the initial outward spiral to find and identify the target. The sequence of Search, CoarseTrack, WalkDown, and FineLock is the standard astrometry target acquisition scenario. No other options are available. *Requirement*: Default "SEARCH" *Reference*: Appendix 1: Target Acquisition

Table 6.3: Position Mode Optional Parameters (Continued)

Optional Parameter	Allowed Values	Comments and Recommendations
COUNT	DEF (default), 1–2621400 Units: FGS PMT counts	Expected count rate [target + background]. When the default is set, the count rate is calculated (by the proposal processing software) from the target V magnitude, filter, and aperture. The default background rate (from in-orbit measurements) is 712 counts/sec for all four PMTs. *Recommendation*: Allow the system to select the default. The default values are calculated using in-orbit photometric calibrations with accuracies appropriate for guiding purposes and for the calculation of exposure times. A few special cases may require non-default values and are discussed in the text. *Reference*: Chapter 7: See sections on Position and Transfer Mode Signal to Noise and Exposure calculation sections.
FESTIME	DEF (default), 0.025, 0.05, 0.1, 0.2, 0.4, 0.8, 1.6, 3.2 Units: seconds	Sets the averaging time for the Fine Error Signal (in seconds). The FESTIME also determines the rate at which the star selectors are adjusted to null the fine error signal. *The default value for Position Mode is calculated from the COUNT parameter if explicitly entered, or if COUNT defaults to the V magnitude and the filter. All Transfer Mode observations use FESTIME = 0.025 seconds.* *Recommendation*: The algorithm that selects the default FESTIMEs from the specified brightness of the target is based on photon statistics and a conversion from photon noise to equivalent positional error. For fainter targets, longer integration times are supplied by the default algorithm to assure that the FGS can track the fringe and remain in FineLock. For non-point sources, the S-Curve amplitude is reduced because of the increased contribution of the background or companion. In these cases, it may be desirable to adjust the FESTIME. Please consult with STScI. *Reference*: Chapter 7: See Sections on Position and Transfer Mode Signal to Noise and Exposure calculation sections.
LOCK	FINE (default), COARSE, 0.0–1.0 Units: None	The method used by the astrometer to track the science or reference target. (Note, this parameter does not specify the HST guiding mode). Because of the excessive wear to bearings inside the instrument, CoarseLock is no longer allowed. *Requirement*: Fine. *Reference:* Chapter 5 and Chapter 7.
NULL	YES, NO (default) Units: None	Determines whether the next FESTIME begins immediately after the previous one or not until the star selectors have been repositioned. This parameter may be applicable for very fast moving target. Observers should consult with STScI before specifying non-default values. *Recommendation*: This use of this parameter is limited to a few specific observation scenarios. Most standard astrometry programs require NULL=NO. *Reference*: STScI will alert the proposer if a non-default value is required.

Table 6.4: Transfer Mode Optional Parameters

Optional Parameter	Allowed Values	Comments and Recommendations
ACQ-DIST	DEF (default = 15), 0.0 - 90.0 Units: arcsec	Determines the size (in arcseconds) of the search region. For ACQ-MODE=SEARCH, ACQ-DIST is the maximum radius of the search spiral. *Recommendation*: Although a search radius of up to 90 arcsec is allowed, larger values must be used with caution, i.e., the larger the search radius, the more potential to acquire a spurious nearby star (spoiler). If the target coordinates are expressed with respect to the Guide Star System, the default value of 15 arcsec (radius) should be sufficient to find the target. HST's pointing accuracy usually places the target within 1 arcsec of the expected location in the FGS. *Reference*: Appendix 1: Target Acquisition
ACQ-MODE	SEARCH (default) Units: arcsec	Determines the strategy for locating the target. The search phase is the initial outward spiral to find and identify the target. The sequence of Search, CoarseTrack, WalkDown, and FineLock is the standard astrometry target acquisition scenario. No other options are available. *Requirement*: Default "SEARCH" *Reference*: Appendix 1: Target Acquisition
SCANS	1 (default)–200 Units: None	Determines the number of separate scan lines. Successive scans are taken in opposite directions. *Recommendation*: Determine the number of scans to achieve the required signal-to-noise. *Reference*: Chapter 7
STEP-SIZE	1.0 (default) 0.3–10.0 Units: mas	The angular distance (in mas) stepped by the IFOV along an interferometric axis in 0.025 seconds. *To achieve the best results, step sizes of 0.6 or 1 mas should be selected.* *Recommendation*: Value depends on the science target and goals of the observation, required resolution and signal-to-noise. *Reference*: Chapter 7

Special Requirements

In this section, we describe several special requirements which are often needed in an FGS Phase II observing proposal.

Visit-Level Special Requirements

Many visit-level special requirements are outlined in the Phase II Proposal Instructions. Those most applicable to FGS programs are:

Spacecraft Orientation ORIENT:

- *Definition*: The angle from North to the +U3 axis of the HST measured in the direction of +U2. The `ORIENT` special requirement is useful for arranging the targets optimally in a field or for aligning an eigenaxis of a science target with an FGS axis with the goal of maximizing the scientific return. Along with the `ORIENT` angle, a tolerance must be specified.
- *Calculation*: Two angles must be known in order to calculate a special `ORIENT` angle: the angle from North to the eigenaxis of the target (measured in the direction of East), and the angle between the +U3 axis to the FGS $+Y_{POSTARG}$ axis measured in the direction of +U2. The latter input angle is given in Table 7.3 of the Proposal Instructions and in Chapter 2. (Note that the values are different for FGS1r and FGS3.)
- *Accuracy*: The HST roll angle precision depends on the relative guide star position errors and the FGS alignment calibration errors (when two guide star FineLock is used). The pre-designated roll angle for a two-guide star FineLock tracking will be accurate to ≤ 0.04 degrees.
- Recommendations when `ORIENT` is used in the proposal:
  - Explain, in the "Additional_Comments" text section of the proposal, the method used to calculate `ORIENT` so that STScI understands the requirements.
  - `ORIENT` is considered a *Special Scheduling Request* and as such, must be justified in the proposal and will affect the schedulability of the visit. Setting the `ORIENT` tolerance to as large a range as possible (and still be within the bounds of the scientific requirements) will help to lessen the scheduling impact.

Timing Requirements:

- *Definition:* Timing links between visits are fairly common for FGS observations. For Position Mode exposures, timing links may be necessary for parallax work in which a subsequent exposure should be taken six months after the previous exposure. Transfer Mode observations may also make use of timing requirements: if a calibration exposure is to be made, it is often prudent to schedule the calibration exposures close in time to the science observation. Timing links on the Visit level include: BEFORE, AFTER, BETWEEN [dates], GROUP [the following visits] WITHIN [xxx hours, or xxx orbits], etc. See the Phase II Proposal Instructions for the complete list.

- *Note*: Timing requirements place restraints on the schedulability of the visit. Specify the largest tolerance on the timing constraint that the science can accommodate.

Exposure-Level Special Requirements

All available exposure-level special requirements are described in detail in the Phase II Proposal Instructions. Of these, the following three types are most often used in connection with FGS observations.

POS TARG:

- *Definition*: The ΔX and ΔY offset of a target from the standard aperture reference position are the POS TARG coordinates. They are specified in arcseconds and with respect to special coordinate systems which are illustrated and described in Chapter 2 and in the Phase II Proposal Instructions. POS TARG is used to position a target at various points in the FGS FOV. For example, a common use in Position Mode observations is to place the science target at a position near the center while also accommodating the largest number of reference targets. In Transfer Mode, since calibrations are only available at the center reference point, the POS TARG is not recommended.
- Recommendations when POS TARG is used in the proposal:
  - The POS TARG reference frame is centered (0,0) at the standard reference position of the aperture and is *not* equivalent to the FGS detector reference frame (the two frames have different parities and different origins). See Chapter 2.
  - The POS TARG specification refers to the final offset position of the target (and not to the motion of the telescope to carry the target to its destination).

SAME POS AS:

- *Definition:* The position and orientation of the spacecraft may be held constant over the course of all observations within a given visit by use of the exposure-level special requirement SAME POS AS. This requirement is virtually *always* used for Position Mode visits.

SEQ NON-INT:

- *Definition:* To ensure that all exposures within a visit are scheduled in the same orbit, the SEQ NON-INT special requirement should be used, otherwise the system may divide the exposures over several orbits, requiring guide star re-acquisitions, each of which takes several minutes to execute (time which could be spent on target).

Do not hesitate to explain the use of any special requirements in the proposal text. The more explanation, the easier for STScI to understand your requirements and schedule the proposal

Overheads

The assessment of the total spacecraft time needed by a program should take into account the overheads associated with various types of observations. Overheads are incorporated into the RPS2 proposal processing algorithm.

Position Mode Overheads

Table 6.5 lists the estimated overheads associated with guide star and astrometry star acquisitions and slewing of the IFOV in the pickle. Columns 2 and 3 in Table 6.6 list an average overhead for each exposure and the recommended total exposure time (see Table 4.5), both presented as a function of target magnitude. *Total spacecraft time* is estimated by combining columns 2 and 3. Note that the overheads in Table 6.5 are based on FGS3 characteristics. Slight modifications (a few seconds) may be needed to accommodate FGS1r characteristics.

Table 6.5: Position Mode Overheads

Activity Description	Duration	Comments
Initial guide star acquisition	6 min	Two-guide star FineLock
IFOV slew to target	17 sec + 6 x dist (in arcmin)	
Astrometry target acquisition: • Search • CoarseTrack • FineLock Acquisition	 • 5 sec • 13 sec or 21 sec • varies with V	(Each science target and reference star) • For a 15 arcsec search radius. • For V < 14 and V > 14 respectively • For V<12: ~3 sec duration; For V>16: ~400 sec duration.
Guide star re-acquisition	5 min	Relevant for contiguous multi-orbit visits.

Table 6.6: Position Mode Overheads and Exposure Time vs. Magnitude for FGS3

V Magnitude	Estimated Overhead per exposure (minutes)	Exposure Time[a] in seconds
8–12	0.6	20
13	0.7	20
14	2	30
15	3	45
16	8	45
17	8	50

a. For total spacecraft time, add columns 2 and 3.

Transfer Mode Overhead

The overheads for the activities which occur during Transfer Mode exposures are listed in Table 6.7. The guide star and astrometry star acquisition scenarios for Position Mode and Transfer Mode are identical through the CoarseTrack phase.

The average overhead for a Transfer Mode exposure is ~2 minutes.

Table 6.7: Transfer Mode Observing Overheads

Activity Description	Duration	Comments
Initial guide star acquisition	6 min	Two-guide star FineLock
Astrometry target acquisition: • Search • CoarseTrack	 • 5 sec • 13, 21 sec	(Each science target and reference star) • For a 15 arcsec search radius. • For V < 14 and V > 14 respectively
Time for IFOV to slow and reverse scan direction	15 sec/scan	
Guide star re-acquisition	5 min	Relevant for contiguous multi-orbit visits.

Proposal Logsheet Examples

This section provides several examples of proposal logsheets for the following types of investigations:

- "1. Parallax Program with Position Mode" on page 95
- "2. Bright Binary with Transfer Mode" on page 99
- "3. Mass Determination: Transfer and Position Mode" on page 102
- "4. Faint Binary with Transfer Mode: Special Background and Roll Angle Measurements" on page 104

1. Parallax Program with Position Mode

- **Goal**: Determine the parallax and proper motion of star, "OGF_1".
- **Scenario:**
  - The program requires three visits, at 0, 6, 12 months intervals. Best results are obtained if these visits are timed to occur at epochs of maximum parallax factor.
  - A special orientation is needed to accommodate target and reference star geometry (for this example). The Orient can be determined from using special tools (e.g., PICKLES or VTT)
  - Target Filter: For Science target (V = 9): F583W.
  - Reference Star Filter: (all reference stars V > 10)): F583W.
  - Reference Star Geometry: Six reference stars near science target; POS TARG required to fit all reference stars in the pickle. See Table 6.1 on page 96.
- **Special Considerations:**
  - The need for special orientation must be explained in the text justification section.
  - The science target must be shifted from FGS1r aperture reference point in order to fit all (i.e., OGF-21-REF) stars in the pickle. Appropriate POS TARG can be determined from PICKLES or VTT. Contact STScI Help desk for assistance if necessary.
- **Target Logsheet:**
  - See Proposal Instructions for guidance.
  - Please include color information on all targets if available so color-related calibrations can be assessed by STScI.

Table 6.1 on page 96 illustrates the field geometry and the orient angles of a typical FGS observation, while Table 6.8 on page 96 summarizes the details of the exposures in the visit.

Figure 6.1: Example 1: Field of View at Special Orientation

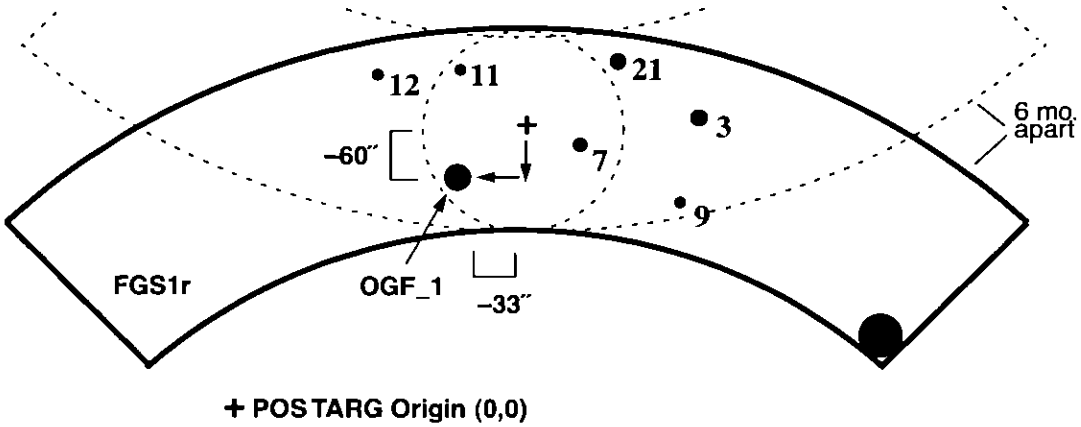

Visits 1 and 3

θ = Off-Nominal Orient Angle = 48°

γ = Nominal Orient Angle = 67°
(6 months later, FOV is rotated 180 degrees)

ORIENT -19° FROM NOMINAL

POS TARG (-60,-33)

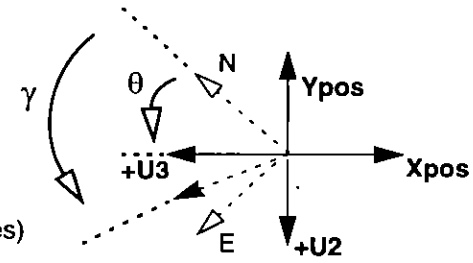

Table 6.8: Target and Exposure Input for Example 1

Target	V	FILTER	FESTIME (default)	Exposure Time (seconds)	~NEA for Single Exposure (mas)
"OGF_1"[a]	9	F583W	0.025	20	< 1.0
OGF-3-REF[a]	11.1	F583W	0.025	20	< 1.0
OGF-7-REF[a]	10.3	F583W	0.025	20	< 1.0
OGF-9-REF	10.2	F583W	0.025	20	< 1.0
OGF-11-REF[a]	13.3	F583W	0.050	30	3.1
OGF-12-REF	13.6	F583W	0.050	30	3.5
OGF-21-REF	11.5	F583W	0.025	20	1.0

a. REF must be included in REFERENCE and CHECK STAR NAMES to inform the planning system that slews between stars are done by moving the FGS IFOV and not the entire HST.

- **Reference/Check Star Pattern:** Check Stars in this observation are REF-7, REF-11, and OGF_1:

OGF_1--> 12 -- 11 -- 7 -- OGF_1 -- 11 -- 21 -- 3 -- 7 -- OGF_1
-----> 9 -- 7 -- 11 -- OGF_1 -- 21 -- 12 -- 11 -- 9 -- OGF_1

- **The RPS2 Exposure Logsheet Template:** The Optional_Parameters entry is missing since, for this example, all Position Mode Optional Parameters are DEFAULT values

```
Visit_Number: 1
Visit_Requirements: BETWEEN 14-MAR-1998 AND 15-MAR-1998
ORIENT -18.5D TO -19.5D FROM NOMINAL
Visit_Comments: Two Guide Star FineLock Required.Exposure_Number: 01
         Target_Name: OGF_1
              Config: FGS
              Opmode: POS
            Aperture: 1
          Sp_Element: F583W
Number_of_Iterations: 1
   Time_Per_Exposure: 20S
Special_Requirements: SEQ 1-4 NON-INT;POS TARG -33,-60.

     Exposure_Number: 02
         Target_Name: OGF-12-REF
              Config: FGS
              Opmode: POS
            Aperture: 1
          Sp_Element: F583W
Number_of_Iterations: 1
   Time_Per_Exposure: 30S
Special_Requirements: SAME POS AS 1;

     Exposure_Number: 03
         Target_Name: OGF-11-REF
              Config: FGS
              Opmode: POS
            Aperture: 1
```

```
          Sp_Element: F583W
Number_of_Iterations: 1
   Time_Per_Exposure: 30S
Special_Requirements: SAME POS AS 1;
Comments:

     Exposure_Number: 04
         Target_Name: OGF-7-REF
              Config: FGS
              Opmode: POS
            Aperture: 1
          Sp_Element: F583W
Number_of_Iterations: 1
   Time_Per_Exposure: 20S
Special_Requirements: SAME POS AS 1;
Comments:
```

...and continues until the orbit is filled.

```
6-months after Visit 1, the HST Nominal Orient
Angle is 180° from the Nominal HST Orientation in
Visit 1.
NOMINAL ORIENT ANGLE = 247°
OFF-NOMINAL ORIENT ANGLE = 228°
POS TARG (+60,+33)
```

```
Visit_Number: 2
Visit_Requirements: BETWEEN 14-SEP-1998 AND 15-SEP-1998;
                    ORIENT -18.5D TO -19.5D FROM NOMINAL
Visit_Comments: Two Guide Star FineLock Required.
Exposure_Number: 01
         Target_Name: OGF_1
              Config: FGS
              Opmode: POS
            Aperture: PRIME
          Sp_Element: F583W
Number_of_Iterations: 1
```

```
   Time_Per_Exposure: 20S
Special_Requirements: SEQ 1-4 NON-INT;POS TARG +33,+60
Comments:
     Exposure_Number: 02
         Target_Name: OGF-12-REF
              Config: FGS
```

...Continues until the orbit is filled.

.....

Visit_Number 3 is similar to Visit 1 since it occurs 1 year later.

Running the proposal template file through RPS2 will inform the observer whether the syntax is correct, whether the exposures fit in an orbit and how much time is left, and finally whether the observing dates are viable for the requested ORIENT angle.

2. Bright Binary with Transfer Mode

- **Goal**: To look for a companion to a highly variable Ae/Be star
- **Scenario:**
  - Program requires four visits, once per month.
  - Special orientation to accommodate target geometry.
  - Target filter: F583W.
  - The target "Twin_Shell" has a magnitude V = 13.0.
  - The target is essentially a point source, i.e., expected separation of binary if present is less than 40 mas.
- **Special Considerations:**
  - The need for Special Orientation must be explained in the text Justification section.
  - Please include color information on all targets especially when Transfer Mode is being used. STScI will use the information to plan the calibration observations of the color reference standard stars.
- **Exposure Time Calculation**
  - Target Magnitude in F583W: 13.0
  - FESTIME: 0.025 for all Transfer Mode observations
  - FGS Count Rate: 10387.9 counts/sec (2 PMTs—from photometric calibration, Chapter 7).
  - Background Count Rate Estimation: 712 counts/sec.
  - ScanLength: 1.6 arcsec.

- StepSize: 0.6mas (but binned later to 1 mas).
- Target Visibility Period: 58 Minutes.
- Total Exposure Time: 39 minutes.
- Exposure Time Calculation:

$$T_{exposure} = 0.025 * [ScanLength/StepSize] * N_{scans}$$

where in this example ScanLength = 1.6 arcsec, StepSize = 0.0006 arcsec, and the number of scans N_{scans} = 35.
Note: This exposure time allows for the overheads described in previous chapters, assuming a target visibility time of ~ 58 minutes.

Figure 6.2 on page 100 illustrates the geometry of the binary with respect to the POS TARG and detector reference frames.

Figure 6.2: Example 2: Field of View at Special Orientation

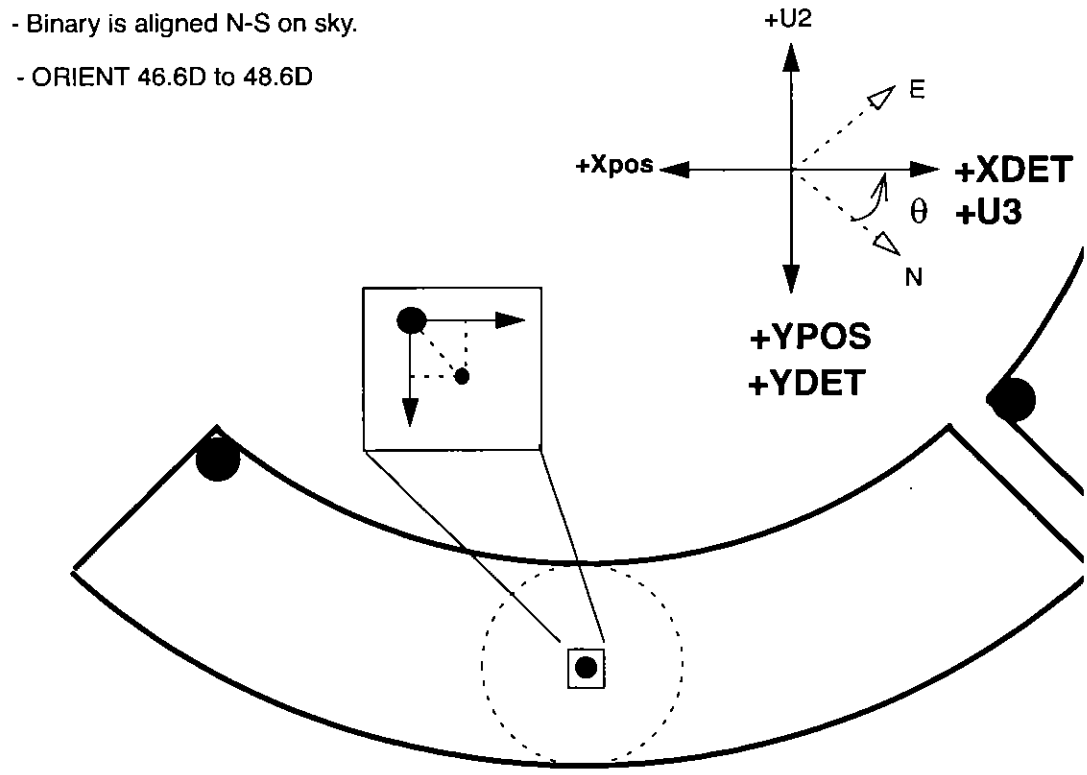

- **The RPS2 Exposure Logsheet Template:**

```
Visit_Number: 1

Visit_Requirements: ORIENT 46.6D TO 48.6D

Visit_Comments: Two Guide Star FineLock Required. Please notify Contact
Scientist if two guide stars cannot be found.


Exposure_Number: 01
```

```
         Target_Name: TWIN_SHELL
              Config: FGS
              Opmode: TRANS
           Aperture: 1
          Sp_Element: F583W
Optional_Parameters: SCANS=35, STEP-SIZE=0.6
Number_of_Iterations: 1
   Time_Per_Exposure: 2333S
Special_Requirements:
Comment:
Visit_Number: 2
Visit_Requirements: AFTER 1 BY 30D TO 32D
                    ORIENT -24D TO -25D FROM NOMINAL
Visit_Comments: Two Guide Star FineLock Required.
Exposure_Number: 01
         Target_Name: TWIN_SHELL
              Config: FGS
              Opmode: TRANS
           Aperture: 1
          Sp_Element: F583W
Optional_Parameters: SCANS=35, STEP-SIZE=0.6
Number_of_Iterations: 1
   Time_Per_Exposure: 2333S
Special_Requirements:
```

And similar Visits for 3 and 4.

Running the proposal template file through RPS2 will inform the observer whether the syntax is correct, whether the exposures fit in an orbit and how much time is left if they do not; and finally, whether the observing dates are viable for the requested ORIENT angle.

3. Mass Determination: Transfer and Position Mode

- **Goal**: Determine the parallax, proper motion, and reflex motion using Position Mode and the relative orbit using Transfer Mode.
- **Scenario:**
  - Program requires two visits every six months for three years.
  - Target Filter: F583W.
  - Reference Star Filter: F583W.
  - Reference Star Geometry: Six reference stars near science target; science target must be placed at aperture reference position for Transfer Mode observations.
- **Special Considerations:**
  - Please include color information on all targets if available so color-related effects can be assessed.
  - Exposure Time Calculation:
  - Target Magnitude in F583W: 13.0
  - FESTIME: 0.025 for all Transfer Mode observations.
  - Exposure Time Estimate FGS Count Rate: 10387.9 counts/sec (From photometric calibration, Chapter 7); Background Count Rate Estimation: 712 counts/sec.
  - ScanLength: 1.6 arcsec.
  - StepSize: 0.6mas (but binned later to 1 mas).
  - Target Visibility: 63 minutes.
  - Total Transfer Mode Exposure Time: 28 minutes.

  - Exposure Time Calculation:

$$T_{exposure} = 0.025 * [ScanLength/StepSize] * N_{scans}$$

where in this example ScanLength = 1.6 arcsec, StepSize = 0.0006 arcsec, and the number of scans $N_{scans} = 25$

Figure 6.3 on page 103 illustrates the geometry of the target and reference stars, while Table 6.9 on page 103 and Table 6.10 on page 104 summarize the details of the exposures in the visit.

Figure 6.3: Example 3: Transfer + Position Mode Visits

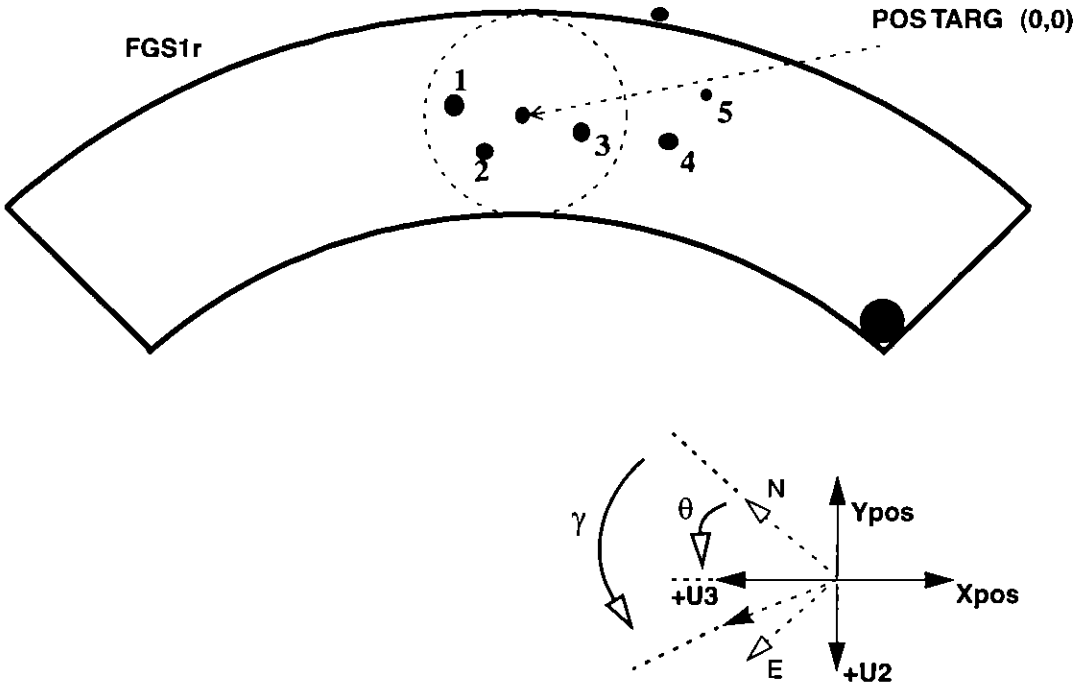

Table 6.9: Target and Exposure Input for Example 3

Target	V	FESTIME	FILTER	Total Exposure	~NEA for one exposure (mas)
FB424242[a] Position Mode	13.0	0.050	F583W	20 sec	2.0
FB424242 Transfer Mode	13.0	0.025	F583W	28 min	$\sigma_{Sx} = 0.008$
BL-1-REF[b]	10.8	0.025	F583W	20 sec	<1.0
BL-2-REF	14.1	0.100	F583W	35 sec	5.0
BL-3-REF	11.5	0.025	F583W	20 sec	1.0
BL-4-REF	12.5	0.025	F583W	20 sec	1.7
BL-5-REF	13.0	0.050	F583W	20 sec	2.5

a. The primary target needs only be listed once in the fixed target list.
b. REF must be included in REFERENCE and CHECK STAR NAMES to inform the planning system that slews between stars are done by moving the FGS IFOV and not the entire HST.

Table 6.10: Reference/Check Star Pattern

Mode	Overhead + Exposure Time (Minutes)
GS ACQ	7
TRANS Mode	
• FB424242	28 + 9
POS Mode:	
• FG424242	2
• BL-3-REF	1
• BL-2-REF	2.5
• BL-1-REF	1
• FB424242	2
• BL-3-REF	1
• BL-4-REF	1
• FB424242	2
POS Mode	
• BL-3-REF	1
• BL-1-REF	1
• FB424242	2

4. Faint Binary with Transfer Mode: Special Background and Roll Angle Measurements

- **Goal**: Observe a faint binary (V = 15.5) in Transfer Mode. Special background observations are needed to insure an accurate background assessment. In addition, the roll angle of HST will be determined empirically using Position Mode observations of the science target and a reference star.
- **Scenario:**
  - Program requires two visits every six months for three years.
  - Program requires two orbits per visit to achieve signal-to-noise in Transfer Function.
  - Target Filter: F583W.
  - Reference Star Filter: F583W.
  - Geometry: Target is placed at center of the FOV; the background observation is obtained in a dark region (specified in the proposal as a pointed target); the reference star for the Position Mode observation is also nearby.
- **Exposure Time Calculations:**
  - Target Magnitude in F583W: 15.5
  - Transfer Mode Parameters:

- FESTIME: 0.025 for all Transfer Mode Observations.
- Exposure Time Estimate: FGS Count Rate: 1039 counts/sec (From the photometric calibration, Chapter 2); Background Count Rate Estimation: 712 counts/sec.
- ScanLength: 1.6 arcsec.
- StepSize: 1 mas.
- Total Visibility Period: 48 minutes.
- Total Transfer Mode Exposure Time: 23 minutes.

- Exposure Time Calculation:

$$T_{exposure} = 0.025 * [ScanLength/StepSize] * N_{scans}$$

where in this example ScanLength = 1.6 arcsec, StepSize = 0.0006 arcsec, and the number of scans $N_{scans} = 20$

- **Background Observation:**
  - A special background observation is needed because the target is faint and its binary characteristics are at the resolution limit of the FGS1r. The implementation of the background exposure incorporates the following:
  - Guide star acquisition: 7 minutes.
  - Total Transfer Mode exposure and overhead time: 32 minutes.
  - Total Position Mode exposure and overhead time: 6 minutes.
  - Select a position of dark sky near the target.
  - Specifying the target coordinates of the dark region in RA and DEC rather than POS TARG will guarantee that the same area of the sky is measured in each visit.
  - Enter the dark target as a unique entry in the Target Position Logsheet, with the suffix "-REF".
  - Specify the dark target to be bright, V = 12, to minimize overheads. The photometry will be available, though the "acquisition" will fail.
  - Create a Position Mode exposure line for the dark target, with an exposure time of ~30 seconds. Position Mode is selected for the background measurement simply because it has fewer overheads.
- **Position Mode Observations for Roll Determination:**
  - Position Mode exposures of the faint binary and a nearby reference star are needed to empirically determine the HST roll angle at the time of the observation.
  - Observe the binary in Position Mode to expedite data analysis. See Chapter 7.

Figure 6.4 illustrates a possible geometry of the field, while Table 6.11 summarizes the FESTIMES and total exposure times for the target, reference star, and dark sky observations.

Figure 6.4: Example 3: Transfer + Position Mode Visits

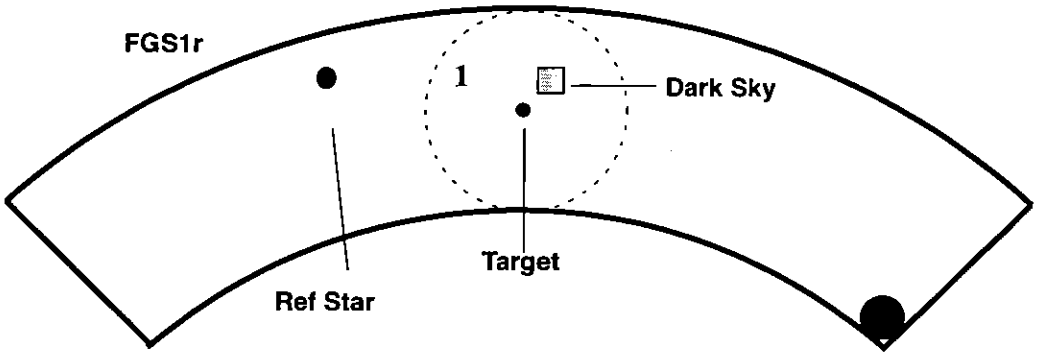

Table 6.11: Target and Exposure Input for Example 4

Target	V	FETIME	FILTER	Total Exposure
HDFAINT Position Mode	15.5	0.40	F583W	45 S
HDFAINT Transfer Mode	15.5	0.025	F583W	23 min
JH-1-REF Position Mode	10.8	0.025	F583W	20 S
DARK_SKY-REF Position Mode	12	0.025	F583W	30 S

- **The RPS2 Exposure Logsheet Template:**

```
Visit_Number: 1
Visit_Requirements: BETWEEN JUN-9-1998 AND JUN-10-198
Visit_Comments:

Exposure_Number: 01
        Target_Name: DARK_SKY-REF
             Config: FGS
             Opmode: POS
```

```
Aperture: 1
          Sp_Element: F583W
Optional_Parameters:
Number_of_Iterations: 1
   Time_Per_Exposure: 30 S
Special_Requirements: SEQ 1-5 NON-INT, SAME POS AS 3
Exposure_Comment: Background Measurement, no target in field.
Special_Requirements: SAME POS AS 03

Exposure_Number: 02
         Target_Name: JH-REF-1
Config: FGS
              Opmode: POS
            Aperture: 1
          Sp_Element: F583W
Optional_Parameters:
Number_of_Iterations: 1
   Time_Per_Exposure: 20 S
Special_Requirements: SAME POS AS 03


Exposure_Number: 03
         Target_Name: HDFAINT
              Config: FGS
              Opmode: TRANS
            Aperture: 1
          Sp_Element: F583W
Optional_Parameters: SCANS=35, STEP-SIZE=1
Number_of_Iterations: 1
   Time_Per_Exposure: 1333S
Special_Requirements:

Visit_Number: 2
Visit_Requirements: AFTER 01 BY 28D TO 32D
.... and so on.
```

CHAPTER 7:

FGS Astrometry Data Processing

In this chapter . . .

Data Processing Overview / 109
Exposure-Level Processing / 110
Visit-Level Processing / 113
Epoch-Level Processing / 115

This chapter describes the FGS astrometry data processing pipeline and analysis tools. The steps to reduce and calibrate the raw data are described along with the sequence in which they are applied.

Data Processing Overview

FGS Astrometry observations are analyzed at three distinct levels, the *exposure-level* (individual observations), the *visit-level* (all observations within the HST orbit), and the *epoch-level* (relating data from one visit to others). The astrometry data pipeline processes the observations up to and including the visit level. Epoch-level analysis requires tools beyond the scope of the FGS data pipeline.

The exposure- and visit-level corrections and calibrations are performed by the observer using *calfgsa* and *calfgsb* which are implemented as tasks in STScI's STSDAS system. These tasks are semi-automated and require little user input to process the individual exposures that comprise the typical astrometry visit. Reference files used by these tasks are maintained by STScI and can be found by following the links to the calibration sections of the FGS Web Site at

http://www.stsci.edu/instruments/fgs/.

Epoch-level analysis of FGS data is not, by its nature, a procedure which lends itself to generic pipeline processing. However, tools to provide the observer with some of the more common manipulations encountered in data analysis of FGS astrometry observations are being made available to the general FGS user. Currently, these tools are not STSDAS tasks, but a collection of stand-alone scripts and executable files to achieve plate solutions for Position Mode observations and the deconvolution of binary star transfer functions from Transfer Mode observations.

The processing and analysis applied at each level is discussed below. Interested readers are encouraged to monitor the STScI newsletter or visit the FGS web site for updates to the status of these tools. More detailed discussions can be found in the *HST Data Handbook*, version 4.0 or later.

Exposure-Level Processing

The term "exposure-level processing" refers to pipeline corrections that are applied to the individual FGS observations. These are discussed in this section.

Initial Pipeline Processing

Regardless of the observing mode, several activities are carried out during the initialization of the astrometry pipeline. This begins with the usual file management, data quality assessments, and the determination of the required reference files and their availability status. At this early stage, the data are inspected to determine the identification of the astrometer FGS, its mode of operation, and the availability of guide star data from the guiding FGSs. The astrometer's data are inspected to evaluate the outcome of the Search, CoarseTrack, and FineLock target acquisitions, while the guide star data are inspected to identify the guiding mode (i.e., was the spacecraft guided by one or two guide stars, and were the guide stars tracked in FineLock?).

If the astrometry target acquisition failed, the FGS flags and status bits are inspected to determine the cause. In this case, data processing proceeds as far as possible (in the event that the observation was a partial success), output files are generated and populated appropriately, and pipeline processing of the observation terminates.

Observing Mode Dependent Processing

After pipeline initialization and data quality assessments, successful observations (i.e., those that acquired the target), are processed according to the FGS observation mode: Position or Transfer.

Position Mode

The goal of exposure-level Position Mode pipeline processing is to determine the centroid of the IFOV while the FGS tracked the object in FineLock. A collateral objective is to analyze the individual PMT data, both to determine the small angle corrections that need to be applied to the centroids as well as to provide photometric information about the target and the sky background.

The guide star data are analyzed in the same way as the astrometer data, over the identical intervals of time. For example, the guide star centroids and average photometry are computed over the time the astrometer was in FineLock.

The corrections applied to the FGS data are as follows:

1. The FineLock centroids are computed by finding the median, from the 40 Hz data - of the X,Y location of the IFOV (computed from the Star Selector A,B encoder angles). PMT data are averaged for astrometer and guiding FGSs.
2. For the astrometer only, the PMT data are evaluated to determine the fine angle adjustments to the centroids.
3. The Optical Field Angle Distortion (OFAD) calibration is applied to remove distortions of the sky in the FOV.
4. Differential velocity aberration correction is applied to the adjusted FineLock centroids of the astrometer and guiding FGSs.

Steps 1 and 2 are carried out in *calfgsa*, while steps 3 and 4 are performed in *calfgsb*. Please see Figure 7.1 on page 118 and Figure 7.3 on page 120, the flow chart descriptions of *calfgsa* and *calfgsb* respectively.

Transfer Mode

During a Transfer Mode observation, the data retrieved from the astrometric FGS will include PMT counts and star selector positions from the slew of the IFOV to the target object, the Search and CoarseTrack target acquisition, and the individual Transfer scans. Corresponding data acquired from the guiding FGSs will include FineLock tracking of the guide stars.

The astrometer's data are analyzed to evaluate the background counts, if available (see Chapter 7), and to locate and extract the individual scans. For each scan, the guide star centroids are computed and corrected for differential velocity aberration. Output files are generated with the appropriate information.

The data from the individual scans are used to compute the Transfer Function over the scan path. The quality of each scan is evaluated for corruption from high amplitude, high frequency spacecraft jitter, and, if unacceptably large, the scan is disqualified from further analysis.

The remaining scans are cross correlated, shifted as needed, binned as desired, and co-added to enhance the signal to noise ratio. The co-added Transfer Function can be smoothed if need be. The analysis tool which performs these functions is available from STScI. It is currently implemented as a standalone executable (FORTRAN + C) in the UNIX environment.

Although not part of pipeline processing, the analysis of observations of binary stars and extended objects will be briefly described here for completeness.

Binary Star Analysis

The Transfer Function of a binary system will be deconvolved, by use of the standard reference S-Curves of single stars from the calibration database, into two linearly superimposed point source S-Curves, each scaled by the relative brightness and shifted by the projected angular separation of the binary's components. This provides the observer with the angular separation and position angle of the components as well as their magnitude difference. These results will be combined with those obtained from observations at different epochs to compute the system's relative orbit.

Extended Source Analysis

For observations of an extended source, such as the resolved disk of a giant star or solar system object, the co-added Transfer Function will be analyzed to determine the angular size of the object. This involves application of a model which generates the Transfer Function of synthetic disks from point source S-Curves from the calibration database.

Transfer Mode observations are processed by *calfgsa* to the point of locating and extracting the individual scans and computing the guide star centroids. Support for additional processing - including the automation of the data quality assessment (identifying those scans which have been unacceptably corrupted by space craft jitter, for example) and the cross correlation and co-adding of the individual scans - are available as data analysis tools. Upgrades to *calfgsa* will be noted on the FGS web site. Figure 7.2 on page 119 displays the processing steps performed by the current version of *calfgsa* for Transfer Mode observations.

Visit-Level Processing

Visit-level processing refers to those corrections that are applied to the individual exposures in order to map each onto a common reference frame. Since the FGS observes the targets sequentially, not simultaneously, any motion of the spacecraft or the FGS's FOV during the course of the visit will introduce uncertainties in the measured positions of the objects. The corrections discussed here restore the cohesiveness of the reference frame.

Position Mode

Position Mode observations during the course of a visit must be corrected for two sources of error which render the FOV somewhat unstable: low frequency HST oscillations and residual drift of the FOV across the sky.

HST Oscillations: Using the Guide Star Data

The mapping of the individual astrometry observations onto a common reference frame begins with the analysis of the guide star data. As part of the exposure-level processing, guide star centroids are computed over the same time interval as for the astrometry targets. Generally HST is guided by two guide stars. The so-called "dominant" guide star is used by the pointing control system (PCS) to control the translational pitch and yaw of the telescope. The "sub-dominant" guide star, also referred to as the roll star, is used to maintain the spacecraft's roll or orientation on the sky. Any change in the guide star centroids over the course of the visit (after corrections for differential velocity aberration) is interpreted by the FGS Astrometry Pipeline as an uncorrected change in the spacecraft's pointing.

The pipeline defines an arbitrary fiducial reference frame based upon the location of the guide stars in the first exposure of the visit. Relative changes in the position of the dominant guide star for subsequent observations are assumed to be a translational motion of the HST focal plane. The pipeline "corrects" the position of the sub-dominant guide star and the astrometric target star. Any change in the angle defined by the line connecting the two guide stars and the spacecraft's V2 axis is interpreted as a rotation of the focal plane, and is removed from the astrometry data.

The correction of the astrometry centroids for vehicle motion (as determined by changes in guide star positions) is referred to as *pos-mode dejittering*. Transient corrections can be as large as 3 to 5 mas, such as when HST enters orbital day, but the adjustments are typically small—less than 1 mas. This underscores the excellent performance of HST's pointing control system under the guidance of the FGSs.

Drift Correction

"Drift", as discussed in Chapter 5, is defined as the apparent motion of the astrometer' s FOV on the sky during the course of the visit as detected by the astrometry targets that are observed more than once during the visit (the *check stars*). Drift must be removed from the measured position of all astrometry targets. This is accomplished by using check star data to construct a model to determine the corrections to be applied. If at least two check stars are available and were observed with sufficient frequency (i.e., at least every seven minutes), a quadratic drift model (in time) can be used to correct for both translation and rotation of the FOV. The availability of only one check star will limit the model to translation corrections only. If the check stars were observed too infrequently, then a linear model will be applied.

If no check stars were observed, the drift cannot be removed and the astrometry will be contaminated with positional errors as large as 15 mas.

It is important to note that the drift is motion in the astrometer which remains after the guide star corrections have been applied. Its cause is not well understood, but with proper check star observing, the residuals of the drift correction are tolerably small (i.e., sub-mas).

With the application of the guide star data for pos-mode dejittering and the check stars to eliminate drift, the astrometry measurements from the individual exposures can be reliably assembled onto a common reference frame to define the *visit's plate*.

The visit level corrections to Position Mode observations, i.e., pos-mode de-jittering and the drift correction are performed by *calfgsb* (Figure 7.3 on page 120).

Transfer Mode

Visit-level corrections to Transfer Mode observations are required only when Position and Transfer Modes are employed in the same visit, and the target object was not observed in Position Mode. In this case, the same adjustments must be applied, namely the pos-mode dejittering from the guide star data and the drift correction from the check stars.

Transfer Mode observations typically last about 20 minutes (or more), much longer than Position Mode exposures (1 to 3 minutes). Therefore, it is far more likely that low frequency spacecraft jitter and FOV drift will have occurred during the Transfer Mode exposure. These do not introduce uncorrectable errors since low frequency FOV motion is implicitly removed from the data by cross correlating the Transfer Function from each individual scan. However, relating the arbitrary coordinate system upon which the Transfer Function is mapped to the system common to the reference stars is an important and necessary prerequisite in linking the Transfer Mode observation to the Position Mode data.

Guide Star Data

Transfer Mode data analysis, as discussed in the exposure level section, involves the cross correlation of the Transfer Functions from each of the individual scans. The first scan is arbitrarily designated as the fiducial; all other scans in the Transfer Function are shifted to align with that of the first (this automatically eliminates jitter and drift local to the observation). Therefore, in order to restore some level of correlation with the other observations in the visit, the guide star centroids are evaluated over each scan, and, along with the shifts, are recorded.

Drift Correction

The cross correlation of the individual scans removes the drift of the FOV from the Transfer Mode data. However, this is a relative correction, local to only the Transfer Mode observation. By recording the shift corrections applied to the individual scans, the visit level pipeline has visibility to the drift that occurred during the Transfer Mode observation.

Transfer/Position Mode Bias

The presence of a small roll error of the Koesters prism about the normal to its entrance face (see "Transfer Mode Scale as a Function of HST Roll Angle" on page 81) introduces a bias in the location of interferometric null as measured by Position Mode when compared to the same location in Transfer Mode. This bias must be accounted for when mapping of the results of the Transfer Mode analysis onto the visit level plate defined by the Position Mode measurements of the reference stars. This bias is removed by applying parameters from the calibration database

Epoch-Level Processing

Astrometry takes time. This is true whether the goal is to determine the parallax, proper motion, or reflex motion of an object measured in Position Mode, or the orbital elements of a binary system observed in Transfer Mode. By its very nature, astrometry looks for changes to the arrangement of objects on the sky, and as a result, observations taken over several different visits must be compared to one another. Relating the observations from different epochs is discussed. A more detailed discussion is provided in the *HST Data Handbook*.

Parallax, Proper Motion, and Reflex Motion

In order to measure the proper motion and parallax of an object observed in Position Mode with the FGS, the data from the individual visits must be combined to form a *virtual plate*. This virtual plate is derived from

an optimal mapping of all of the visit level plates onto a common plate using the method of least-squares to minimize the residuals of all reference stars (the plate solution). This mapping function is used to map the science target at each visit onto the virtual plate. In this way, the parallax, proper motion, and perhaps reflex motion (perturbations caused by a gravitationally bound companion) can be determined.

If enough reference stars are available (> 5), six parameter plate solutions - allowing for independent scale adjustments along each of the astrometer's X and Y axes - can be applied. Otherwise the four parameter model must be applied.

The residuals of the reference stars in the plate solution determine the overall astrometric performance of the telescope as a function of the number of visits expended. FGS3 achieved ~1.2 mas (rms) precision per HST orbit, while FGS1r has demonstrated ~0.8 mas rms precision per HST orbit. Given that the overall astrometric accuracy scales as $\sqrt{1/n}$ while random (Poisson) errors dominate, it can be anticipated that, for example, FGS1r will yield parallax measurements accurate to 0.3 mas in as little as 12 HST orbits if an optimal observing strategy is employed. (Below ~0.2 mas irreducible systematic errors dominate, such as the conversion of relative to absolute parallax.)

STScI can provide the analysis tools (developed by the STAT at the University of Texas) needed to perform a plate solution from multiple Position Mode visits. These tools are available as stand-alone software packages and scripts that can be delivered via ftp from STScI. Supporting documentation is being developed. Please see the FGS web page for further updates.

Binary Stars and Orbital Elements

Transfer Mode observations of binary stars provide the angular separation and position angle of the components at each epoch (as well as their difference in brightness). Once the binary has been observed at a sufficient number of phases in its orbit, the system's orbital parameters can be solved. The result will be knowledge of the orbit's inclination, eccentricity, period, and angular extent of its semi-major axis. If the parallax of the object is known, then the physical size of the orbit can be computed to yield the total mass of the system.

For a binary that was observed along with Position Mode observations of reference stars, it is possible to determine the binary's parallax and proper motion, and the motion of the components about the system's barycenter, which then yields the component masses. This, along with the differential and system photometry (also measured by the FGS), provides the mass-luminosity relation.

STScI can provide observers, via ftp, with the appropriate analysis tools needed to analyze Transfer mode observations of binary star systems.

These tools are standalone software packages written by STScI based upon algorithms developed by the STAT at the Lowell Observatory. These packages allow one to *deconvolve* the binary star Transfer Mode data in order to determine the angular separation and relative brightness of the components at each epoch of observation. Documentation of these packages will be made available during Cycle 11. Check the FGS Web pages for updates.

Figure 7.1: CALFGSA Common Processing Tasks

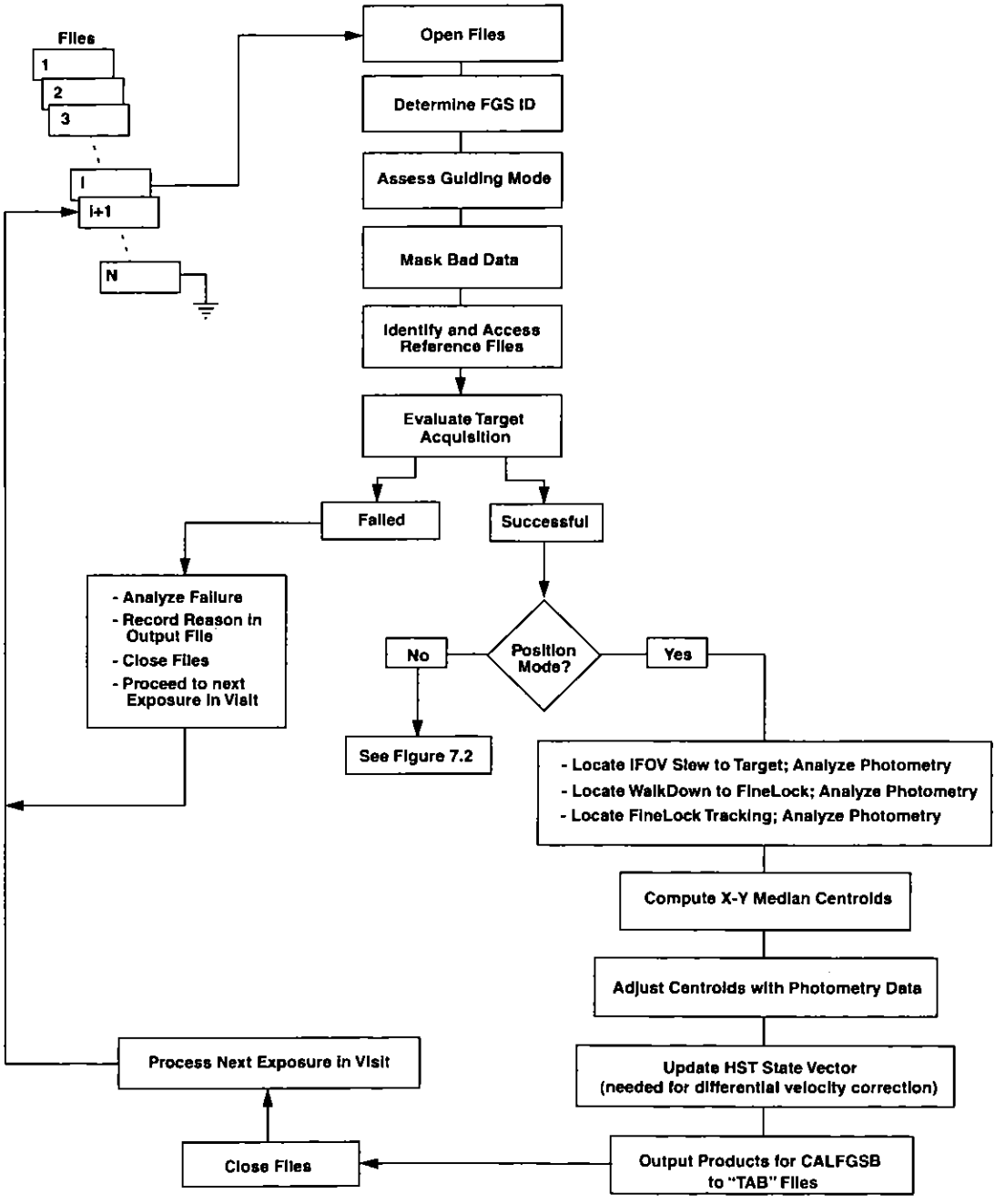

Figure 7.2: CALFGSA Transfer Mode Processing Tasks

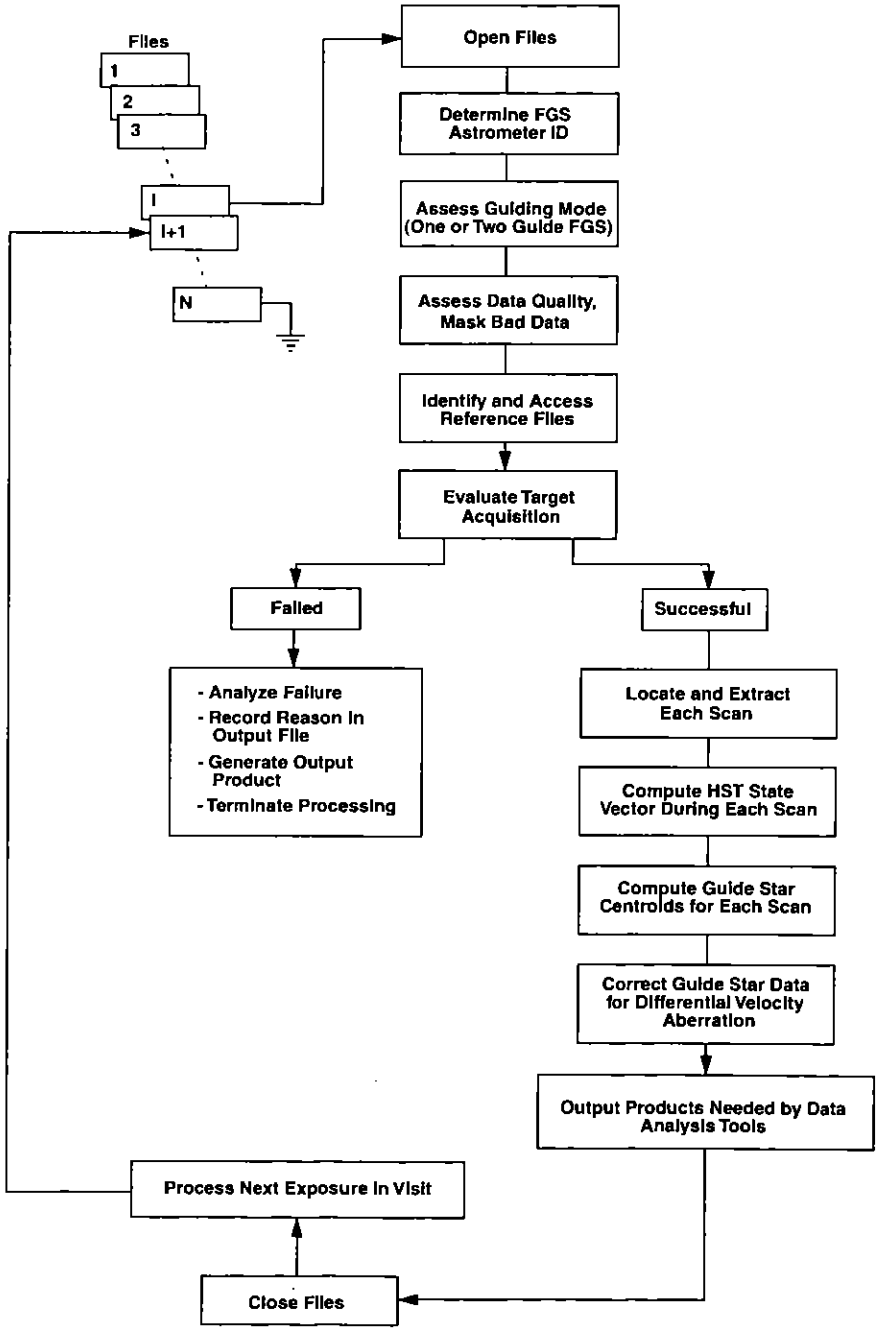

Figure 7.3: CALFGSB Position Mode Processing

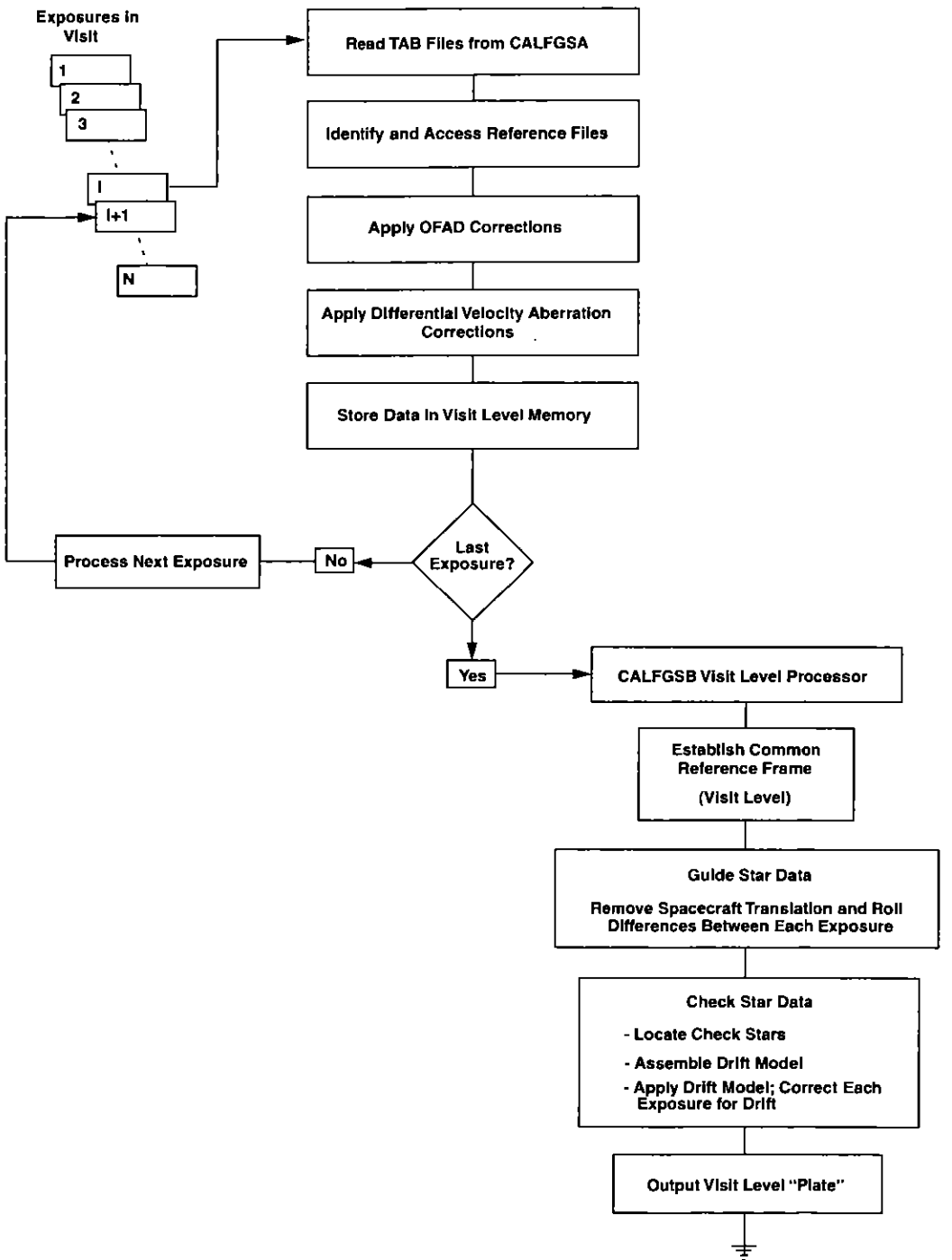

APPENDIX 1:

Target Acquisition and Tracking

In this appendix . . .

FGS Control / 121
Target Acquisition and Position Mode Tracking / 122
Transfer Mode Acquisition and Scanning / 127
Visit Level Control / 127

This chapter describes the acquisition of targets in both Position and Transfer Modes. In addition to the "science exposure", the dataset for a given observation includes photometric measurements of the background as well as the acquisition of the target. The background data are used by the calibration pipeline in the reduction of data. The acquisition data can be helpful in the analysis of failed observations.

FGS Control

Two different computers interface with and control an FGS at various times. The first is the 486, which controls the HST spacecraft and its pointing control system. The second is the Fine Guidance Electronics (FGE) microprocessor associated with each FGS. Both the 486 and the FGEs control the FGSs while they are guiding HST. During astrometric science observations, control is shared by the two computers: the FGE operates the FGS during Position Mode, while the 486 operates the FGS during Transfer Mode scans.

Target Acquisition and Position Mode Tracking

In this section we review the acquisition and tracking sequence. The flags and status bits are defined in detail in the FGS section of the *HST Data Handbook*.

Slew to the Target

To initiate the acquisition of a target, the 486 slews the FGS Instantaneous Field of View (IFOV) to the expected location of the target. Upon arrival, the FGE initiates the search and track sequence: Search, CoarseTrack, and FineLock. Figure 1.1 on page 123 demonstrates the actual movement of the IFOV during a target acquisition.

1. The end of the slew to the target's expected location.
2. A short spiral search.
3. CoarseTrack nutations to locate the photocenter.
4. WalkDown to locate interferometric null.
5. Tracking in FineLock.

Note: The example depicted in Figure 1.1 was chosen for its clear demonstration of the phases of the acquisition. *This example is atypical, as the 7″ difference between the expected location and the true location of the target is unusually large. More typical miss-distances are 0.3" to 1.00".*

Figure A1.1: Location of IFOV as FGS Acquires a Target

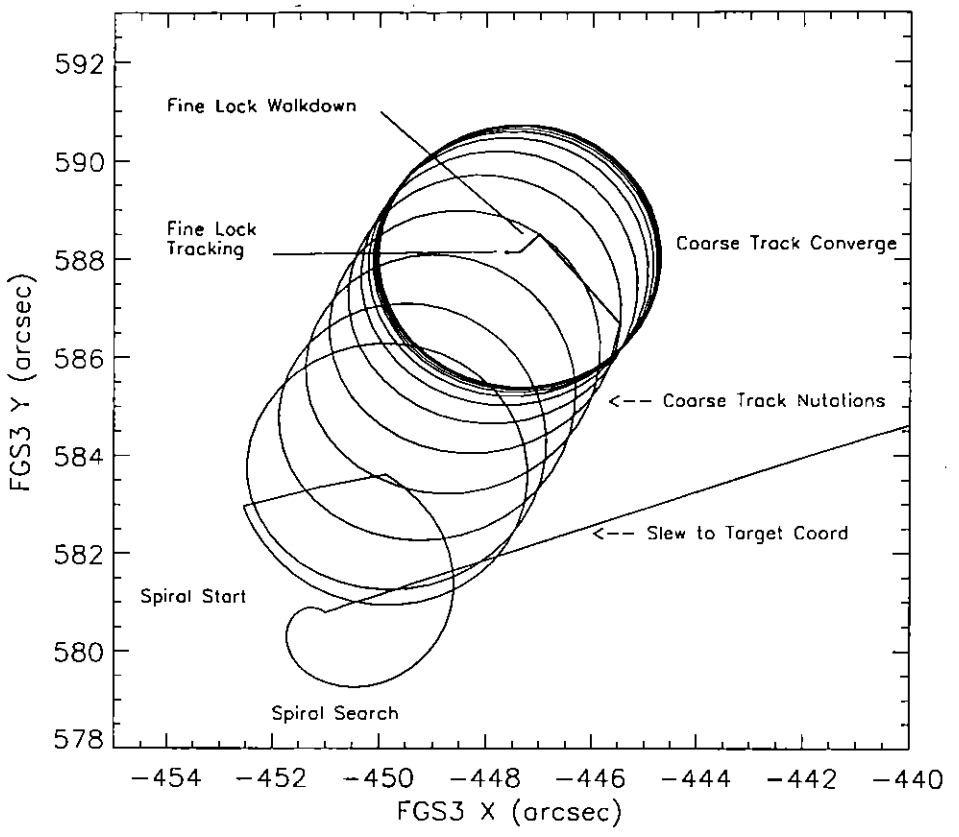

Search

In the search phase, the IFOV, under FGE control, steps every 25 msec along an outward spiral while the PMTs count the photons received from the 5″ x 5″ patch of sky observed in the IFOV. When the counts fall within a specified tolerance, the FGE declares the spiral search a success, and the instrument transitions to CoarseTrack. By default, the radius of the spiral search is 15 arcsec, but can be a large as 90 arcsec.

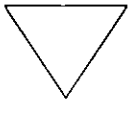

Unless the target's position is highly uncertain, there is no benefit in specifying a search larger than the default, since the HST Pointing Control System points the telescope with an accuracy of about 0.3". Large search spirals consume time better spent on science measurements.

CoarseTrack

After a successful search, the FGE attempts to acquire and track the star in CoarseTrack. The FGS locates the photocenter by comparing the photon counts from the four PMTs as the IFOV nutates in a 5" diameter circular path around the target.

If the PMT data ever indicate the star is no longer present, the FGS reverts back to Search mode, beginning where it left off on the search spiral to resume its outward search for the star.

FineLock

Upon completion of the CoarseTrack, the FGS attempts to acquire the target in FineLock. This activity involves the acquisition and tracking of an object's interferogram. The fundamental interval of time during FineLock is the Fine Error averaging time (denoted as FESTIME - see Chapter 7). During an FESTIME the FGS integrates the PMT counts while holding the IFOV fixed.

The acquisition begins with the "WalkDown to FineLock," or simply *the WalkDown*. The FGE commands the FGS's IFOV to a position offset or "backed-off" from the photocenter (determined by CoarseTrack). Here at the very beginning of the WalkDown, while the IFOV is far from the fringe, the FGE collects data from the two PMTs on each of the X and Y channels to compute an average sum (SUM) and difference (DIFF) of the PMT counts on each channel. The integration time is 0.4 sec or one FESTIME, whichever is larger. The FGE then uses these values to compensate for any difference in the response of the two PMTs on a given axis. Thus, the X-axis Fine Error Signal (FES) for the remainder of the Position Mode observation will be:

$$Q_X = (A_X - B_X - DIFF_X) / (SUM_X)$$

where A_x and B_x are the average photon counts/25 msec (from PMTXA and PMTXB) integrated over the FESTIME, and $DIFF_x$ and SUM_x are the average difference and sum of the PMTXA, PMTXB counts per 25 milliseconds (as computed at the start of the walkdown). The Y-axis FES is computed in a similar fashion.

Figure 1.2 on page 125 shows the instantaneous value of the normalized difference of the PMT counts along the Y-axis during a WalkDown to FineLock. The fact that the null lies to the positive side of the Y-axis S-Curve ($S(y) > 0.0$) clearly demonstrates the need for the DIFF-SUM adjustment to locate the true interferometric null. The reference to "pipeline corrected null" in Figure 1.2 refers to the true values of DIFF and SUM as computed by the astrometry pipeline, which uses the photometry

during the entire WalkDown to achieve a better signal-to-noise for these values. (See Chapter 7 for additional details on the FGS pipeline.)

Figure A1.2: Offset of True Null from $S_y = 0$

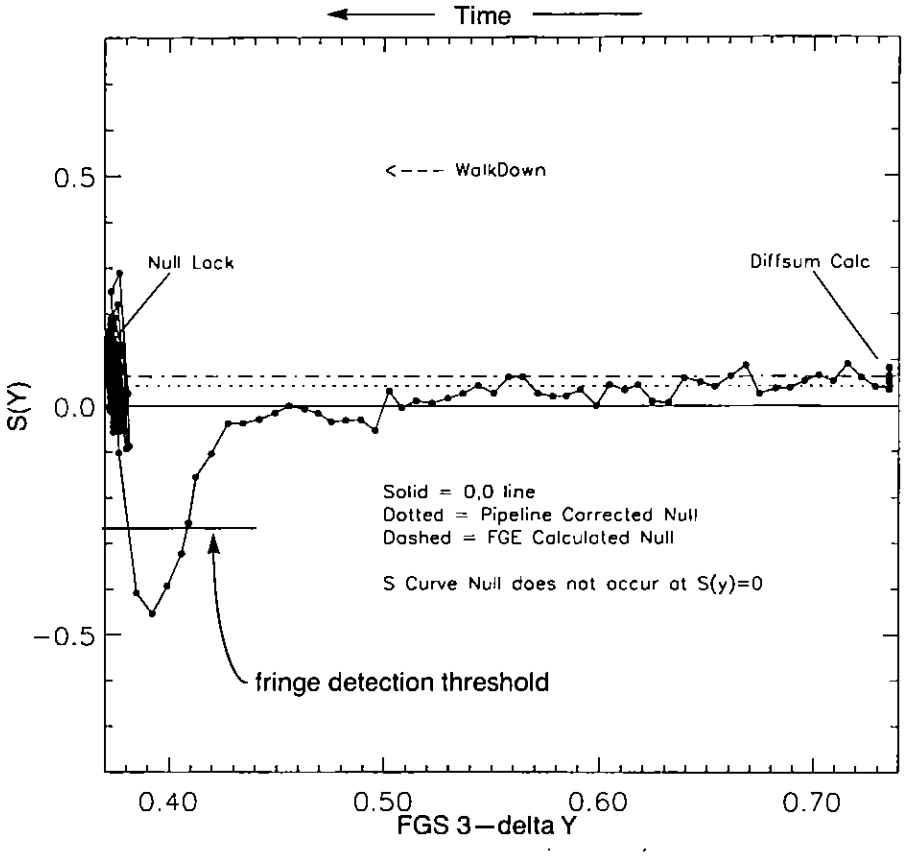

During the WalkDown, the IFOV creeps towards the photocenter in a series of equal steps of approximately 0.006" in X and Y. The IFOV is held fixed for an FESTIME after each step while the PMT data are integrated to compute the fine error signal on each axis. If the absolute value of the fine error signal for a given axis exceeds a specified threshold for three consecutive steps (satisfying the *3-hit algorithm*), the FGE concludes it has encountered the S-Curve on that axis. From this point, a continuous feedback loop between the star selector servos and the FES value governs the repositioning of the IFOV along that axis. For the remainder of the observation, the FGS continuously adjusts the star selector positions by small rotations every FESTIME to set the FES to zero. This repositioning of the IFOV ensures the wavefront at the face of the Koesters prism has zero tilt.

If the FGS does not detect the S-Curve after 130 steps (i.e., after having "walked" 810 mas), the FineLock acquisition fails and the "scan step limit

exceeded" flag is set. The IFOV will then remain positioned at the end of the WalkDown path until the 486 slews it to the expected location of the next target in the observing sequence. The observer will be provided with the 40 Hz photometry and star selector angles from which the Fine Error Signal can be reconstructed and analyzed to determine the cause of the failure. *The star must be acquired on both axes for the observation to succeed.*

When the S-Curves on both axes have been encountered and the 3-hit algorithm satisfied, the FGS is said to be tracking the object in FineLock. Figure 1.3 shows the IFOV's position for both the WalkDown and FineLock tracking in local detector space. Notice the interferometric null is first encountered along the Y-axis. The IFOV must walk an additional 0.2" along the X-axis to find its interferometric null. This is typical FGS3, and is due to a bias in the CoarseTrack photocenter and the FineLock (interferometric) null. FGS1r has a different bias, with the X-axis null encountered some 0.440" before the Y-axis null. These biases do not degrade the instruments scientific performance.

Figure A1.3: X,Y Position in Detector Space of FGS 3's IFOV During WalkDown to FineLock and Subsequent Tracking of a Star in FineLock

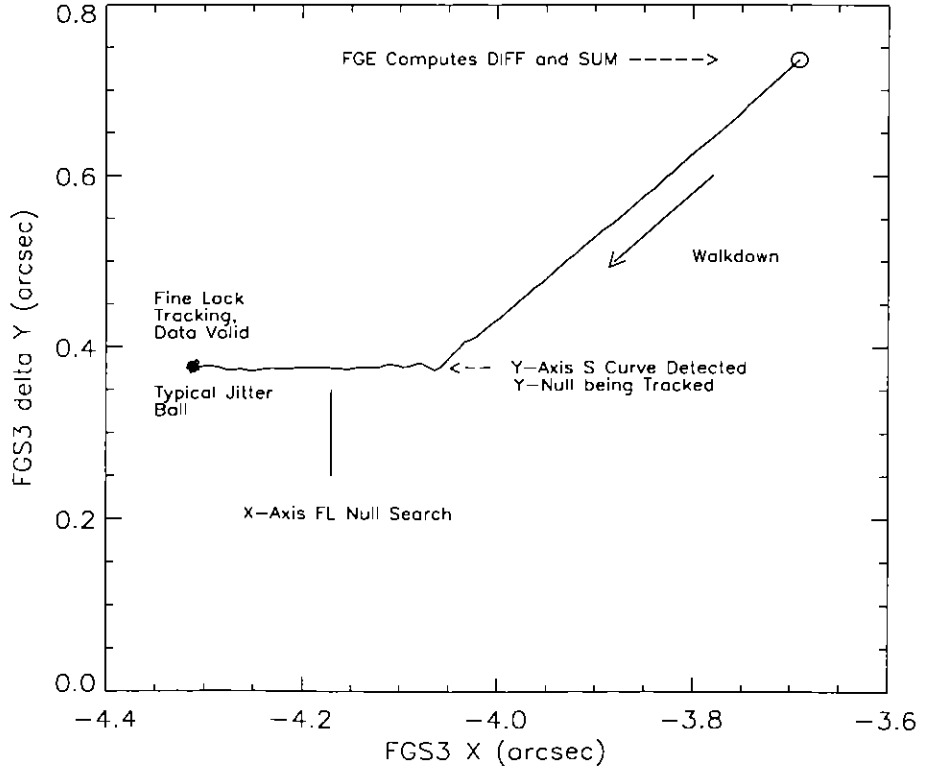

Transfer Mode Acquisition and Scanning

When the FGS is operated in Transfer Mode, the acquisition is implemented in the same sequence as described in the previous section, with the exception that the FGS *remains in CoarseTrack until a specified spacecraft time*. Thereafter, the 486 slews the IFOV to the starting point of the first scan and steps it across the object along a diagonal path in detector space for a distance specified in the Phase II proposal. Each sweep across the target is referred to as a scan. After completing a scan, the 486 reverses the IFOV's direction and scans the object again until the total number of scans (as specified in the Phase II proposal) has been completed. Every 25 milliseconds, the PMT data and star selector rotation angles are reported in the telemetry. The FGS samples the entire S-Curve and its wings with sub-milliarcsecond resolution. The interferogram can be reconstructed by post-observation data processing.

Visit Level Control

After an observation is completed, the FGS's IFOV - under control of the 486 - is slewed to the expected location of the next target in the observing sequence. The search/track acquisition is initiated and the object, if acquired, is observed in either Position or Transfer Mode. This process is repeated until all the exposures in the visit have been executed.

APPENDIX 2:

FGS1r Performance Summary

In this appendix . . .

FGS1r's First Three Years in Orbit / 129
Angular Resolution Test / 132
FGS1r's Angular Resolution: Conclusions / 136
FGS1r: Final AMA Adjustment / 136

FGS1r's First Three Years in Orbit

As a result of the misfigured HST primary mirror, the FGSs must contend with a spherically aberrated wavefront. As discussed in Chapter 2, this aberration amplifies the degrading effect of any misalignment of FGS optical elements that produces a shift of the beam at the Koesters prism. The result is a deformed S-Curve with reduced modulation. In order to provide an in-flight means to align FGS1r and thereby guarantee its interferometric performance, a stationary mirror was remounted on a commandable mechanism capable of tip/tilt articulation. This Articulating Mirror Assembly (AMA) is currently available in FGS1r and FGS2r. Without the AMA, FGS1r would most likely not have been suitable as a science instrument.

The first year of FGS1r's tenure in orbit is best described as an adjustment process. Upon reaching orbit, the instrument's interferometric response had already degraded, presumably due to a shift of the pupil at the Koesters prism induced by the launch stresses and gravity release. Early in the commissioning process, the AMA was adjusted to correct the instrument's alignment and restore its S-Curves to near ideal. Figure 2.1 on page 130 compares the full aperture (F583W) S-Curves before and after the initial AMA adjustment.

Figure A2.1: FGS1r S-Curves: Before and After AMA Adjustment

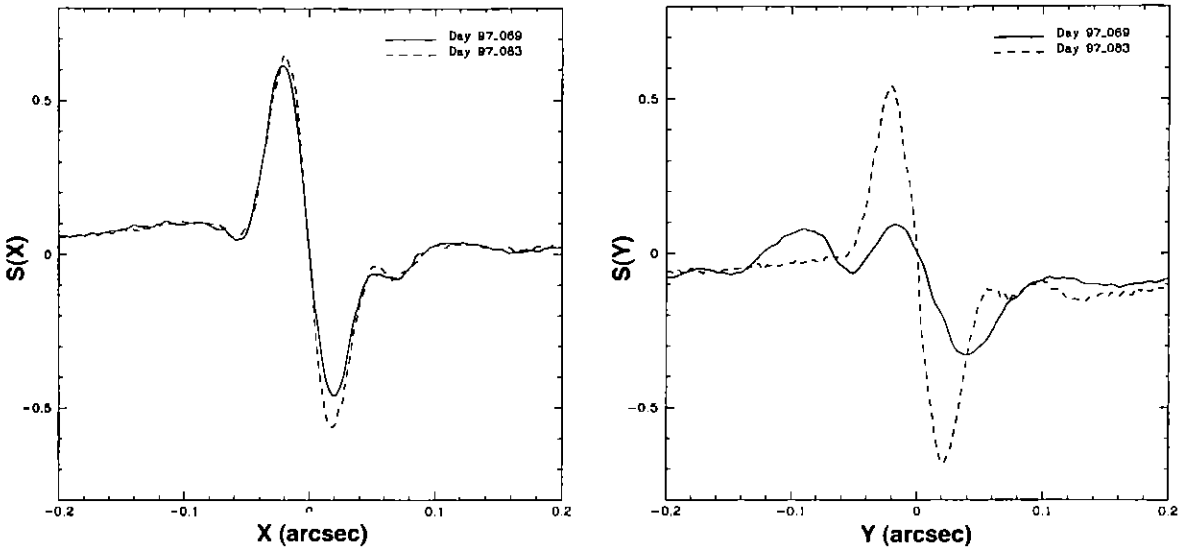

It was anticipated that FGS1r's performance would evolve during its first year in orbit due to the outgassing of the graphite epoxy composites upon which the instrument's optical bench is mounted. To monitor the changes, a standard star was observed in Transfer mode, once per month for the first 120 days, and then approximately every 3 months afterward. Consistent with the outgassing hypothesis, the S-Curves on both the X and Y axis were seen to change (degrade) quickly at first but eventually reached an approximate steady state by the first quarter of 1998. Figure 2.2 on page 131 shows the early evolution of the full aperture (F583W) S-Curves, from initial optimization on March 24, to August 10, 1997, and Figure 7.4 on page 131 shows the evolution from September 19, 1997 through February 23, 1998.

Figure A2.2: FGS1r S-Curves: First Six Months After AMA Adjustment

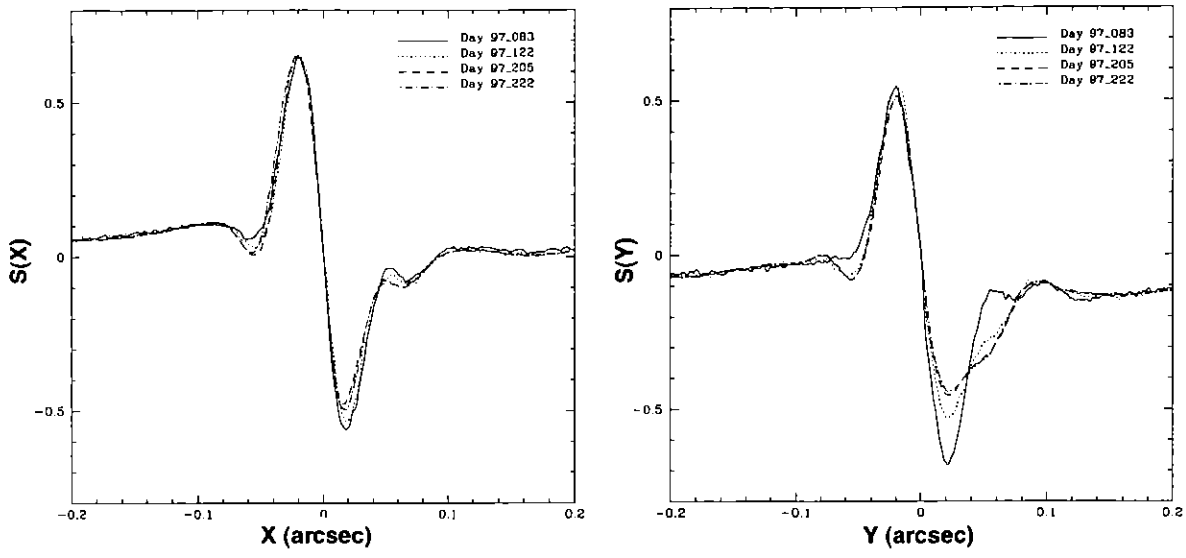

Figure 7.4: FGS1r S-Curves: Second Six Months After AMA Adjustment

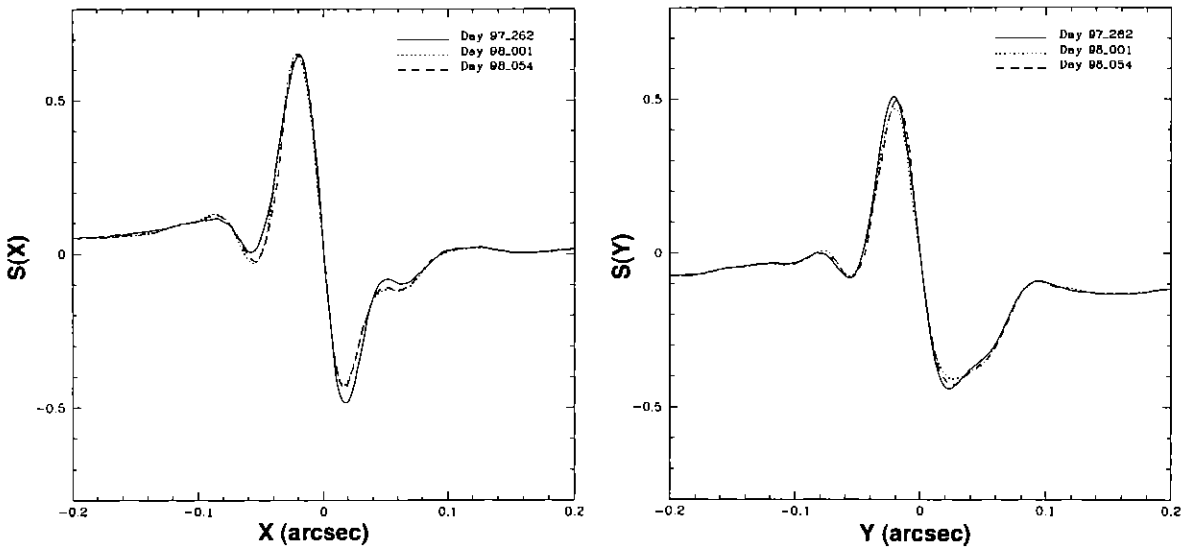

On May 8, 1998, the AMA was once again adjusted to restore the interferometer's performance to yield the S-Curves displayed in Figure 2.3 on page 132. With near ideal S-Curves on both the X and Y axis, STScI executed an angular resolution test to assess FGS1r's potential as an astrometric instrument.

Figure A2.3: .Optimized FGS1r S-Curves Used in Angular Resolution Test

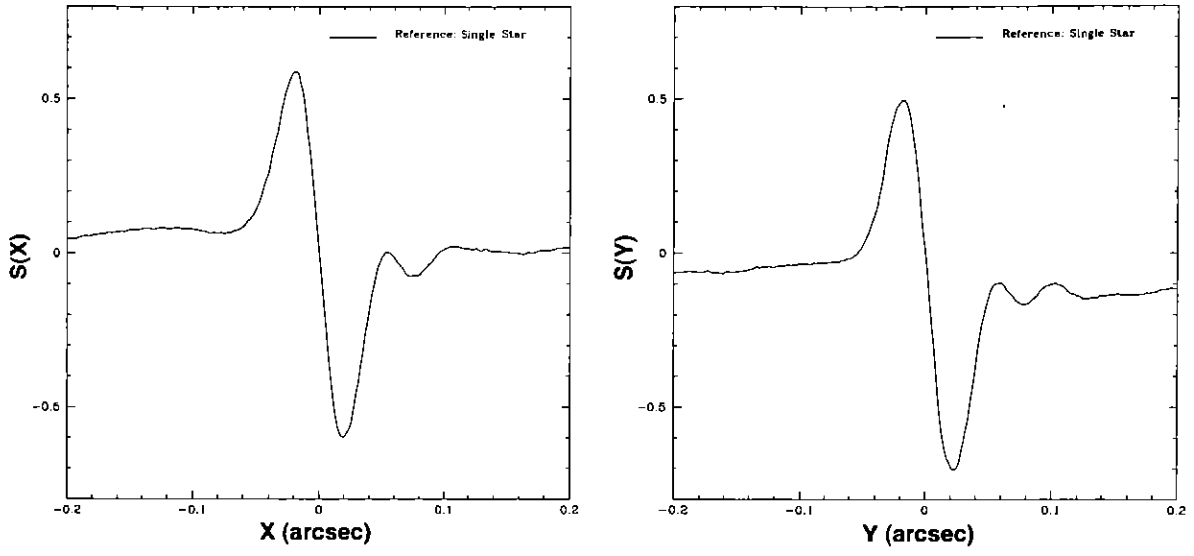

Angular Resolution Test

Following the FGS1r re-optimization in early May 1998, STScI executed a test to determine the angular resolution limits of FGS1r and FGS3 by observing a known binary system at several small increments of telescope roll angle. The binary ADS11300 is an 9th magnitude system with components having a magnitude difference $\Delta m = 0.6$. At the time of the test, the predicted angular separation of the components was 0.085" (Franz and Wasserman, private communication). The test was designed such that the predicted position angle of the binary was (almost) aligned with the Y axis of the FGS, i.e., the projected angular separation of the two stars was large along the Y axis but small along the X axis. By rolling the HST in 6 increments, the projected separation along the X axis varied from the predicted angular resolution limit of FGS1r (~6 mas) to the resolution limit of FGS3 (~20 mas).

The true position angle and separation of the components were determined from both the FGS1r and FGS3 observations with the stars separated by 23 mas along the X axis. These values were used to determine the actual angular separation of the stars along FGS1r's X axis as a function of spacecraft roll, and the Transfer mode observations were analyzed to assess the instrument's ability to measure these separations. The test included actual separations of 7, 9, 12, 14, 17, and 23 mas (as compared with the intended separations of 6, 8, 10, 12, 15, and 20 mas).

FGS3 was tested only at the component separations of 14 and 23 mas since simulations of its X axis performance indicated that this instrument would not "resolve" the binary for separations less than 20 mas.[1]

Figure A2.4: FGS1r Transfer Function: Change in Angular Separation of a Binary

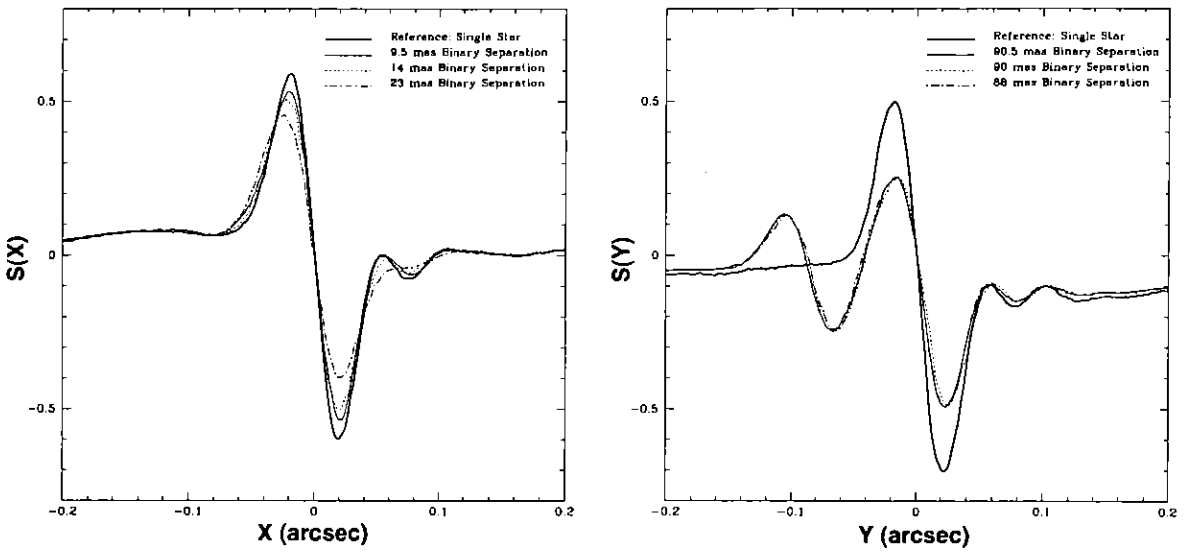

Test Results: The Data

For the six observations with FGS1r, Figure 2.4 compares the observed Transfer functions, and hence the response of the instrument to the angular separation of the stars as projected along the interferometer's X- and Y-axis. It is evident from these data that FGS1r easily detected the non-singularity of the source, and is sensitive to the change in separation of the two stars. Figure 2.5 on page 134 plots the predicted vs. observed amplitude of the Transfer Function as a function of the binary's projected separation.

1. We express our greatest appreciation to O. Franz and L. Wasserman for researching the binary.

Figure A2.5: FGS1r Transfer Function Amplitude w/ Binary Separation

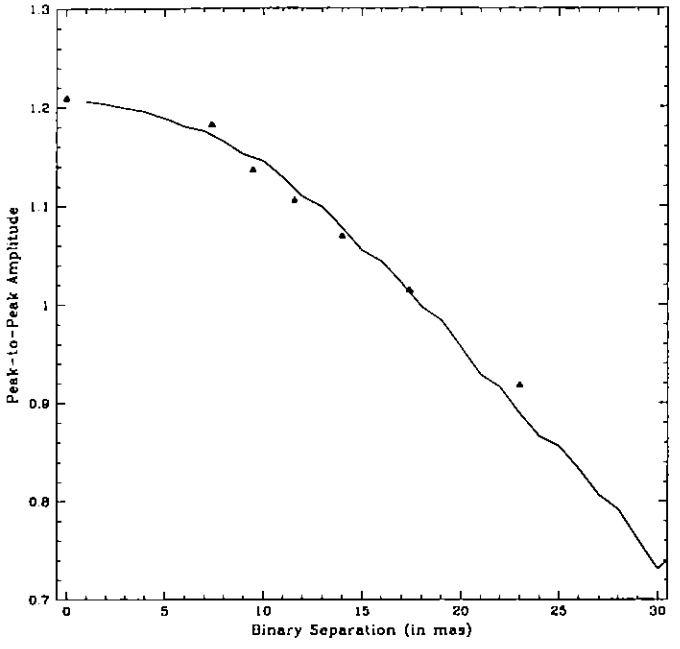

The true "signal" in these observations can be thought of as the difference between the peak-to-peak amplitude of the binary star's Transfer Function and that of the standard single star S-Curve. The statistical contribution to the noise can be calculated from the standard deviation of the normalized difference of the PMT counts in the wings of the fringe. With signal and noise defined in this way, Table 2.1 displays the signal-to-noise ratio for these six observations. These values underscore the validity of the instrument's response displayed in Figure 2.4 and Figure 2.5.

Table A2.1: FGS1r Angular Resolution Test: Effective Signal-to-Noise Ratios

Angular Separation (in mas)	Peak-to-Peak Amplitude	S/N
Single star	1.209	–
+7.4	1.182	48.9
+9.5	1.136	63.2
+11.7	1.105	105.7
+14.0	1.069	128.6
+17.4	1.014	156.7
+23.0	0.918	194.7

Test Results: Binary Star Analysis

The observations were analyzed, as described in Appendix 2, by finding a linear superposition of point source S-Curves that have been scaled and shifted to reproduce the observed Transfer function. Two separate techniques were employed. The most general model solves for the magnitude difference, angular separation, and parity of the binary's components. The second technique constrains the magnitude difference and solves for both the separation and parity.

Table 2.2 reports the results of these fits along the X axis for the FGS1r observations. In this table, a negative separation corresponds to a parity such that the faint star is to the "left" of the bright star, i.e., it is displaced in the –X direction of the scan. Likewise, a positive separation places the faint star to the right of the bright star. For these observations, the parity was positive so a negative parity is incorrect. The formal error of each of these fits is about 0.5 mas.

Along the Y axis, where the components are widely separated by about 90 mas, the fits to the Transfer functions yielded accurate results for both the FGS1r and FGS3 observations.

The FGS3 observations succeeded in detecting the non-singularity of the source when the stars were separated by 14 mas along its X axis, but could not yield an accurate measurement of the separation. The observation with the 23 mas separation succeeded (as expected).

Table A2.2: FGS1r Angular Resolution Test: Binary Star Analysis

Predicted Angular Separations (in mas)	Computed Separations (in mas)	
	No Constraints	Δmag Constrained
+7.4	+6.9	+7.5
+9.5	-11.1	+11.5
+11.7	-12.2	+12.5
+14.0	+13.6	+14.1
+17.4	+16.9	+18.0
+23.0	+23.0	+23.0

For FGS1r, as can be seen in Table 2.2, the unconstrained solution yields an incorrect parity for angular separations less than 14 mas. The models that constraining the magnitude difference reproduced the correct angular separations to within ~ 5%, even at the smallest separation of 7.3 mas (though, not for the test at 9.5 mas separation).

FGS1r's Angular Resolution: Conclusions

Figure 2.4 on page 133 shows that FGS1r detects duplicity at component separations as small as 7 mas, and Table 2.2 shows that this instrument can accurately measure these separations if the magnitude difference is constrained (for projected separations < ~15 mas, no constraints are necessary for larger separations).

Details of the angular resolution test design and results are currently available on the FGS Web site.

FGS1r: Final AMA Adjustment

The final adjustment to FGS1r's AMA was performed on October 12, 1998. The results included near-ideal S-curves, essentially similar to those displayed in Figure 2.3 on page 132. Since then, STScI has continued to monitor the temporal stability of these interferograms. Small changes in the amplitude and morphology of the y-axis S-curve have been seen. These appear to be due to a continuing, but very slow, shift of the y-axis Koester prism w.r.t. HST's OTA. To assure the reliability of measurements made by FGS1r on close (< 25mas) binary systems, standard calibration reference stars are observed once per cycle (if that spectral type is needed by GO programs during the cycle).

Glossary of Terms

The following terms and acronyms are used in this Handbook.

articulating mirror assembly (AMA): Commandable adjustable mirror assembly (replaces FF3 in FGS1r) capable of tip/tilt motion; allows for in-flight re-alignment of the beam at the Koesters prism to mitigate deleterious effects of HST's spherical aberration.

back-off distance: Distance ($+dx$,$+dy$) from target photocenter to which the FGS IFOV is moved before starting the Walkdown to FineLock phase of target acquisition.

beam walk: Movement of the axis of tilt of the collimated beam on the face of the Koesters prisms; results from clocking errors and misalignments of the SSA and SSB assemblies with respect to the Koesters prisms.

breathing (thermal breathing): Change in telescope focus possibly resulting from temperature changes incurred as HST crossed the day/night terminator during each orbit.

check star: Targets observed more than once per POS mode visit; used as positional references to detect and allow for the removal of the apparent motion of the FOV during the visit.

CoarseTrack: Search algorithm used by the Fine Guidance Electronics which compares the counts from all four PMTs to continuously update the estimate of the target's photocenter.

COSTAR: Corrective Optics Space Telescope Axial Replacement; set of corrective optics installed in the 1993 HST servicing mission to correct the FOC, FOS, and GHRS for the spherically aberrated wavefront due to the misformed HST primary mirror. COSTAR does not correct the wavefront as seen by the FGS.

de-jittering: The process of correcting a POS mode observation for the effects of spacecraft jitter and oscillations by establishing a fixed, though arbitrary reference frame determined by the x,y centroids of guide stars observed with the guiding FGSs and compensating for motions of those guide stars during post-observation processing.

dominant guider: The FGS used to control the HST's translational attitude during an observation.

drift: Relative motions between FGS 3 and FGSs 1 and 2; thought to be a result of thermal effects.

F583W: FGS "Clear" filter, effective central wavelength of 5830 Å, with a bandpass of 1500 Å.

F5ND: FGS neutral-density filter; attenuates by 5 magnitudes.

FGE: Fine Guidance Electronics, on-board microprocessors which control the FGSs during the search for, acquisition of, and Position Mode tracking of the target.

FGS: Fine Guidance Sensors, term used to describe one of the three white light Koesters prism (shearing) interferometers aboard HST.

FES: Fine Error Signal.

FESTIME: Fine error averaging time; time over which PMT data are averaged for computation of the Fine Error Signal.

FGS X,Y detector coordinates: Coordinate system defined for each FGS originating from the telescope's optical axis (the V1 bore sight); easily maps to the HST V1,V2,V3 coordinate system.

field dependency: Variations of measured quantities of the Transfer Function (i.e., morphology and modulation) as a function of location in the FOV.

FineLock (FL): Stage of target acquisition in which the star selectors are moved to continuously zero the FES via a closed loop feedback between the position of the IFOV and PMT counts.

FITS: Flexible Image Transport System; the standard astronomical data interchange and archival format.

fold flat mirror (FF3): Non-adjustable mirror assembly employed by FGS2 and FGS3 to redirect the light emergent from the star selector and filter wheel assemblies onto the faces of the Koesters prisms.

FOV: Field of view, for an individual FGS is approximately a quarter annulus with inner and outer radii of 10.2 and 14.0 arcminutes respectively. The total field of view is sometimes referred to as the FGS *pickle*.

GEIS: Generic Edited Information Set; HST file format, similar in many ways to the FITS format standard; data consists of a header file and a binary data file with multiple data groups.

GO: General Observer.

GTO: Guaranteed Time Observer.

guide star: A star acquired in FineLock by the FGS and used by the HST pointing control system to make continuous corrections to the telescope's pointing; used to eliminate translational and rotational drift of the telescope during observations.

HIPPARCOS: High-Precision Parallax Collecting Satellite; European Space Agency satellite launched in 1989 to determine astrometric position and parallax measurements of bright stars to an accuracy of 1 milliarcsecond and 2 milliarcseconds/year respectively.

HST: Hubble Space Telescope.

IFOV: Instantaneous Field of View, the roughly 5″ x 5″ aperture located by the positions of the two star selectors for FGS observations.

IRAF: Image Reduction and Analysis Facility, the suite of analysis tools developed by NOAO to process general astronomical data.

Koesters prism: Prism at the heart of FGS interferometer; constructed of two halves of fused silica and joined along a surface coated to act as a dielectric beam splitter.

LTSTAB: Long Term Stability Monitoring; program of short POS Mode observations of an astrometric field made in the F583W filter to monitor the long term stability of the OFAD and plate scale calibration; usually repeated monthly or bi-monthly.

M35: Open cluster in Gemini (RA 06^h 08.9^m, Dec +24° 20′; $m_V \sim 5.3$) from which several stars are used in *LTSTAB* observations.

NEA: Noise Equivalent Angle.

NOAO: National Optical Astronomy Observatories.

null (interferometric null): Position in IFOV corresponding to the zero-point crossing of the transfer function for a given interferometric axis.

OFAD: Optical Field Angle Distortion, distortion incurred as a result of the combined effects of the FGS/OTA optical train and errors in SSA and SSB encoder values; alters the measured relative angular separations of stars distributed across the FGS pickle from their true angular separations.

ORIENT angle: Angle measured from North (through East) to the HST U_3 axis. This angle definition is used in proposals and should not be confused with roll angle. (See "roll angle").

OTA: Optical Telescope Assembly.

parallax: Angular displacement in the apparent position of a celestial body when observed from separated points.

PI: Principle Investigator.

pickle: The total field of view (FOV) of a given FGS, roughly 69 square arcminutes in (angular) area.

pick-off mirror: Pickle-shaped plane mirror used to deflect light from the HST Optical Telescope Assembly (OTA) to the FGS; defines the field of view (FOV) of a given FGS.

pitch: Rotation of HST in the V1,V3 plane.

plate scale: Magnification of the combined OTA and FGS optical system.

PMT: Photo-Multiplier Tube.

Position (POS) Mode: FGS mode in which a star is observed in FineLock; used to measure the parallax, proper motion, or reflex motion of a given target or targets.

POS TARG coordinate system: FGS coordinate system originating from the center of the FGS field of view, with the Y-axis positive in the radial direction from the FGS center and the X-axis rotated 90 degrees counter-clockwise to the A-axis.

Proper Motion: Apparent angular motion of a star on the celestial sphere over time.

PUPIL: A 2/3 pupil stop used to block the portion of the wavefront originating from the outer 1/3 of the HST primary mirror, reducing the deleterious effects of spherical aberration.

reflex motion: angular motion of an object about its local barycenter (e.g., as in binary stars).

roll: Rotation of HST along the V1 axis.

roll angle: Angle measured from North (through East) to the HST V_3 axis. This angle definition is relative to the V_3 axis as projected on the sky and should not be confused with the orient angle. (See "ORIENT angle").

RPS2: Graphical software system for designing HST Phase II observing programs.

SAA: South Atlantic Anomaly; lower extension of the Van Allen radiation belts lying in a region above South America and the South Atlantic Ocean; no HST scientific or calibration observations are possible during spacecraft passages through the highest SAA contours.

S-Curve: The FGS's interferometric fringe from a point source (also, see Transfer Function).

SM3: 1999 HST Servicing Mission.

SMOV: Servicing Mission Orbital Verification.

S/N: Signal-to-noise ratio.

Spiral Search: Search algorithm during which the star selectors command the IFOV in an outward spiral search around a target's expected position.

Spoiler: A star nearby the intended target inadvertently acquired by the FGS.

SSA: Star Selector A Assembly; a two-mirror and five element optical corrector group used to correct for optical aberrations induced by the OTA and aspheric pickoff mirror; along with the SSB, defines and locates the IFOV aperture.

SSB: Star Selector B Assembly; a four-mirror optical group used to pilot the collimated beam through the filter assembly and onto the polarizing beamsplitter; along with the SSA, defines and locates the IFOV aperture.

STAT: Space Telescope Astrometry Science Team.

step-size: Angular distance covered by the IFOV during one photon integration period (FESTIME); default step-size is 1.0 mas.

strfits: STSDAS routine to convert FITS files to GEIS images, STSDAS tables or text files.

STScI: Space Telescope Science Institute.

STSDAS: Space telescope Science Data Analysis System, the set of data analysis and calibration routines used to process HST data; based on the IRAF set of analysis tools produced by National Optical Astronomy Observatories (NOAO).

sub-dominant (roll) guider: The FGS used to maintain control of HST's rotation about the V1 axis during an observation.

SV: Science Verification, the process of taking observations used for HST instrument calibration and verification of science capabilities.

tilt: Angle of wavefront at face of Koesters prism.

Transfer Function (TF): The difference in counts of the two PMTs for a given interferometric axis, normalized by the sum of those counts, versus the tilt angle of the wavefront at the entrance face of the Koesters prism.

Transfer (TRANS) mode: FGS observing mode used primarily to measure the angular separations and relative magnitudes of multiple stars or the angular size of extended targets.

U1,U2,U3 Orient Reference Frame: Coordinate system fixed in the HST focal plane as projected onto the sky; U1 corresponds to the V1 axis, while U2 and U3 correspond to the negative directions of V2 and V3 respectively.

Upgren69: FGS standard reference star (RA $00^h\ 37^m\ 51.9^s$, Dec $+84^o$ 57' 47.8"; $m_V \sim 9.58$; B-V = 0.49) used to monitor the interferometric response of the FGS over time.

URL: Universal Resource Locator (or Link); the unique address used to define the "location" of a WWW-based document.

V1,V2,V3 reference frame: Fixed telescope coordinate system, with the V1 axis lying along the optical axis, V2 parallel to the solar-array rotation axis, and V3 perpendicular to the solar-array axis.

vehicular jitter: Variations in the HST pointing measured by the FGS's tracking of guide stars; thought due to mechanical or thermal transients over the course of the orbit.

WalkDown (WalkDown to FineLock): Target acquisition mode in which the IFOV is moved toward target photocenter in equal steps along x,y until FineLock is achieved.

yaw: Rotation of HST within the V1,V2 plane.

zero-point crossing: Point at which the difference in PMT counts along a given interferometer axis is zero; ideally, this crossing should occur at interferometric null.

List of Figures

FGS Interferometric Response (the "S-Curve") 6
FGSs in the HST Focal Plane (Projected onto the Sky) 7
FGS Star Selector Geometry 8
FGS1r Optical Train Schematic 13
Light Path from Koesters Prisms to the PMTs 14
The Koesters Prism: Constructive and Destructive Interference ... 16
Full Aperture S-Curves of the Original FGSs 20
Improved S-Curves for Original FGSs when Pupil is in Place 21
FGS1r S-Curves in Full Aperture Across the Pickle 22
FGS Proposal System and Detector Coordinate Frames 25
FGS1r Filter Transmission 26
PMT Efficiency 27
Comparison: PC Observation v. FGS Observation 32
Simulated PC Observations v. FGS Observations of a 70mas Binary 33
Comparison of FGS1r and FGS3 Transfer Mode Performance 34
Relative Orbit of the Low-Mass Binary System Wolf 1062 AB 36
Mira-type variable with a resolved circumstellar disk 37
Flare Outburst of Proxima Centauri as Observed with FGS3 38
Triton Occultation of the Star TR180 as Observed by FGS 3 38
Default FESTIME as a Function of V Magnitude for F583W FGS1r: NEA as a Function of Magnitude and FESTIME 48
A Sample Visit Geometry 54
.Binary S-Curves Generated from FGS1r X-Axis Data 56
FGS1r (F583W) S-Curves: Single and Co-Added 62
Evolution of S-curve morphology along the FGS1r Y-axis 64

Overlay of the pointings used for the FGS3 OFAD calibration..... 71
Overlay of pointings used for the FGS1r OFAD calibration 71
FGS3: Residuals of OFAD Calibration in the X-axis (top panel) and Y-axis (bottom panel)..... 72
FGS2 Guide Star Motion at the Onset of a Day/Night Transition..... 74
Effects of Jitter on an FGS1r S-Curve (single scan) 78
Temporal Stability: FGS3 v. FGS1r..... 80
Example 1: Field of View at Special Orientation 96
Example 2: Field of View at Special Orientation 100
Example 3: Transfer + Position Mode Visits 103
Example 3: Transfer + Position Mode Visits 106
CALFGSA Common Processing Tasks..... 118
CALFGSA Transfer Mode Processing Tasks..... 119
CALFGSB Position Mode Processing 120
Location of IFOV as FGS Acquires a Target..... 123
Offset of True Null from S_y= 0 125
X,Y Position in Detector Space of FGS 3's IFOV During WalkDown to FineLock and Subsequent Tracking of a Star in FineLock 126
FGS1r S-Curves: Before and After AMA Adjustment..... 130
FGS1r S-Curves: First Six Months After AMA Adjustment..... 131
FGS1r S-Curves: Second Six Months After AMA Adjustment 131
.Optimized FGS1r S-Curves Used in Angular Resolution Test... 132
FGS1r Transfer Function: Change in Angular Separation of a Binary..... 133
FGS1r Transfer Function Amplitude w/ Binary Separation 134

List of Tables

FGS1r Dark Counts 17
Approximate Reference Positions of each FGS in the HST Focal Plane 24
Available Filters 26
FGS1r TRANSFER Mode Performance: Binary Star 34
Filters for which FGS1r will be Calibrated for Cycle 8 46
Default FES Times 48
FGS1r: Background + Dark 49
F-factor Transmission Estimator for Combination of Filter and Color 49
Recommended FGS1r Exposure Times 50
FGS1r Transfer Mode Filters to be Calibrated During Cycle 8 59
Suggested Minimum Number of Scans for Separations < 15 mas 62
FGS1r Position Mode Calibration and Error Source Summary 68
FGS1r Transfer Mode Calibrations and Error-Source Summary 76
FGS1r Transfer Mode - F583W Observed Reference Star Colors 81
FGS Instrument Parameters 87
Summary of Calibrated Mode and Filter Combination 87
Position Mode Optional Parameters 88
Transfer Mode Optional Parameters 90
Position Mode Overheads 93
Transfer Mode Observing Overheads 94
Position Mode Overheads and Exposure Time vs. Magnitude for FGS3 94
Target and Exposure Input for Example 1 96

Target and Exposure Input for Example 3 103
Reference/Check Star Pattern 104
Target and Exposure Input for Example 4 106
FGS1r Angular Resolution Test: Effective Signal-to-Noise Ratios 134
FGS1r Angular Resolution Test: Binary Star Analysis 135

Index

A

aberrations
  differential velocity 69
  optical 17
accuracy
  summarized 29
ACQ-DIST
  POS mode 88
  TRANS mode 90
ACQ-MODE
  POS mode 88
  TRANS mode 90
alignment
  minimizing effect of misalignment 20
angular diameter
  non-point source 36
aperture 87
  parameter, Phase II 87
astrometer
  designated 22
astrometry
  pipeline 109
  Position Mode 43
  Transfer Mode 55

B

background
  bright 51
  measurements 64
  noise 48
  special, faint binary observation 104
  subtraction, TRANS 77
beam decenter
  S-curve 19
bibliography
  special topics 40
binary star 50, 55, 99, 104, 112, 116
binary star studies 4
brightness
  limits 45

C

calculation
  exposure time, Position Mode 49
calibration
  background subtraction, TRANS 77
  color, POS 72
  cross-filter, POS 75
  Cycle 7 monitoring 83
  dark subtraction, TRANS 77
  drift, POS 74
  drift, TRANS 78
  jitter, POS 73
  jitter, TRANS 77
  modes maintained by STScI 27
  OFAD distortion, POS 70
  pipeline, astrometry 109
  plate overlay, POS 76
  plate scale, POS 75
  position centroid, POS 69
  Position Mode 67
  S-curve, TRANS 79
  Transfer Mode 76
  velocity, POS 69
centroid adjustment
  Position Mode 69
check stars 46

CoarseTrack
target acquisition 124
Transfer Mode acquisition 127
color
lateral 72
Transfer Mode 59
combined mode
calibration 82
strategy, described 30
control
FGS 121
cosmic rays 48
COUNT 89
cross filter observation 54

D

dark
background 48
subtraction, TRANS 77
dark counts
FGS1R 17
decenter beam
FGS1R 22
designated astrometer 22
detector
description 17
diamter
measurement 4
differential velocity aberration 69
drift
astrometry pipeline 114, 115
calibration, POS 74
calibration, TRANS 78
exposure sequence 53

E

error sources
Position Mode 67
Transfer Mode 76
exposure
Position Mode 44
Transfer Mode 57
exposure sequence
drift 53
exposure time
calculation, Position Mode 49
Transfer Mode 61
extended source studies 50, 82, 112

F

faint binary 104
FES-TIME
POS mode 89
FGS
control 121
instrument overview 1
operating modes 7
science investigations suited to 30
web page 41
field
crowded, components 52
target 45
field dependence
S-curve 19, 21
field of view
position in pickel 24
filter
cross, calibration 75
spectral elements 87
filters
available 5, 25
fine bit error
star selector encoder
star selector encoder
fine bit error 69
FineLock
target acquisition 124
forward steering section
optical path 12

G

guide star
astrometry pipeline 113, 115

I

instrument
  parameters 87
  parameters, Phase II 87
interference
  Koesters prism 16
interferometer
  described 13
investigations
  suitable for FGS 30

J

jitter
  calibration, POS 73
  calibration, TRANS 77

K

Koesters prism 4
  described 13

L

lateral color 72
light path
  see "optical path"
limits
  brightness 45
  target geometry 45
linked modes
  see "combined mode"
LOCK 89
logsheet
  proposal, examples 95

M

mass determination 102
misalignment
  minimizing effect of 20
mixed mode
  see "combined mode"
modes
  bias, astrometry pipeline 115
  described 7
motion
  reflex 115
moving target 39, 54

N

NULL 89

O

operating modes
  see "modes"
opmode
  parameter, Phase Ii 88
optical aberrations 17
optical field angle distortion
  calibration, POS 70
optical path
  FGS 11
  forward steering section 12
  interferometer 13
optional parameter 87, 88
  ACQ-DIST, POS mode 88
  ACQ-DIST, TRANS mode 90
  ACQ-MODE, POS mode 88
  ACQ-MODE, TRANS mode 90
  COUNT, POS mode 89
  FESTIME, POS mode 89
  LOCK, POS mode 89
  NULL, POS mode 89
  POS mode 88
  SCANS, TRANS mode 90
  STEP-SIZE 90
optional parameters
  Phase II 88
ORIENT 91
orientation
  target 59
overheads
  Position Mode 93
  Transfer Mode 94

P

parallax 95, 115
parameters
  instrument, Phase II 87
  optional, Phase II 88
Phase II
  logsheet examples 95
  proposal, preparing 85
photometry
  Position Mode 37
  relative 4
photomultiplier tube
  described 13
  PMT calibration, TRANS 77
pickel
  described 23
pipeline
  drift correction 114, 115
  epoch level 115
  exposure level 110
  mode bias 115
  Position Mode 111, 113
  processing 109
  Transfer Mode 111, 114
  visit level 113
plate overlay
  calibration, POS 76
plate scale
  calibration, POS 75
POS TARG 92
Position Mode
  astrometry 43
  astrometry pipeline 111
  bibliography 40
  calibration 67
  centroid adjustment 69
  combined with Transfer 82
  exposure 44
  exposure time 49
  observation planning 45
  overheads 93
  photometry 37
  pipeline 113
  pupil 47
Position mode
  described 7
proper motion 95, 115
proposal
  logsheet examples 95
  Phase II 85
pupil
  Position Mode 47

R

reference stars 46
references
  special topics 40
reflex motion 115
roll angle
  faint binary observation 104

S

SAME POS 92
scan length
  Transfer Mode 57, 58
SCANS 90
scattered light 48
science
  investigations suited to FGS 30
S-curve 5
  beam decenter 19
  calibration, TRANS 79
  field dependence 19
  ideal 18
  properties 18
  wavelength dependence, TRANS 80
search
  target acquisition 123
SEQ NON-INT 92
slewing
  described 23, 122
South Atlantic Anomaly 48

special requirement
exposure-level 92
orient 91
POS TARG 92
SAME POS 92
SEQ NON-INT 92
timing 91
visit-level 91
special requirements
Phase II 90
spectral coverage 5
spectral element
parameter, Phase II 87
star selector
described 6
stellar mass 35
STEP-SIZE 90
step-size 90

T

target acquisition
CoarseTrack 124
FineLock 124
Transfer Mode 127
target selection
Transfer Mode 58
timing requirement 91
Transfer Mode
astrometry 55
bibliography 40, 41
calibration 76
color 59
combined with Position 82
exposure 57
exposure time 61
overheads 94
pipeline 111, 114
S-curve 80
target acquisition 127
Transfer mode
described 8

V

velocity
differential, aberration 69
virtual plate 115

W

WalkDown
target acquisition, FineLock 124
World Wide Web
FGS page 2, 41